THE ROLE OF PROSTAGLANDIN E2 ON THE DEVELOPING HIPPOCAMPUS – LINK TO AUTISM SPECTRUM DISORDER

SHALINI IYER

A THESIS SUBMITTED TO THE FACULTY OF GRADUATE STUDIES IN PARTIAL FUFILLMENT OF THE REQUIREMENTS FOR THE DEGREE OF

MASTER OF SCIENCE

GRADUATE PROGRAM IN KINESIOLOGY AND HEALTH SCIENCE
YORK UNIVERISTY
TORONTO, ONTARIO

JUNE 2022

ABSTRACT

Autism spectrum disorder (ASD) is a neurodevelopmental disorder characterized by deficits in social communication, increased repetitive/restricted behaviours and anxiety. The prevalence of autism has been drastically increasing over the past few decades with an associated increase in socioeconomic burden, imposing hardship on many families. Currently, 1 in 66 Canadians are impacted by the disorder and males are four times as likely to be diagnosed with ASD. There is a growing need to understand the underlying mechanisms during development that are contributing to the pathology of ASD in both sexes. Clinical and epidemiological studies suggest exposure to environmental risk factors during pregnancy can impact lipid signaling during development, contributing to the pathology of ASD in children. Previous literature has provided evidence that a bioactive lipid signalling molecule in the brain, known as prostaglandin E2 (PGE2) can be perturbed due to exposure to environmental risk factors during pregnancy, impacting critical processes such as neuronal migration, differentiation and proliferation. Moreover, deficits in hippocampal function are known to contribute to the major symptoms that characterize ASD. In this study, we investigated how prenatal exposure to PGE2 impacts the developing hippocampus in males and females. We examined the effect of PGE2 exposure on dendritic morphology using Golgi-cox staining and proteins that may be driving these morphological changes using western blotting. Our findings suggest that prenatal PGE2 exposure impacts hippocampal dendritic morphology in a sex-dependent manner, which is associated with changes in the expression of proteins involved in cytoskeletal architecture. Ultimately, this study provides us with insight on how perturbed PGE2 signaling impacts cytoskeletal dynamics in the developing hippocampus, contributing to the pathology of autism.

ACKNOWLEDGEMENTS

Beginning my MSc at the peak of the pandemic, I was faced with uncertainty, obstacles, and challenges I would have never imagined. However, I would have not been able to complete my thesis without the support of many individuals – it truly took a village. First and foremost, I would like to express my sincerest gratitude to my supervisor Dr. Dorota Crawford for her incredible support and kindness over these past few years. I have immensely grown as a researcher over the course of my training due to her guidance and encouraging me to step out of my comfort zone. I would also like to thank my committee members, Dr. Steven Connor and Dr. Ali Abdul-Sater for providing me with guidance and insightful feedback throughout my project.

Additionally, I would like to thank my lab mates – Aisha Abdul Rahiman, Ilham Abbasi and Sasha Udhesister for their friendship and feedback. I would especially like to extend my deepest gratitude to my mentor and friend, Dr. Ashby Kissoondoyal, for not only providing me with extensive support, technical training, and valuable feedback, but inspiring me to pursue a career in research. Additionally, thank you to Dr. Ashby Kissoondoyal for preparing the PN30 Golgi-Cox samples and Ilham Abbasi for assisting with the PN90 data collection.

Thank you to Magdalena Jaklewicz from the York University Imaging Facility, Debra Reid and Wendy Lezama from the Animal Facility for their training and expertise.

Finally, I am indebted to all my family and friends who provided me with emotional support and encouragement during the challenging times**.** Thank you to my parents and sister, Ravi Iyer, Shanthi Iyer, Jana Iyer, who endlessly supported me by encouraging me to pursue my passion and inspired me to continuously persevere. Thank you to my closest friends for listening to my experiences, helping me destress and providing words of encouragement – Maya El-Zahed, Nimrat Randhawa and Vidhi Barot.

TABLE OF CONTENTS

LIST OF TABLES

LIST OF FIGURES

FIGURE 12. PROTEIN EXPRESSION OF B-ACTIN AND AMPA IN THE HIPPOCAMPUS AT PN90. 83

LIST OF ABBREVIATIONS

AA – Arachidonic acid

AIC – Akaike Information criteria

AMPA – Alpha-amino-3-hydroxy-5-methyl-4-isoxazole propionic acid

ASD – Autism spectrum disorder

CNS – Central nervous system

CA – Cornu ammonis

COX1 – Cyclooxygenase-1

COX2 – Cyclooxygenase-2

COX2-KI – Cyclooxygenase-2 knock-in

DG – Dentate gyrus

DHA – Docosahexaenoic acid

dmPGE2 – Dimethyl prostaglandin E2

EEDC – Estrogen-like endocrine disrupting chemicals

EP – E-Prostanoid receptors

EPA – Eicosapentaenoic acid

EPSP – Excitatory-post-synaptic potential

EPSC – Excitatory-post-synaptic current

G0, G11, G17 – Gestational day 0, 11, 17

GABA - Gamma-amino-butyric-acid

GAPDH - Glyceraldehyde-3-phosphate dehydrogenase

HRP – Horseradish peroxidase

IL – Interleukin

LTD – Long-term depression

LTP – Long-term potentiation

MRI – Magnetic resonance imaging

NDD – Neurodevelopmental disorder

NE4C – Neuroectodermal stem cells

NMDA – N-methyl-D-aspartate

NO – Nitric oxide

OR – Odds ratio

PFA – Paraformaldehyde

PGE2F – PGE2-exposed female

PGE2M – PGE2-exposed male

PLA2 – Phospholipase A2

PN30, 90 – Postnatal day 30 or 90

PUFA – Polyunsaturated fats

PBS – Phosphate-buffered saline

SD – Standard deviation

SDS-PAGE – Sodium dodecyl-sulfate polyacrylamide gel electrophoresis

SEM – Standard error of the mean

SNT – Simple neurite tracer

TBS – Tris buffered saline

TBS-T – Tris buffered saline, Tween 20

VPA – Valproic acid

Wnt – Wingless-related integration site

WTF – Wildtype female (saline-exposed female)

WTM – Wildtype male (saline-exposed male)

CHAPTER 1: BACKGROUND LITERATURE

1.1 Autism Spectrum Disorder

Autism Spectrum Disorder (ASD) is a neurodevelopmental disorder (NDD) characterized by atypical behavioural patterns in three major domains, which includes social communication, restricted interests, and repetitive behaviours (American Psychiatric Association, 2014). Further, individuals with ASD may also experience delayed cognitive function, sensory, motor development and increased anxiety (Posar & Visconti, 2018; Travers *et al.*, 2018; Zaboski & Storch, 2018). Detection of ASD can occur as early as one year of age, however, symptoms are more pronounced and easily detectable between two to three years of age (American Psychiatric Association, 2014). Males are also four times as likely to be diagnosed with ASD, indicating a large sex-bias (Public Health Agency of Canada, 2018). Interestingly, over the past few decades, there has been a substantial increase in the prevalence of ASD **(Figure 1)**. Specifically, in the United States of America (USA), between 1990 and 1999 the prevalence of ASD per 1000 children was an average of 7.6. The prevalence doubled in the next decade, where an average prevalence of 14.4 per 1000 children between 2000 to 2009 was detected (CDC, 2018; Cakir *et al.*, 2020). The prevalence of ASD continued to increase in the recent decade, where an average prevalence of 24.7 per 1000 children between 2010 to 2019 was observed (Cakir et al., 2020; Zablotsky, Black, & Blumberg, 2014). The CDC estimates that the prevalence of ASD increases by 10% each year and reached a prevalence of 1 in 54 in 2020 (Knopf, 2020). Between 2020-2029, the prevalence of ASD is predicted to double reaching 44.6 cases per 1000 people (Cakir et al., 2020; Zablotsky, Black, & Blumberg, 2014). In Canada, similar prevalence rates have been observed, where currently 1 in 66 children are impacted by ASD (Public Health Agency of

Canada, 2018). Although there is some postulation that the alarming increase in the prevalence of ASD diagnosis may be associated with factors such as increased awareness of the disorder, improved diagnostic tools, earlier diagnosis and women having children at an older age, studies have demonstrated that these factors only account for over 50% of the observed increase **(Figure 2)**. The remaining fifty percent is unaccounted for and largely unknown. (Hertz-Picciotto & Delwiche, 2009; Weintraub, 2011). In the last few decades, it is becoming more evident from clinical and epidemiological studies that the influence of various environmental risk factors (discussed below) affects the developing brain, resulting in ASD related outcomes (Hinz *et al.*, 2008; Tamiji & Crawford, 2010a, 2010b; Liew *et al.*, 2016; Hajisoltani *et al.*, 2019). Specifically, maternal exposure to environmental risk factors are known to affect the levels of biolipids such as prostaglandin E2 (PGE2), which are critical for neurodevelopment and have been linked to ASD (Bandim *et al.*, 2003; Tamiji & Crawford, 2010a, 2010b; Brandlistuen *et al.*, 2013; Wong & Crawford, 2014). Thus, it is becoming increasingly critical to understand the contributing factors to the etiology of ASD.

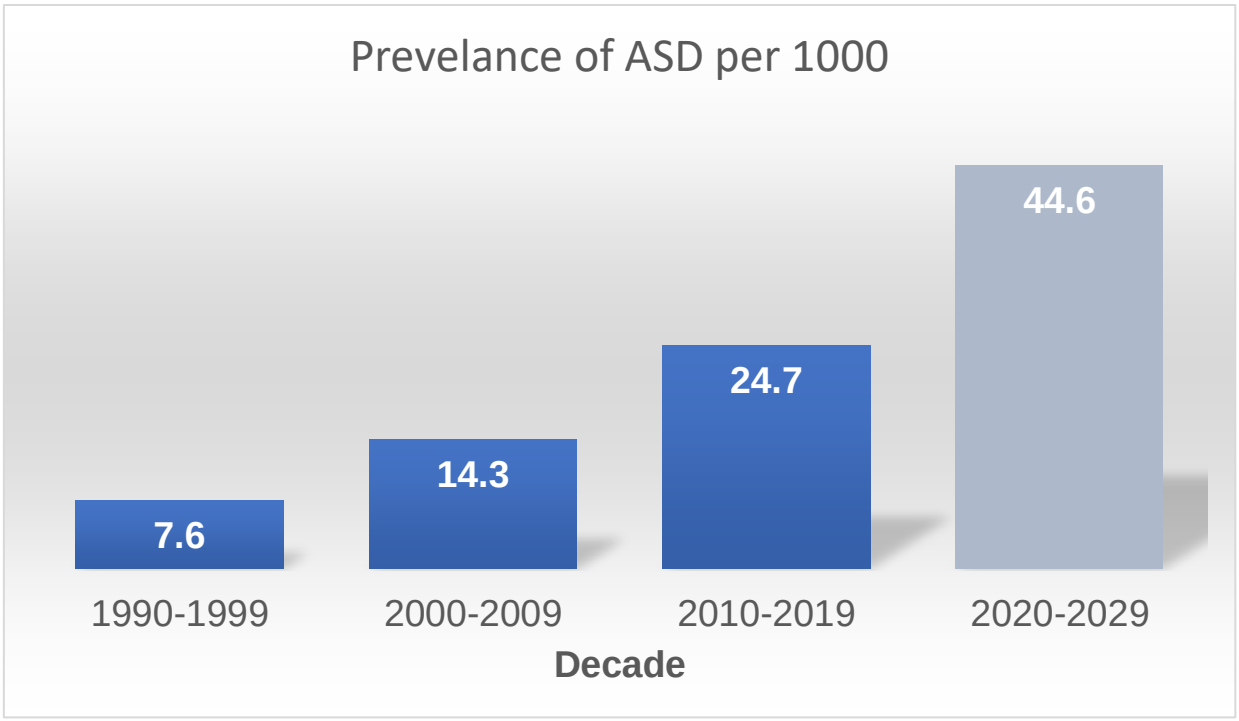

Figure 1: Prevalence of ASD over the past few decades.
The prevalence of ASD has been drastically increasing over the past few decades, with a projected increase of 44.6 per 1000 children in the 2020s. The data is obtained from CDC's Autism and Developmental Disabilities Monitoring Network (ADDM) (CDC, 2018) and the projection data is obtained from Zablotsky *et al.* (2014).

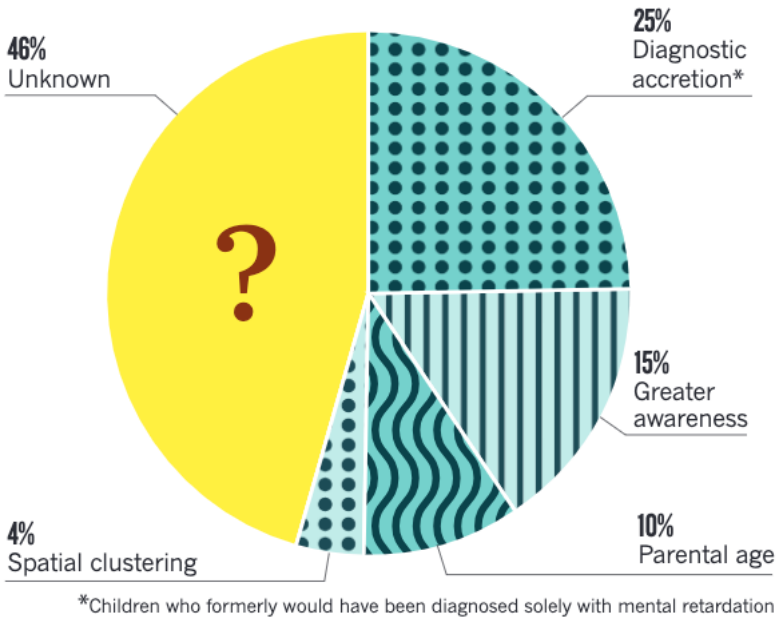

Figure 2: Factors contributing to the increased prevalence of ASD.
More than 50% of the rise in ASD prevalence in the United States is accounted for by various factors, however the remaining is still unaccounted for. Figure and copyright obtained from: (Weintraub., 2011).

1.2 Lipid Signalling

1.2.1 Lipid signalling in the neurotypical brain

Fatty acids are an integral component of cell membranes and can be classified as saturated, monosaturated or polyunsaturated. Interestingly, the human brain has the greatest lipid content, where 60% of its dry mass is composed of lipids, specifically phospholipids and polyunsaturated fats (PUFAs). Lipids are critical for neurodevelopment, specifically during postnatal development there is a high requirement for PUFAs (Sastry, 1985; Bennett & Horrobin, 2000; Boland *et al.*, 2009; Wong & Crawford, 2014). Additionally, lipids have diverse functions in brain, they are critical for functions such as vision, neuroplasticity, inflammation, circadian rhythm, learning and memory (Ferrucci *et al.*, 2006; Wu *et al.*, 2008; Hoffman *et al.*, 2009; Su, 2010; Ladesich *et al.*, 2011).

The two major categories of PUFAs are omega-3-linoleic acid, which is metabolized into docosahexaenoic acid (DHA) or eicosapentaenoic acid (EPA) and omega-6-linoleic acid, which is metabolized into arachidonic acid (Haag, 2003; Yehuda & Rabinovitz, 2016). One of the most common derivatives of PUFAs and of primary interest is arachidonic acid (AA), which is released from the cell membrane by the enzyme phospholipase A2 (PLA_2) **(Figure 3)**. AA is further metabolized into prostaglandin E2 (PGE2), the major bioactive lipid signalling molecule in the brain often produced during neurodevelopment and in response to inflammation, either by cyclooxygenase 1 (COX1) or cyclooxygenase 2 (COX2). Following the production of PGE2, it binds to transmembrane G-protein coupled receptors, known as E-prostanoid receptors (EP1-4), which leads to various downstream signalling cascades (Andreasson, 2010; Wong & Crawford, 2014). During development, PGE2 is involved in cell proliferation, migration, differentiation,

synaptic plasticity, learning and memory (Chen & Bazan, 2005; Andreasson, 2010; Wong & Crawford, 2014; Wong *et al.*, 2016).

As COX1 and COX2 are both involved in the production of PGE2, they are differentially expressed in human tissues. The COX1 enzyme is constitutively expressed in majority of human tissues and in microglial cells in the brain (Hoozemans *et al.*, 2001). In contrast, the COX2 enzyme is primarily induced in most human tissues in response to cytokines, growth factors and inflammatory signals. However, the COX2 enzyme is constitutively expressed in specific organs, including the kidney, the intestinal tract, female reproductive system and neuronal cells in the brain (Nørregaard *et al.*, 2015; Kirkby *et al.*, 2016). Interestingly, COX2 expression is known to be the greatest within dendrites (Yamagata *et al.*, 1993). Additionally, the primary source of PGE2 production is from COX2 during the perinatal period and continues to rise during early development. In contrast, COX1 enzymes have shown to be consistently low during the developmental period (Peri *et al.*, 1995; Li *et al.*, 1997). This suggests COX2/PGE2 signalling plays a crucial role during early development.

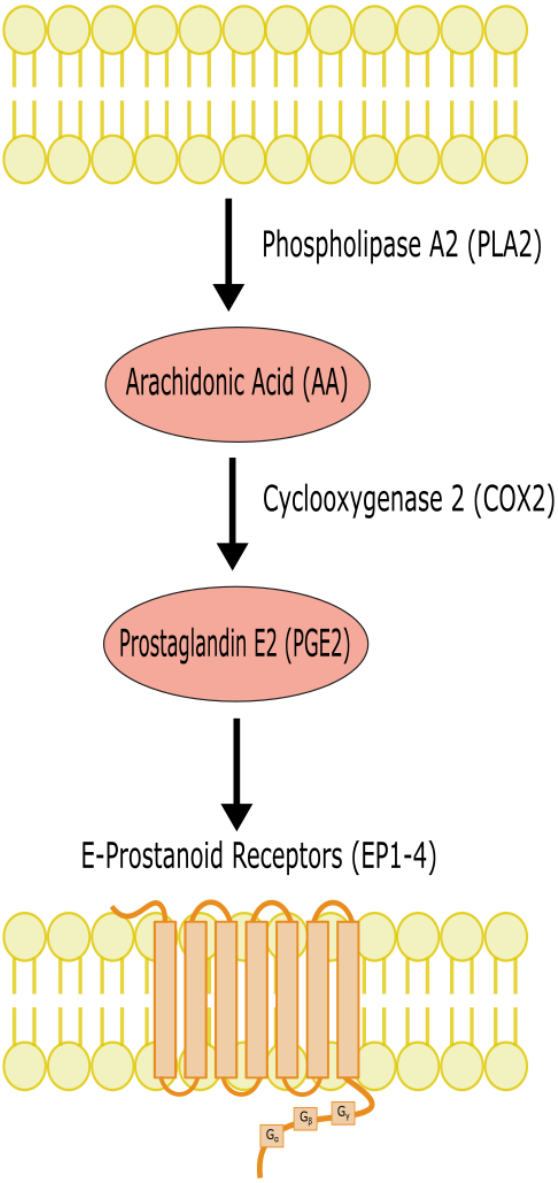

Figure 3. The synthesis of prostaglandin E2.
Arachidonic acid freed from the cell membrane by phospholipase A2 (PLA2) is further converted into prostaglandin E2 (PGE2) by COX2. PGE2 can further stimulate various signalling cascades by binding onto the receptors, EP1-EP4.

1.2.2 The relationship between lipid signalling and autism

Irregular lipid content in the brain has been implicated in ASD, specifically the bioactive lipid molecule, PGE2. Exposure to environmental factors such as heavy metals, pollutants, exposure to specific drugs and infections has known to modulate COX2/PGE2 signalling resulting in detrimental effects. A previous study provided evidence of lower AA levels, the PGE2 precursor, in the plasma of males and females with ASD. The lower AA acid levels may suggest a greater rate of metabolization into other lipid metabolites such as PGE2 (Yui *et al.*, 2016). Studies examining the levels of lipid markers in blood samples of children with ASD demonstrated a significant increase in COX2 and PGE2 levels compared to control individuals (Qasem *et al.*, 2018; Kordulewska *et al.*, 2019). More recently, one study investigated the levels of COX2 and the PGE2 receptor EP2 in blood samples of individuals with ASD and found they were elevated compared to the control group. The study also investigated whether COX2 and EP2 could be used as biomarkers for early detection of ASD, they found that EP2 provided good predictive value of ASD for individuals who are at low and high risk (El-Ansary *et al.*, 2021). Additionally, the specificity and sensitivity of these markers for ASD diagnosis has been investigated, revealing COX2 and PGE2 can potentially be used as ASD predictive markers (Qasem *et al.*, 2018).

1.3 Exposure to environmental risk factors and link to autism

During prenatal and perinatal development, exposure to exogenous risk factors can lead to irregularities in lipid content in the brain which has been implicated in ASD (Wong & Crawford, 2014; Wong *et al.*, 2015). Specifically, environmental factors such as insufficient fatty acid diet, exposure to drugs such as misoprostol and acetaminophen, exposure to air pollutants and toxins, oxidative stress, inflammation and infections can disrupt PGE2 levels (Tamiji &

Crawford, 2010b, 2010a; Wong & Crawford, 2014; Wong *et al.*, 2015; T Schultz & G Gould, 2016).

1.3.1 Drug exposure

Valproic Acid

The exposure of certain drugs and medications *in utero* has been associated with an increased risk of the child developing ASD. A potent teratogen known as valproic acid (VPA), an anticonvulsant, also used to treat mood disorders and severe migraines is known as a major risk factor for ASD. A population-based study looking at the adverse effects of prenatal VPA exposure in Scotland determined anticonvulsant drugs such as VPA are a risk factor for ASD. Specifically, 8.9% of the children in the study developed ASD due to prenatal VPA exposure (Rasalam *et al.*, 2005). More recently, another population based study on children born between 1996-2006 in Denmark provided evidence of increased risk of 4.42% in developing autism with maternal use of VPA, while accounting for maternal epilepsy (Christensen *et al.*, 2013). In rodent models, maternal exposure to VPA contributed to ASD-related behavioural symptoms including decreased social behaviour, increased repetitive/restricted behaviours, increased anxiety, hyperactive behaviour and attention-deficits (Schneider & Przewłocki, 2005; Markram *et al.*, 2007; Roullet *et al.*, 2010; Kim *et al.*, 2011). In addition to behavioural changes in the VPA rodent model, studies have also provided evidence of molecular changes in the brain. VPA has shown to decrease COX2 levels in the rat brain, contributing to a corresponding decrease in COX2 metabolites, including AA (Bosetti *et al.*, 2003). Furthermore, prenatal VPA exposure has also shown to affect inflammatory mediators, including *Ptgs2* (gene for COX2) and the expression of COX2 itself in the cerebral cortex of rats (Gąssowska-Dobrowolska *et al.*, 2020). Studies have also provided evidence of VPA-exposure resulting in decreased brain-derived neurotrophic factor (BDNF), hyperacetylation of histones during embryonic stages, increased

cellular apoptosis, decreased cell migration, changes in dendritic spine density and synapse-related proteins, heavily impacting neurodevelopment and contributing to the etiology of ASD (Roullet *et al.*, 2010; Kataoka *et al.*, 2013; Lan *et al.*, 2021).

Misoprostol

Furthermore, the misuse of the prescription drug misoprostol during pregnancy, often used to treat stomach ulcers, induce labour, and terminate pregnancies, contributing to the development of Mobius syndrome, ASD and intellectual disability. (Gonzalez *et al.*, 1998). Studies have also shown that individuals diagnosed with Mobius syndrome due to misoprostol exposure, are at a greater risk of also developing ASD compared to the normal population. Misoprostol acts similarly to PGE2, as it stimulates the same EP receptors as PGE2, leading to alterations in intracellular calcium levels, which is critical for neuronal communication, development and migration (Tamiji & Crawford, 2010a) **(Figure 4)**. Changes in intracellular calcium levels can heavily impact long-term potentiation (LTP), a critical mechanism involved in memory consolidation in the brain. (Esplugues, 2002a; Tian *et al.*, 2008). In addition, neural stem cells exposed to PGE2 and misoprostol, result in disruption of neuronal growth cone formation, a decrease in the length and number of dendritic extensions, which can influence neuronal communication and plasticity in the brain (Tamiji & Crawford, 2010b).

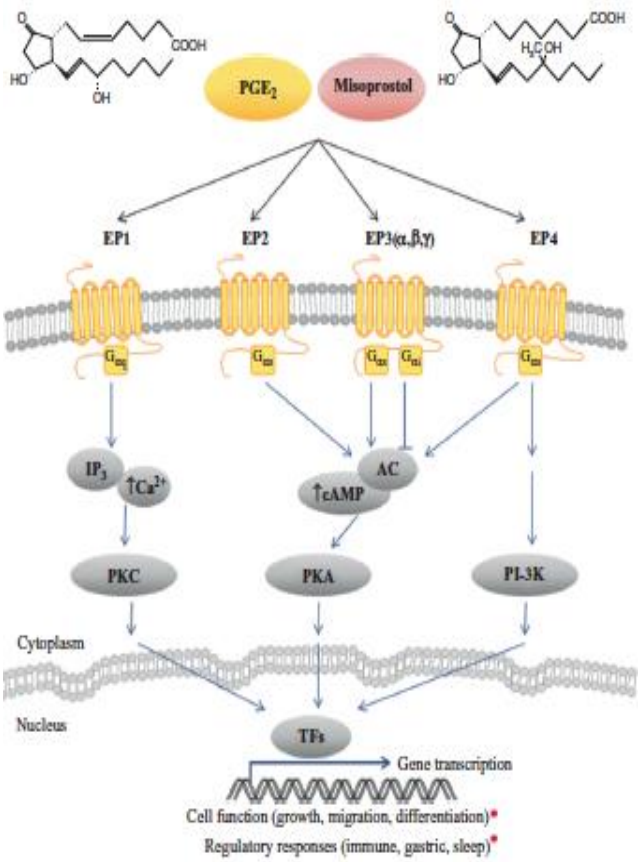

Figure 4. The interaction between PGE2 signalling and misoprostol.
Stimulation of EP1-4 receptors leads to downstream signalling cascades and transcription of genes involved in cell function and regulator responses, which have been implicated in ASD. Figure and copyright obtained from: (Wong & Crawford, 2014).

Acetaminophen

More recently, studies have determined that the use of certain over-the-counter drugs, such as acetaminophen can increase the risk of ASD in the offspring. Studies have shown long-term use of acetaminophen during pregnancy increased the risk of developing ASD and related symptoms, such as poor psychomotor development, communication, reduced emotionality and sociability (Brandlistuen *et al.*, 2013; Liew *et al.*, 2016). Acetaminophen leads to inflammatory responses and oxidative stress, which can compromise brain development and contribute to the risk of developing ASD (Andrade, 2016). A recent study determined that children exposed to acetaminophen during pregnancy for a long duration had greater DNA methylation, which can impact critical genes involved in neurodevelopment (Gervin *et al.*, 2017). An *in-vivo* study on rats revealed that acetaminophen exposure during critical periods of prenatal neurodevelopment increased the expression of immune-related genes and cytokine production (Koehn *et al.*, 2020). As previously mentioned, PGE2 is produced in response to inflammation, suggesting inflammatory responses triggered by acetaminophen can potentially impact the COX2-PGE2 pathway in the brain (Esplugues, 2002; Tian *et al.*, 2008; Korbecki *et al.*, 2013; Wong and Crawford, 2014).

Exposure to various drugs during critical times in pregnancy, including prescription drugs such as valproic acid and misoprostol and over-the-counter drugs such as acetaminophen, can result in disruptions in synaptic plasticity in the brain, contributing to deficiencies in learning and memory associated with ASD (Tamiji & Crawford, 2010b, 2010a; Wong & Crawford, 2014; Wong *et al.*, 2015; T Schultz & G Gould, 2016).

1.3.2 Pollutants and pesticides

Prenatal exposure to exogenous risk factors such as air pollution, heavy metals, pesticides and consumer products such as cosmetics, can potentially result in atypical neurodevelopment and contribute to neurodevelopmental disorders such as ASD (Wong *et al.*, 2015). There is evidence that prenatal exposure to air pollution results in oxidative stress and inflammation in the brain (Calderón-Garcidueñas *et al.*, 2007, 2015; Møller *et al.*, 2014). Subsequently, inflammation is one of the major factors that leads to increased AA release, followed by increased PGE2 production (Dumuis *et al.*, 1988; Lafon-Cazal *et al.*, 1993; Shelat *et al.*, 2008).

Pesticides are another risk factor contributing to atypical brain development and increasing the risk of ASD. Pesticides have the ability to cross the blood brain barrier and the placental barrier during pregnancy using specific transporters that normally transport PGE2 (Alebouyeh *et al.*, 2003; Bahn *et al.*, 2005; Koepsell, 2013). Additionally, pesticides act as estrogen-like endocrine disrupting chemicals (EEDCs), which disrupt hormone levels (Soto *et al.*, 1994; Kojima *et al.*, 2004; Evseenko *et al.*, 2006). Previous literature has demonstrated that PGE2 can be induced in response to exposure to estrogen compounds in rodents. Estrogen induced PGE2 production contributes to changes in the brain, such as masculinization (Amateau & McCarthy, 2004).

Exposure to environmental factors such as pollutants and pesticides prenatally can result in inflammation and oxidative stress, which influence downstream signalling pathways such as the COX-PGE2 and NO pathway (Wong *et al.*, 2015).

1.3.3 Infection and Inflammation

Interestingly, various studies have demonstrated that there is an association between exposure to bacterial infection during pregnancy and the diagnosis of ASD in children. (Meyer *et al.*, 2007). A recent metanalysis study analyzing the risk of ASD due to maternal infection during pregnancy, revealed that exposure to bacterial infections can increase the ASD incidence rate (Jiang *et al.*, 2016). Another study provided evidence that exposure to a bacterial infections during a hospital admission increases the risk of delivering a child who will develop ASD (Zerbo *et al.*, 2015). One of the most common bacterial infections that increase the risk delivering a child who will be diagnosed with ASD, are urinary tract infections (Atladóttir *et al.*, 2010; Zerbo *et al.*, 2015).

Inflammatory responses triggered by maternal infection, lead to the production of pro-inflammatory molecules, cytokines and interleukins, which can impact fetal brain development (Zerbo *et al.*, 2015). In the central nervous system (CNS), cytokines can impact critical processes involved in neurodevelopment, including synaptic transmission, cell survival, differentiation and maturation (Aarum *et al.*, 2003; Jiang *et al.*, 2018). Interleukin-6 (IL-6) is a major neuroimmune factor released in response to infection and has been shown to be elevated in individuals diagnosed with ASD, potentially due to activated glia or maternal immune activation leading to disruption in neuronal plasticity and neuroanatomy (Wei *et al.*, 2011, 2012, 2013). An *in-vivo* study on rats revealed prenatal IL-6 treatment resulted in hippocampal apoptosis, increased expression of the receptor NMDA (N-methyl-D-aspartate) and resulted in deficits in learning and memory behaviour (Samuelsson *et al.*, 2006). Additionally, other studies have provided evidence that other cytokines are involved in modulating LTP in the brain; elevated IL-1ß, IL-18, IFN- γ, impair LTP in the hippocampus (Vereker *et al.*, 2000; Maher *et al.*, 2006; Tong *et al.*, 2012).

This suggests that inflammatory responses triggered due to factors such as infection and injury, can impact synaptic plasticity in the brain.

1.3 Molecular Evidence of Abnormal PGE2 Signalling and link to Autism

Both *in-vitro* and *in-vivo* studies in our lab have provided evidence that altered PGE2 levels disrupts key signalling molecules and genes involved in neurodevelopment, contributing to ASD-related behaviours in mice models (Wong *et al.*, 2016, 2019). *In-vitro* studies using neuroectodermal (NE4C) stem cells, derived from mice, demonstrated an increase in proliferation, early differentiation, increased neurite length and neurite loops when exposed to higher levels of PGE2 (Wong *et al.*, 2016; Kissoondoyal & Crawford, 2021). PGE2 has also shown to elevate ß-catenin levels, a transcription factor involved in regulating gene transcription in the wingless canonical (Wnt) pathway in NE4C cells (Wong *et al.*, 2016). Additionally, research in mice models have revealed that maternal exposure to PGE2 during critical stages of neurodevelopment impacts developmental genes including, Mmp7, Wnt2 and Wnt3a, which are genes involved in the Wnt canonical pathway (Rai-Bhogal, Wong, *et al.*, 2018). The Wnt pathway is highly involved in neurodevelopment, including anterior-posterior patterning of the brain and dysregulation of this pathway has been related to ASD (Abu-Khaklil *et al.*, 2004). Our lab has also observed ASD-related behaviours in the COX2-KI (COX2 knock-in) and PGE2-exposed model, which include hyperactivity, anxiety, repetitive behaviours, impaired motor strength and social interaction (Wong *et al.*, 2019; Kissondoyal *et al.*, Unpublished).

More recently, our lab has provided evidence of abnormal cerebellar development due to abnormal PGE2 signalling. Specifically, there were changes in dendritic morphology and expression of proteins involved in cytoskeletal architecture during cerebellar development in COX2 deficient mice and PGE2-exposed mice (Kissoondoyal *et al.*, 2021; Kissondoyal *et al.*,

Unpublished). Furthermore, not only does PGE2 contribute to molecular changes in the cerebellum, but it also contributes to cerebellar related motor deficits (Kissondoyal *et al.*, Unpublished).. Similar studies by McCarthy and colleagues, found a direct injection of PGE2 and COX2-inhibitors in the cerebellum resulted in abnormal dendritic development and differential expression of proteins critical for cytoskeletal architecture (Dean, Knutson, *et al.*, 2012; Dean, Wright, *et al.*, 2012). These studies provide strong evidence that the COX2-PGE2 signalling can impact neurodevelopment, specifically cerebellar development, and results in associated behavioural deficits, contributing to the pathophysiology of ASD. However, the impact of prenatal PGE2 exposure on hippocampal development is currently unknown.

1.4 The Relationship between the Hippocampus and Autism

In addition to the three major impairments that characterize ASD, which include deficits in social communication, the presentation of anxious behaviours, repetitive and restricted behaviours, individuals with ASD also demonstrate impairments in sensory and cognitive functioning which has been associated with deficits in hippocampal development (Reinhardt *et al.*, 2020a). Impairments in hippocampal dependent memory and the link to ASD has often been overlooked, as such deficits are not defined by the core domains. However, research suggests that hippocampal impairments contribute to the pathophysiology of ASD in concordance with deficits in other brain regions **(Figure 5)**. Individuals with ASD exhibit hippocampal-dependent learning and memory impairments across a variety of domains, including executive functioning, spatial reasoning, working and episodic memory (Hartley *et al.*, 2014; Cooper *et al.*, 2017a; Reinhardt *et al.*, 2020a).

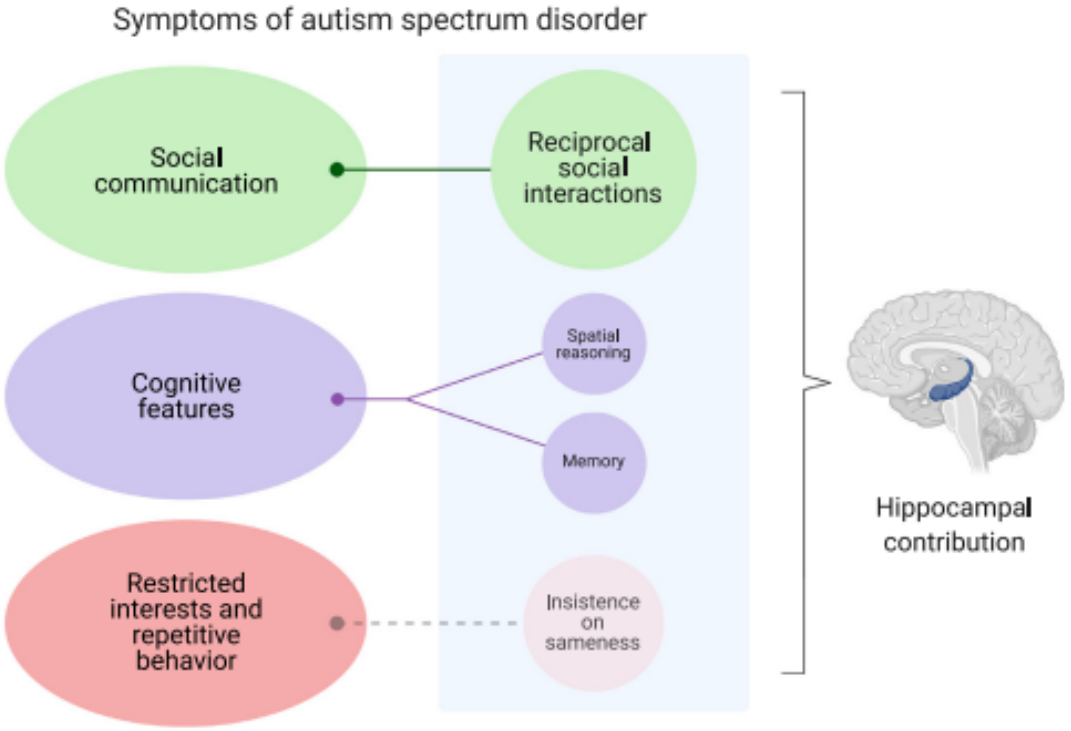

Figure 5: Hippocampal dysfunction and the relationship to the diagnostic criteria of autism. The highlighted blue area indicates functions the hippocampus is involved in. The solid lines indicate an interaction, while a dotted line indicates a potential interaction. The size of the circle indicates the severity of the function. Figure and copyright obtained from: (Banker *et al.,* 2021).

1.4.1 Memory and Spatial Reasoning

Individuals with ASD have reduced memory encoding and retrieval, which has been linked to attenuated hippocampal connectivity with other regions of the brain. Specifically, adult individuals with ASD demonstrated reduced capability in memory retrieval following a memory task, which was associated with reduced network activity in the hippocampus using fMRI compared to neurotypical individuals (Cooper *et al.*, 2017b). Another study provided evidence that children between 8-16 years of age with high-functioning ASD demonstrate significantly reduced memory for complex visual and verbal information, as well as, spatial working memory, which are all critical functions executed by the hippocampus (Williams *et al.*, 2006). Interestingly, a previous study provided evidence that in addition to impairments in working memory, adults with ASD experience difficulty remembering faces, social scenes and visual stimuli, which play a role in social communication, one of the major deficits observed individuals with ASD (Williams *et al.*, 2005).

In addition to memory, the hippocampus also plays a critical role in spatial reasoning. Studies have demonstrated the involvement of specific spatial cells in the hippocampus (Hartley *et al.*, 2014), structural MRI studies have suggested the involvement of the hippocampus in spatial reasoning (Brown *et al.*, 2014) and navigation experience has been associated with dynamic changes in the hippocampus (Maguire *et al.*, 2000; Morgan *et al.*, 2011). Individuals with ASD demonstrate spatial navigation deficits (Ring *et al.*, 2018), diminished time exploring novel environments (Kawa & Pisula, 2010) and an ability to generate spatial maps of their environment (Lind *et al.*, 2013).

Moreover, studies have also demonstrated similar deficits in well-established ASD rodent models. Specifically, a previous study provided evidence that prenatal exposure to VPA in rats, a

well-known model used to study ASD, demonstrated that VPA exposure led to increased escape latency during the Morris Water Maze (MWM), an indication of hippocampal-dependent memory and spatial reasoning impairments. In addition, prenatal VPA exposure led to reduced docosahexaenoic acid (DHA), antioxidant activity and increased neuronal loss in the hippocampus. Interestingly, the addition of DHA reversed the hippocampal dependent memory and spatial reasoning deficits, increased both neuronal survival and antioxidant levels in the hippocampus (Gao *et al.*, 2016). Another study evaluating ASD-related behaviours in the VPA-rodent model also demonstrated impaired spatial learning and memory using the MWM and reduced GABAnergic signalling in the hippocampus (Hou *et al.*, 2018). Similar hippocampal dependent learning, memory and spatial reasoning deficits have been observed in other well-stablished ASD rodent models, including the Shank3 (SH3 and multiple ankyrin repeat domains 3) and Fmr1 (Fragile X Mental Retardation 1) knockout models (Tian *et al.*, 2017; Song *et al.*, 2019). Additionally, in the Fmr1, Shank3 knock-out models and other ASD-rodent models, deficits in the novel objection recognition task have been observed, an indication of memory impairments (Kane *et al.*, 2012; Christensen *et al.*, 2013; Lee *et al.*, 2015; Schiavi *et al.*, 2020). Overall, there is growing evidence of the relationship between hippocampal dependent memory and spatial reasoning deficits and autism.

1.4.2 Social Interaction

Although the hippocampus is primarily involved in memory and spatial reasoning, research suggests the emerging role of the hippocampus in social interaction. Specifically, the hippocampus is involved in mediating social behaviours, such as reciprocal interaction, navigating social space and even the perception of emotions (Perry *et al.*, 2011; Immordino-Yang & Singh, 2013; Montagrin *et al.*, 2018; Schafer & Schiller, 2018). Interestingly,

individuals with hippocampal damage have demonstrated diminished social functioning, suggesting the involvement of the hippocampus in social behaviour (Davidson *et al.*, 2012). Although, impairments in hippocampal development and the relationship to deficits in social functioning in individuals with autism is less understood, there is some suggestion the two may be related. Specifically, individuals with ASD experience difficulty conceptualizing interpersonal space, maintaining an appropriate distance from other individuals and experience deficits in joint attention, which involves the capability to focus on visual stimuli with another individual (Dawson *et al.*, 2004; Kennedy & Adolphs, 2014), which may potentially be related to altered hippocampal function. Although diminished social interaction has been observed in ASD rodent models (Spencer *et al.*, 2005; Bozdagi *et al.*, 2010; Kim *et al.*, 2013; Wong *et al.*, 2019), hippocampal involvement in social functioning is not yet fully understood.

1.5 Abnormalities in the Hippocampus

In addition to changes in hippocampal associated behaviours, abnormalities in the hippocampus have been reported in individuals with ASD. Many studies have provided evidence of changes in shape, volume and symmetry of the hippocampus in individuals with ASD compared to healthy individuals (Schumann *et al.*, 2004; Barnea-Goraly *et al.*, 2014; Richards, Greimel, *et al.*, 2020a). Interestingly, the heterogeneity of ASD may be reflected in hippocampal abnormalities, as studies have demonstrated inconsistent findings. Some studies have provided evidence of increased hippocampal volume in children and adolescents with ASD (Schumann *et al.*, 2004; Barnea-Goraly *et al.*, 2014). However, studies have also shown reduced hippocampal volume in individuals with ASD (Aylward *et al.*, 1999). Recently, a longitudinal study of males and females examined hippocampal development in children with ASD and neurotypical children between 2-7 years of age. They determined that hippocampal growth rates did not

significantly differ between males and females. However, hippocampal volume was larger in children with ASD, compared to neurotypical individuals who have similar hemisphere volume. Ultimately, they provided novel evidence of larger hippocampal volume in individuals with ASD by adjusting for hemisphere volume (Reinhardt *et al.*, 2020a), which may account for discrepancies in hippocampal volume observed in previous studies. More recently, a study conducted radiomic analyses on MRI images, which is used to quantify patterns and textures of specific regions that cannot be normally observed on MRI images. Preliminary results from this study demonstrate significant differences in hippocampal texture features in individuals with ASD, which can potentially be used as a diagnostic biomarker (Chaddad *et al.*, 2017).

1.6 Dendritic Morphology and Autism

In the neurotypical brain, dendrite morphogenesis is tightly regulated by three major physiological requirements: 1) neuronal dendrites must sufficiently encompass the dendritic field to ensure sensory inputs are correctly processed (Shepherd *et al.*, 2005; Wen & Chklovskii, 2008), 2) the dendritic arborization pattern and spine density must be appropriate for signal processing (Losonczy *et al.*, 2008; Spruston, 2008) and 3) dendrites must maintain flexibility in response to experience, which is often driven by changes in cytoskeletal architecture and expression of receptors involved in synaptic signalling (Hu *et al.*, 2008; Espinosa *et al.*, 2009).

One of the major factors contributing to impaired neurodevelopment in individuals with ASD, may be due to aberrant dendritic growth and dendritic spine formation, impacting neuronal communication (Martínez-Cerdeño, 2017). During development, there is initially a significant outgrowth in dendritic arbour and formation of immature dendritic spines, followed by a reduction of inactive arborization due to pruning and the development of more mature spines (Riccomagno & Kolodkin, 2015). However, individuals with ASD may experience defects in the

pruning mechanism, contributing to increased brain volume, hyperconnectivity and higher density of immature dendritic spines (Schumann *et al.*, 2004; Hutsler & Zhang, 2010; Barnea-Goraly *et al.*, 2014). A previous study examining dendritic spine densities in post-mortem brain samples from ASD patients, determined that there was a greater spine density in the superficial layers, than in the deep layers of the cortices. The superficial layer is the last layer to develop during neurodevelopment and experiences the greatest level of pruning, which may be indicative of dysregulated pruning mechanisms in ASD patients (Hutsler and Zhang, 2010). Additional studies on postmortem brains from ASD patients have consistently found aberrant dendritic branching or spine density in regions of the brain compared to healthy controls, including an increase in spine density in cortical pyramidal neurons in the temporal lobe (Tang *et al.*, 2014), the amygdala (Weir *et al.*, 2018), decreased branching in the CA1 and CA4 (CA, Cornu Ammonis) region of the hippocampus (Raymond *et al.*, 1996) and prefrontal cortex (Mukaetova-Ladinska *et al.*, 2004).

Similar findings of significant changes in dendritic growth have been reported in ASD animal models. In the *C58/J* ASD mouse model there was a decrease in spine density in the prefrontal cortex and decreased mature spines in the hippocampus, related to dysregulation of cytoskeletal and synaptic plasticity proteins (Barón-Mendoza *et al.*, 2021). Similarly, there were longer dendritic arbours in the hippocampus during early postnatal development in the *BTBR* ASD rodent model (Cheng *et al.*, 2017), increased dendritic arborization in the hippocampus of and decreased dendrite length in the Shank3 knockout mice (Reichova *et al.*, 2020) and dendritic arborization in the dentate gyrus of Frm1 knockout mice (Yau *et al.*, 2019). Overall, there is strong evidence from both autism patients and animal models of ASD, that dendritic growth is heavily impacted contributing to the pathophysiology of autism.

1.6.1 PGE2 Signaling and Dendritic Morphology

Previous studies have provided evidence of abnormal COX2/PGE2 signaling impacting dendritic morphology in various regions of the brain, impacting overall brain function. Previously, a study demonstrated that direct PGE2 injection into the cerebellum contributes to a reduction in dendritic length, complexity, and the expression of spinophilin (Dean, Wright, *et al.*, 2012). In contrast, another study by the same group provided evidence that direct injection of COX2-inhibitors in the cerebellum of both male and female mice during early postnatal development increases dendritic arborization and spine density contributing to motor deficits (Dean, Knutson, *et al.*, 2012). The morphological changes observed in the cerebellum are thought to be associated with changes in PGE2 levels during a critical time interval during neurodevelopment, which coincides with the aromatase enzyme, which is involved in the conversion of androgen into estrogen. Ultimately, this time interval is particularly susceptible to inflammation which leads to changes in PGE2 levels, contributing to abnormal dendritic morphology. Recently, the same group determined a similar critical time window in cerebellar development exists in humans by examining post-mortem brain samples (Wright *et al.*, 2019). Interestingly, our lab has recently provided the first evidence that prenatal PGE2 exposure has a sex-dependent effect on dendritic arborization, looping, spine density, morphology and proteins critical for cytoskeletal architecture, contributing to cerebellar deficits (Kissondoyal *et al.*, Unpublished). We have also previously shown in our COX2 knock-in model (COX2-KI), there was an increase in dendritic arborization closer to the cell soma, likelihood of observing loops, spine density and morphology (Kissoondoyal *et al.*, 2021).

However, the effects of prenatal PGE2 exposure on hippocampal development has not been directly studied. Previous literature has demonstrated high expression of COX2 and

prostaglandin E synthases in dendritic spines, suggesting PGE2 synthesis is highly involved in dendritic spine morphogenesis (Sang *et al.*, 2005). The same group demonstrated that PGE2 exposure increases the amplitude of exictatory-post-synaptic potentials (EPSPs) in hippocampal neurons. In contrast, another study demonstrated the inhibition of COX2 contributes to decreased amplitudes of EPSPs, which is reversed with PGE2 exposure, suggesting PGE2 is involved in the regulation of hippocampal membrane exictability and synaptic tranmission (Sang *et al.*, 2005). The changes in EPSPs observed due to abnormal PGE2 levels may be linked to improper dendritic formation, as this has known to highly impact synaptic transmission (Markram *et al.*, 1997). Overall, we aim to further investigate the effects of prenatal PGE2 exposure on dendritic morphology during hippocampal development.

CHAPTER 2: OBJECTIVES AND HYPOTHESIS

2.1 Overall Objectives and Hypotheses

The overall objective of this study is to investigate the morphological and molecular consequences of abnormal prenatal COX2/PGE2 signalling on hippocampal development and whether these changes are sex specific. As previously mentioned, our lab determined that changes in PGE2 levels (COX2 knock-in and PGE2-exposed mice) impacts dendritic arborization, looping, spine density, morphology and proteins critical for cytoskeletal architecture in the cerebellum. However, the implications of prenatal PGE2 exposure have not been investigated in the hippocampus. Specifically, in this study I will quantify how *in-utero* PGE2-exposure contributes to changes in hippocampal dendritic morphology and expression of proteins crucial for hippocampal function in offspring at critical postnatal stages.

Based on previous literature and research in our lab **I hypothesize** that maternal exposure to PGE2 during pregnancy: 1) contributes to sex-dependent changes in dendritic morphology in the developing hippocampus and 2) will result in a downregulation of proteins critical for cytoskeletal architecture and hippocampal function.

2.2 Experimental Model

My hypothesis will be tested using the *in-vivo* mouse model, PGE2-exposed offspring at PN30 and PN90 (postnatal day 30 and 90). Pregnant C57BL/6 females were injected with a single subcutaneous injection of 0.25µg/g 16, 16 dimethyl prostaglandin E2 (dmPGE2; Cayman Chemical) on G11, a stable analogue of PGE2, diluted in saline to a final volume of 200µL. Although dmPGE2 is an analogue of PGE2, it is metabolized at a decreased rate compared to PGE2, thus, remaining active for a longer period of time (Steffenrud, 1980; Ohno *et al.*, 1985).

Control animals were injected with 200µL of saline. Injections were performed on G11, as it marks the beginning of neurogenesis (Semple *et al.*, 2013). In the mouse, neurogenesis occurs between G11 and G17 in various brain regions (Rodier, 1980; Takahashi *et al.*, 1995; Clancy *et al.*, 2007). Additionally, this time interval is when pregnant females were administered the drug misoprostol to terminate pregnancies, which resulted in detrimental effects, such as Moebius syndrome and autism (Pastuszak *et al.*, 1998; Bandim *et al.*, 2003).

2.3 Aim 1: Investigating hippocampal dendritic morphology at PN30 and PN90

2.3.1 Rational

As previously mentioned, our lab has provided evidence that COX2-deficient (COX2-KI) and prenatally PGE2-exposed mice offpsring have abnormal cerebellar dendritic morphology and associated motor deficits (Kissoondoyal *et al.*, 2021; Kissondoyal *et al.*, Unpublished). This study will investigate the effect of maternal PGE2 exposure on the developing hippocampus in males and females at postnatal stages.

2.3.2 Objectives and Hypothesis

The first aim of this study is to examine the effects of prenatal exposure to PGE2 during a critical timepoint in neurodevelopment at gestation day 11 (G11), which marks the onset of neurogenesis, on dendritic morphology at PN30 and PN90. Based on previous literature and research in our lab **I hypothesize** that maternal exposure to PGE2 during pregnancy will contribute to sex-dependent changes in dendritic morphology. Based on our previous study on the cerebellum of PGE2-exposed mice (Kissondoyal *et al.*, Unpublished)., I specifically hypothesize there will be an increase in dendritic arborization.

2.3.3 Methodology

Whole brain samples of mice offspring exposed to saline and PGE2 at G11 were extracted on PN30 and PN90 from males and females for Golgi-Cox staining, a technique used to specifically stain neurons and examine dendritic morphology as described previously (Zaqout & Kaindl, 2016; Kissoondoyal *et al.*, 2021). The brain was sliced at 100 µm thickness to allow visualization of dendritic morphology. Following staining, confocal microscopy was conducted to image the hippocampus.

Images of the whole hippocampus were taken at 20X on the confocal microscope and were used to examine *dendritic arborization, primary branch length, branch order, the cross-sectional area of the neuronal soma and dendritic looping* using the open-source software, ImageJ and the plugin simple neurite tracer (SNT). Individual images of the neuron were taken at 100X on the confocal microscope to examine dendritic spine morphology. The NIS-Elements Artificial Intelligence software system was used to quantify dendritic *spine morphologies*, such as thin, stubby, and mushroom shaped spines. The dendritic spines measurements were obtained and classified using the Nikon NsAi software (Nikon).

2.4 Aim 2: Investigating the expression of proteins critical for hippocampal function

2.4.1 Rational

Previously, our lab has demonstrated that abnormal dendritic morphology in the cerebellum due to changes in PGE2 levels *in vivo* (COX2-KI and PGE2-exposed) is associated with differential expression of, β-actin, a protein critical for cytoskeletal architecture and spinophilin (SPN), a protein highly enriched in dendritic spines (Kissoondoyal *et al.*, 2021; Kissondoyal *et al.*, Unpublished). Additionally, our lab has previously provided evidence that genes associated with glutamate signaling and synaptic plasticity are impacted in COX2-KI mice

in early embryonic stages (Rai-Bhogal, Ahmad, *et al.*, 2018a). Specifically, ASD-risk genes known to be involved in synaptic transmission such as GRM5 (receptor involved in glutamate signaling) and GRIA2 (receptor involved in long-term potentiation) were impacted in the COX2-KI model in early embryonic stages. In addition, non-ASD risk genes which are also involved in synaptic transmission such as calmodulin-kinase 2b (CAMK2b), a downstream enzyme involved in long-term potentiation, was also impacted (Rai-Bhogal, Ahmad, *et al.*, 2018a). Based on previous research and our lab's studies, we selected four candidate proteins which are critical for memory consolidation in the hippocampus and have known to be dysregulated in neurodevelopmental disorder, SPN, β-actin, NMDA (N-methyl-D-aspartate or GluN2A subunit) and AMPA (Alpha-amino-3-hydroxy-5-methyl-4-isoxazole propionic acid or GluR1) receptors (Lee *et al.*, 2003; Lujan *et al.*, 2012; Anna *et al.*, 2016; Cercato *et al.*, 2016; Danesi *et al.*, 2019)

2.4.2 Objectives and Hypothesis

The second aim of my study is to investigate the effects of prenatal PGE2 exposure on the expression of proteins involved in dendritic morphology and hippocampal function in the mature brain at PN90. Based on previous literature and research in our lab **I hypothesize** that maternal exposure to PGE2 during pregnancy will contribute to sex-dependent changes in the expression of proteins at PN90. Specifically, based on previous studies investigating PGE2-exposure on cerebellar proteins, I hypothesize PGE2 exposure will contribute to a downregulation in proteins involved in cytoskeletal architecture in a sex-dependent manner.

2.4.3 Methodology

Hippocampal tissue was extracted from saline and PGE2 exposed mice on PN90. Following homogenization of the tissue, protein was isolated from three saline and PGE2-exposed male and female mice from three individual litters and pooled for western blot analysis.

To examine protein expression the following proteins were probed, spinophilin, beta-actin, GluN2A (component of the NMDA receptor) and GluR1 (component of the AMPA receptor).

CHAPTER 3: METHODOLOGY

3.1 Animals

Male and female C57BL/6 mice (Jackson Laboratories) were housed at the York University animal facility. Male and female C57BL/6 mice were housed together overnight for breeding and the females were checked for the presence of a vaginal plug each morning. The day a vaginal plug was observed in a female was designated as gestational day 0 (G0). Following G0, females were housed separately from their male counterpart for the remainder of the pregnancy. On G11, females were injected with a single subcutaneous injection of 0.25µg/g 16, 16 dimethyl prostaglandin E2 (dmPGE2; Cayman Chemical), a stable analogue of PGE2, diluted in saline to a final volume of 200µL (PGE2-exposed) (Wong *et al.*, 2015; Kissoondoyal et al., Unpublished). dmPGE2 is metabolized at a slower rate compared to PGE2, thus, remaining active for a longer period of time (Steffenrud, 1980; Ohno *et al.*, 1985). Control animals were injected with 200µL of saline (saline-exposed). Subcutaneous injections were performed on G11, which is the start neurogenesis in mice (Semple *et al.*, 2013). In the mouse, neurogenesis occurs between G11 and G17 in various brain regions (Rodier, 1980; Takahashi *et al.*, 1995; Clancy *et al.*, 2007). Furthermore, studies have shown that this critical time window is when pregnant females administered the drug misoprostol to terminate pregnancies, which resulted in detrimental effects, including Moebius syndrome and autism (Pastuszak *et al.*, 1998; Bandim *et al.*, 2003). All experiments and protocols performed in accordance with the ethical guidelines of York University's Animal Care Committee and was approved by the Research Ethics Board of York University.

3.2 Golgi-Cox Staining

The whole brain was extracted from 3 litter-matched males and females from 3 separate litters from PGE2-exposed and saline-exposed C57BL/6 mice at PN30 and PN90. A total of 12 animals were used. Golgi-Cox staining was performed using previously established protocols (Zaqout & Kaindl, 2016). Following the extraction, the brain was bisected, washed in 1X PBS solution, and transferred to a 4% paraformaldehyde (PFA) solution for 24 hours for fixation. Subsequently, the fixed brain samples were washed in double-distilled (dd)-H20 and transferred to the Golgi-Cox solution. After 24 hours, each brain tissue sample was replaced with fresh Golgi-Cox solution and kept in the dark at room temperature up to 7-10 days. The Golgi-Cox solution was prepared by dissolving potassium dichromate, mercuric chloride and potassium chloride in ddH20, with a 5% weight-to-volume ratio (w/v). After impregnation with the Golgi-Cox solution was complete, the brain samples were transferred to a tissue protectant solution in the dark at 4°C. After 24 hours, each brain tissue sample was transferred to fresh tissue protectant solution and stored for an additional 7 days in the dark at 4°C. The tissue protectant solution was prepared by dissolving 30% w/v sucrose, 20% w/v ethylene glycol, and 1% polyvinylpyrrolidone in ddH20.

The brain samples were sliced along the sagittal plane, 100µm in thickness using cryostat sectioning by the research histology lab located at the University Health Network (Toronto, Ontario; www.uhnresearch.ca). The brain slices were mounted onto gelatin coated slides and the staining was developed using a 3:1 ammonia to H20 solution, followed by 5% w/v sodium thiosulfate in H20. Subsequently, serial dehydration of the slices was conducted using 70%, 95% and 100% ethanol, followed by immersion in xylene and sealed with a cover-slip.

3.3 Confocal Microscopy

The hippocampal Golgi-Cox-stained slides were imaged on the Carl Zeiss Observer Spinning Disk confocal microscope (LMS 700; Advanced Light and Electron Microscopy, York University), using brightfield microscopy. The entire hippocampus of each animal was imaged at 20X magnification, z-stacked every 1-3 µm (50-150 stacks on average). An individual dendrite projecting from the neuronal soma located in the hippocampus was imaged at 100X magnification using oil immersion and z-stacked every 0.1-0.3 µm (500-1000 stacks on average).

3.4 Image Analysis

3.4.1 Analysis of Dendritic Arborization, length, branch order, soma area and looping

Image analysis was completed using the open-source software Fiji Image J and the images were blinded for analysis. For the images of the whole hippocampus obtained at 20X, 5 neuronal cells were quantified per animal, for a total of N=60 cells (N=15 per condition). The Simple Neurite Tracer (SNT) plugin on Fiji Image J was used for sholl analysis (Longair *et al.*, 2011; Schindelin *et al.*, 2012; Rueden *et al.*, 2017). The SNT plugin produces concentric circles every 20µm starting at the center of the neuronal soma. The number of intersections were measured at each of the circles that were generated. The average primary dendrite length and the branch order was obtained from the dendritic arbours that were defined using SNT. The cross-sectional area of the cells was obtained using the area tool on ImageJ to outline and compute the area of the neuronal soma. Quantification of dendritic looping was performed using established guidelines (Kissoondoyal & Crawford, 2021; Kissoondoyal *et al.*, 2021). The greatest turning angle of each dendrite was quantified using the traced dendrites from SNT. Specifically, dendrites with a maximum turning angle greater than 270° was classified as a loop (Kissoondoyal & Crawford, 2021).

3.4.2 Dendritic Spine Analysis

Individual images of the neuron taken at 100X were used to quantify dendritic spine morphology and spine density. Images were blinded during analysis. The dendritic spines measurements were obtained and classified using the Nikon NsAi software (Nikon). The SegmentAI software was trained using a representative image set and a training loss of 0.02 was designated as the cut-off for indication of successful training. DenoiseAI and high contrast settings were used to reduce background detection. Following the detection of dendritic spines using SegmentAI, false positives were filtered from the data set by length (>0.2 µm), width(>0.2 µm), circularity(<0.88 µm) measurements. Dendritic spine classification was conducted using previously established guidelines (Risher *et al.*, 2014; Kissoondoyal *et al.*, 2021). Dendritic spines with a length > 1.4 µm were first classified as thin. Subsequently, in the remaining pool of dendritic spines, those with a width > length were classified as stubby, and the remaining were classified as mushroom shaped. Thin and stubby shaped spines were classified as immature and mushroom shaped spines were classified as mature spines for statistical analyses. Dendritic spine density was determined as the number of spines per length of the dendrite.

3.5 Protein Isolation and Western Blotting

Hippocampal tissue was collected at PN90 from saline-exposed and PGE2-exposed mice. Protein isolation was performed using the 10X lysis buffer RIPA (abcam, ab156034). The 10X RIPA was diluted to 1X using ddH20 and the protease inhibitor cocktail (abcam, ab271306) was added at a 1:100 dilution prior to homogenization. The hippocampal tissue was homogenized using the polytron power homogenizer using the 1X RIPA and transferred to the shaker at 4°C for 2 hours. Following agitation, the homogenized tissue was centrifuged for 20 minutes at 12, 000 rpm at 4°C. The supernatant was aspirated into a fresh microfuge tube and the pellet was

discarded. Protein concentrations were determined using the Pierce BCA protein assay kit (thermofisher, PI23225), where a concentration of 1-5mg/ml was optimal. Protein samples were pooled from saline and PGE2-exposed males and females. For each sample 10 μg was loaded onto a 10% SDS-PAGE gel. Protein samples were separated using PAGE electrophoresis in 1X running buffer (BioRad, 1610772EDU) and transferred to a 0.2μM nitrocellulose membrane (BioRad, 1620112) in cold transfer buffer (BioRad, 1610771EDU). Following the transfer, membranes were washed using 1X TBS (Tris buffer saline; 24g Tris Base, 88g NaCl dissolved in 900mL ddH20 and pH adjusted to 7.6) four times for 5 minutes. The membranes were then blocked using 5% milk in 1X TBS-T (Tris buffer saline 0.01% tween 20) for 1 hour at room temperature. Protein samples were probed using the following primary antibodies diluted in 5% milk in TBS-T, rabbit polyclonal anti-spinophilin (abcam, 1:1000, ab1856, Cambridge, MA, USA), mouse monoclonal anti-beta actin (abcam, 1:10,000, ab6276, Cambridge, MA, USA), mouse monoclonal anti-NMDA2A (abcam, 1:2500, ab133265, Cambridge, MA, USA), rabbit-monoclonal anti-GluR1 (abcam, 1:2500, ab183797, Cambridge, MA, USA) and mouse monoclonal anti-GAPDH (Abcam; 1:10,000, ab8245, Cambridge, MA, USA) overnight at 4°C. After incubation with the primary antibody, the membranes were washed four times for 5 minutes using 1X TBS-T. Following the washes, the membranes were probed using the following HRP-tagged secondary antibodies diluted in 5% milk diluted in TBS-T, goat-anti-rabbit (Abcam, 1:10000, ab6721, Cambridge, MA, USA), and Goat-anti-mouse (Abcam, 1:10000, ab6789, Cambridge, MA, USA) for 1 hour at room temperature. The membranes were washed four times for 5 minutes with TBS-T. The probed membranes were imaged using the ChemiDoc XRS+ System (Biorad). Protein signal intensity was quantified using ImageJ and normalized to GAPDH signal intensity. Following this, fold change of protein expression was

determined relative to the protein in saline-exposed males (protein expression in saline males = 1).

3.6 Statistics

All image analyses and data collection were conducted blinded to the condition and subsequently, unblinded for statistical analyses. The open-source software R was used for all statistical analyses. Dendritic arborization, length, branch order and cell soma size were analyzed using linear mixed effect modeling, which takes interactions and confounding variables into consideration (Bates *et al.*, 2015). Variables of interest were assigned as the main effect, which includes dendritic arborization, length, branch order and cross-sectional area of the neuronal soma. Confounding variables were assigned as random effects, which includes litter or technical replicate. The model of *best- fit* was identified using Akaike Information criteria (AIC) values. Following determination of the model of best fit, pairwise comparisons were performed. Specifically, t-tests were conducted using Satterwaite's adjustment. Categorial data, which includes the likelihood of dendritic loops and dendritic spine morphologies were analyzed using binomial logistical regression with the data presented as odds ratios (95% confidence intervals), where an odds ratio greater than 1 indicates an increased odds of observing the phenomenon and vice versa (Croissant, 2020). All measurements were obtained from males and females from three separate litters. Sample size was calculated using G*Power 3 software and an effect size of 0.3 was used (Faul *et al.*, 2007). $*p<0.05$, $**p<0.01$, $***p<0.001$ was considered statistically significant.

CHAPTER 4: RESULTS

4.1 Dendritic Arborization

Sholl analysis using ImageJ and the simple neurite tracer plugin was conducted to examine the extent of dendritic branching in the hippocampus at PN30 and PN90, where concentric circles were drawn every 20 μm from the centre of the cell soma. **(Figure 6A).** Previously our lab has found an increase in dendritic arborization closer to the cell soma in the cerebellum of COX2-KI and PGE2-exposed mice (Kissoondoyal *et al.*, 2021; Kissondoyal *et al.*, Unpublished). In this study, we investigated the effect of prenatal PGE2-exposure on dendritic arborization in the hippocampus of offspring at PN30 and PN90 offspring using linear mixed effects modeling. Based on the *model of best-fit*, we examined the fixed effects of condition, sex, stage and distance from the centre of the soma, as well as their interactions. Litter was assigned as a random an effect to detect litter bias. There was no significant interaction between condition, sex, distance ($t(1430) = -0.82$, $p = 0.410$) and condition, stage, distance ($t(1430) = 0.130$, $p = 0.900$). However, there was a significant effect in the interaction between condition, sex, stage and distance ($t(1430) = 2.98$, $p = 0.000$). Thus, we further conducted pair-wise comparisons at each distance between saline- and PGE2-exposed male and female offspring at PN30 and PN90.

4.1.1 Postnatal Day 30

Sex Differences in the Healthy Brain

First, we examined whether there are sex-differences in dendritic arborization within the healthy controls by comparing saline females (WTF) and saline males (WTM) offspring at PN30 every 20 μm from 0 μm to 240 μm **(Figure 6B, Table 1).** Saline females (WTF) had significantly greater dendritic arborization compared to saline males (WTM) at 40 μm ($t(1430) = -2.023$, $p = 0.043$, WTM = 4.200, WTF = 5.600), 60 μm ($t(1430) = -2.458$, $p = 0.014$, WTM =

1.900, WTF = 3.600) and 100 μm (t(1430) = -2.168, p = 0.0302, WTM = 0.700, WTF = 2.200). There were no significant difference in dendritic arborization between saline females and saline males at 0 μm (t(1430) = 0, p = 1.000, WTM = 0, WTF = 0), 20 μm (t(1430) = 1.157, p = 0.247, WTM = 6.200, WTF = 5.400), 80 μm (t(1430) = -1.590, p = 0.112, WTM = 1.7, WTF = 2.8), 120 μm (t(1430) = -1.301, p = 0.193, WTM = 0.7, WTF = 1.6), 140 μm (t(1430) = -0.578, p = 0.563, WTM = 0.400, WTF = 0.800), 160 μm (t(1430) = -0.144, p = 0.885, WTM = 0.400, WTF = 0.500), 180 μm (t(1430) = -0.433, p = 0.665, WTM = 0.000, WTF = 0.300), 200 μm (t(1430) = -0.433, p = 0.665, WTM = 0.400, WTF = 0.800), 220 μm (t(1430) = -0.289, p = 0.773, WTM = 0.000, WTF = 0.200) and 240 μm (t(1430) = 0.000, p = 1.000, WTM = 0.000, WTF = 0.000).

Sex Differences in the PGE2-exposed Brain

Further, we also compared dendritic arborization between PGE2-exposed female (PGE2F) and male offspring (PGE2M) **(Figure 6B, Table 1)**. Similarly to the saline offspring, we found PGE2F had significantly greater dendritic arborization at 40 μm (t(1430) = -2.243, p = 0.025, PGE2M = 5.000, PGE2F = 6.267), 60 μm (t(1430) = -4.485, p < 0.001, PGE2M = 3.600, PGE2F = 6.133), 80 μm (t(1430) = -3.541, p = 0.004, PGE2M = 3.333, PGE2F = 5.333) and 100 μm (t(1430) = -2.832, p = 0.005, PGE2M = 2.867, PGE2F = 4.467). However, there were no significant differences between PGE2M and PGE2F at 0 μm (t(1430) = 0.000, p = 1.000, PGE2M = 0.000, PGE2F = 0.000), 20 μm t(1430) = -0.708, p = 0.479, PGE2M = 6.467, PGE2F = 6.133), 120 μm (t(1430) = -1.652, p = 0.099, PGE2M = 2.067, PGE2F = 3.000), 140 μm (t(1430) = 0.118, p = 0.906, PGE2M = 1.730, PGE2F = 1.670), 160 μm (t(1430) = 0.708, p = 0.479, PGE2M = 1.333, PGE2F = 0.933), 180 μm t(1430) = 0.708, p = 0.479, PGE2M = 1.000, PGE2F = 0.600), 200 μm (t(1430) = 0.236, p = 0.813, PGE2M = 0.533, PGE2F = 0.400), 220 μm (t(1430) = -0.354, p = 0.723, PGE2M = 0.000, PGE2F = 0.200), 240 μm (t(1430) = -0.118, p

= 0.906, PGE2M = 0.000, PGE2F = 0.200). Overall, at PN30 we observed sex differences in both healthy offspring (WTF vs WTM) and in PGE2-exposed offspring (PGE2F vs PGE2M) with females have increased arborization at the intermediate length, between 40 μm to 100 μm.

PGE2-exposure in Males

Furthermore, we also examined the effect of PGE2 exposure on neuronal arborization within male and female offspring **(Figure 6B, Table 1)**. In males, we found that PGE2 exposure increased dendritic arborization compared to saline males at 60 μm ($t(1430) = -2.266$, $p = 0.024$, WTM = 1.900, PGE2M = 3.600), 80 μm ($t(1430) = -2.165$, $p = 0.031$, WTM = 1.700, PGE2M = 3.333), and 100 μm ($t(1430) = -2.974$, $p = 0.003$, WTM = 0.700, PGE2M = 2.87). However, there were no significant difference in dendritic arborization between PGE2 males (PGE2M) and saline males (WTM) at 0 μm ($t(1430) = 0.000$, $p = 1.000$, WTM = 0.000, PGE2M = 0.000), 20 μm ($t(1430) = -0.0911$, $p = 0.927$, WTM = 6.200, PGE2M = 6.467), 40 μm ($t(1430) = -0.900$, $p = 0.369$, WTM = 4.200, PGE2M = 5.000), 120 μm ($t(1430) = -1.760$, $p = 0.0792$, WTM = 0.700, PGE2M = 2.067), 140 μm ($t(1430) = -1.709$, $p = 0.088$, WTM = 0.400, PGE2M = 1.733), 160 μm ($t(1430) = -1.102$, $p = 0.270$, WTM = 0.400, PGE2M = 1.333), 180 μm ($t(1430) = -1.052$, $p = 0.29353$, WTM = 0.100, PGE2M = 1.00), 200 μm ($t(1430) = -0.495$, $p = 0.620$, WTM = 0.000, PGE2M = 0.533), 220 μm ($t(1430) = 0.00$, $p = 1.00$, WTM = 0.000, PGE2M = 0.000) and 240 μm ($t(1430) = 0.00$, $p = 1.00$, WTM = 0.000, PGE2M = 0.000).

PGE2-exposure in Females

The effect of PGE2-exposure on females had a similar effect as PGE2-exposed males **(Figure 6B, Table 1)**. PGE2 females have increased dendritic arborization at 60 μm ($t(1430) = -3.530$, $p = 0.005$, WTF = 3.600, PGE2F = 6.13), 80 μm ($t(1430) = -3.530$, $p < 0.001$, WTF = 2.800, PGE2F = 5.333) and 100 μm ($t(1430) = -3.125$, $p = 0.002$, WTF = 2.200, PGE2F =

4.467). However, there were no significant differences in dendritic arborization between PGE2 females (PGE2F) and saline females (WTF) at 0 μm (t(1430) = 0.000, p = 1.000, WTM = 0.000, PGE2F = 0.000), 20 μm (t(1430) = 0.000, p = 1.000, WTF = 0.000, PGE2F = 0.000), 40 μm (t(1430) = -0.698, p = 0.369, WTF = 5.600, PGE2F = 6.267), 120 μm (t(1430) = -1.810, p = 0.071, WTF = 1.600, PGE2F = 3.000), 140 μm (t(1430) = -1.001, p = 0.317, WTF = 0.800, PGE2F = 1.667), 160 μm (t(1430) = -0.343 p = 0.731, WTF = 0.500 PGE2F = 0.933), 180 μm (t(1430) = 0.010, p = 0.992, WTF = 0.400, PGE2F = 0.600), 200 μm (t(1430) = 0.161, p = 0.872, WTF = 0.300, PGE2F = 0.400), 220 μm (t(1430) = 0.313, p = 0.754, WTF = 0.200, PGE2F = 0.200) and 240 μm (t(1430) = 0.212, p = 0.832, WTF = 0.000, PGE2F = 0.067). Overall, at PN30 both PGE2 males and females had increased dendritic arborization between 60 μm and 100 μm compared to the saline counterparts.

4.1.2 Postnatal Day 90

Sex Differences in the Healthy Brain

We also examined whether there are sex-differences in dendritic arborization within the healthy controls by comparing saline females (WTF) and saline males (WTM) offspring at PN90 every 20 μm from 0 μm to 240 μm **(Figure 6B, Table 1)**. WTF have significantly increased dendritic arborization compared to WTM at 20 μm (t(1430) = 7.790, p < 0.001, WTM = 6.600, WTF = 11.000) and 40 μm (t(1430) = -2.950, p = 0.003, WTM = 1.800, WTF = 3.460). However, there were no significant difference in dendritic arborization between saline females (WTF) and saline males (WTM) at 0 μm (t(1430) = 0.000, p = 1.000, PGE2M = 0.000, PGE2F = 0.000), 60 μm (t(1430) = -0.944, p = 0.345, WTM = 0.467, WTF = 1.000), 80 μm (t(1430) = -0.437, p = 0.662, WTM = 0.200, WTF = 0.267), 100 μm (t(1430) = 0.118, p = 0.906, WTM = 0.200, WTF = 0.133), 120 μm (t(1430) = -1.653, p = 0.193, WTM = 0.133, WTF = 0.067), 140

μm t(1430) = -0.118, p = 0.906, WTM = 0.000, WTF = 0.067), 160 μm, 180 μm, 200 μm, 220 μm and 240 μm (t(1430) = 0.000, p = 1.000, WTM = 0.000, WTF = 0.000).

Sex Differences in the PGE2-exposed Brain

Additionally, we also examined sex differences in dendritic arborization in PGE2-exposed offspring **(Figure 6B, Table 1)**. PGE2F have significantly decreased arborization compared to PGE2M at 20 μm (t(1430) = -0.590, p = 0.555, PGE2M = 7.867, PGE2F = 3.467) only. There was no significant difference in dendritic arborization between PGE2F and PGE2M at 0 μm (t(1430) = 0.000, p = 1.000, PGE2M = 0.000, PGE2F = 0.000), 40 μm (t(1430) = -1.587, p = 0.128, PGE2M = 1.400, PGE2F = 0.467), 60 μm t(1430) = -0.590, p = 0.555, PGE2M = 0.467, PGE2F = 0.133), 80 μm (t(1430) = 0.472, p = 0.637, PGE2M = 0.333, PGE2F = 0.067), 100 μm, 120 μm, 140 μm, 160 μm, 180 μm, 200 μm, 220 μm and 240 μm (t(1430) = 0.000, p = 1.000, PGE2M = 0.000, PGE2F = 0.000). Overall, we observe contrasting sex differences, specifically we observed an increase in dendritic arborization in saline females compared to saline males (20-40 μm), however PGE2 females had a decrease in arborization compared to PGE2 males closer to the cell soma (20 μm).

PGE2-exposure in Males

We further examined the effect of PGE2 exposure on dendritic arborization in males and females **(Figure 6B, Table 1)**. We observed that PGE2M had significantly greater dendritic arborization at 20 μm (t(1430) = 0.000, p = 1.000, WTM = 6.600, PGE2M = 7.860). However, PGE2M did not have significantly different levels of dendritic arborization compared to WTM at 0 μm (t(1430) = 0.000, p = 1.000, WTM = 0.000, PGE2M = 0.000), 40 μm (t(1430) = 0.4628, p = 0.643, WTM = 1.800, PGE2M = 1.400), 60 μm (t(1430) = -0.212, p = 0.832, WTM = 0.467, PGE2M = 0.467), 80 μm (t(1430) = -0.437, p = 0.662, WTM = 0.200, PGE2M = 0.333), 100 μm

(t(1430) = 0.125, p = 0.900, WTM = 0.200, PGE2M = 0.000), 120 μm (t(1430) = 0.012, p = 0.990, WTM = 0.133, PGE2M = 0.000), 140 μm, 160 μm, 180 μm, 200 μm, 220 μm and 240 μm (t(1430) = 0.000, p = 1.000, WTM = 0.000, PGE2M = 0.000).

PGE2-exposure in Females

We observed the opposite effect in dendritic arborization due to PGE2 exposure in PN90 females **(Figure 6B, Table 1)**. PGE2F have significantly decreased dendritic arborization compared to WTF at 20 μm (t(1430) = 2.501, p <0.001, WTF = 11.000, PGE2F = 3.467) and 40 μm (t(1430) = 4.738, p < 0.001, WTF = 3.467, PGE2F = 0.467). Dendritic arborization did not significantly differ between PGE2F and WTF at 0 μm (t(1430) = 0.000, p = 1.000, WTF = 0.000, PGE2F = 0.000), 60 μm (t(1430) = -1.250, p = 0.212, WTF = 1.000, PGE2F = 0.133), 80 μm (t(1430) = 0.125, p = 0.900, WTF = 0.267, PGE2F = 0.067), 100 μm (t(1430) = 0.012, p = 0.990, WTF = 0.133, PGE2F = 0.000), 120 μm (t(1430) = -0.099, p = 0.921, WTF = 0.067, PGE2F = 0.000), 140 μm (t(1430) = -0.095, p = 0.924, WTF = 0.067, PGE2F = 0.000), 160 μm, 180 μm, 200 μm, 220 μm and 240 μm (t(1430) = 0.000, p = 1.000, WTF = 0.000, PGE2F = 0.000). Ultimately, we observe that PGE2-exposure has opposite effects on males and females, PGE2-exposed males have increased arborization and PGE2-exposed females have decreased arborization closer to the cell soma (20 μm) compared to their counterparts.

4.1.3 Over Development

Saline-exposed Males and Females

Furthermore, we examined the effect of developmental stage on dendritic arborization by comparing PN30 and PN90 offspring within each condition (WTF, WTM, PGE2F and PGE2M) every 20 μm from 0 μm to 240 μm **(Figure 6B, Table 2).** PN90 WTM have significantly lower dendritic arborization compared to PN30 WTM at 40 μm (t(1430) = 4.265, p < 0.001,

PN30WTM = 4.200, PN90WTM = 1.800), 60 μm (t(1430) = 2.756, p = 0.006, PN30 WTM = 1.900, PN90 WTM = 0.467) and 80 μm (t(1430) = 2.860, p = 0.004, PN30 WTM = 1.700, PN90 WTM = 0.200). However, dendritic arborization was not significantly different between PN30 WTM and PN90 WTM at 0 μm (t(1430) = 0.000, p =1.000, PN30 WTM = 0.000, PN90 WTM = 0.000), 20 μm (t(1430) = -0.106, p = 0.916, PN30 WTM = 6.200, PN90 WTM = 6.600), 100 μm (t(1430) = 1.299, p = 0.194, PN30 WTM = 0.700, PN90 WTM = 0.200), 120 μm (t(1430) = 1.403, p =0.161, PN30 WTM = 0.700, PN90 WTM = 0.133), 140 μm (t(1430) = 1.143, p = 0.253, PN30 WTM = 0.400, PN90 WTM = 0.000), 160 μm (t(1430) = 1.143, p = 0.253, PN30 WTM = 0.400, PN90 WTM = 0.000), 180 μm (t(1430) = 0.674, p = 0.500, P30WTM = 0.100, P90WTM = 0.000), 200 μm, 220 μm and 240 μm (t(1430) = 0.000, p =1.000, PN30 WTM = 0.000, PN90 WTM = 0.000).

Further, we also examined the effect of developmental stage in saline-exposed females **(Figure 6B, Table 2)**. PN90 WTF had significantly increased dendritic arborization at 20 μm (t(1430) = 8.222, p < 0.001, PN30 WTF = 5.400, PN90 WTF = 11.000) and significantly reduced dendritic arborization 40 μm (t(1430) = 3.859, p < 0.001, PN30 WTF = 5.600, PN90 WTF = 3.460), 60 μm (t(1430) = 4.577, p < 0.001, PN30 WTF = 3.600, PN90 WTF = 1.000), 80 μm (t(1430) = 4.472, p < 0.001, PN30 WTF = 2.800, PN90 WTF = 0.260), 100 μm (t(1430) = 3.744, p < 0.001, PN30 WTF = 2.200, PN90 WTF = 0.133) and 120 μm (t(1430) = 2.912, p = 0.004, PN30 WTF = 1.600, PN90 WTF = 0.067). However, PN90 WTF did not significantly differ in dendritic arborization from PN30 WTF at 0 μm (t(1430) = 0.000, p = 1.000, PN30 WTF = 0.000, PN90 WTF = 0.000), 140 μm (t(1430) = 1.663, p = 0.096, PN30 WTF = 0.800, PN90 WTF = 0.067), 160 μm (t(1430) = 1.299, p = 0.194, PN30 WTF = 0.500, PN90 WTF = 0.000), 180 μm (t(1430) = 1.143, p = 0.253, PN30 WTF = 0.400, PN90 WTF = 0.000), 200 μm (t(1430)

= 0.987, p = 0.323, PN30 WTF = 0.300, PN90 WTF = 0.000), 220 μm (t(1430) = 0.831, p = 0.406, PN30 WTF = 0.200, PN90 WTF = 0.000) and 240 μm (t(1430) = 0.000, p = 1.00, PN30 WTF = 0.000, PN90 WTF = 0.000). In the healthy brain, we observe a decrease in dendritic arborization in in PN90 males and females at an intermediate distance (40-80 μm) from the cell soma over development, however in females only, we also observe an increase arborization closer to the cell soma (20 μm).

PGE2-exposed Males and Females

We also examined the effect of developmental stage on dendritic arborization in PGE2-exposed males and females **(Figure 6B, Table 2)**. In PGE2-exposed males, the later developmental stage, PN90 significantly affected dendritic arborization compared the earlier stage, PN30. PN90 PGE2M have significantly increased arborization at 20 μm (t(1430) = 8.222, p < 0.001, PN30 PGE2M = 6.470, PN90 PGE2M = 7.867) and decreased arborization at 40 μm (t(1430) = 6.374, p < 0.001, PN30 PGE2M = 5.000, PN90 PGE2M = 1.400), 60 μm (t(1430) = 4.577, p < 0.001, PN30 PGE2M = 3.600, PN90 PGE2M = 0.467), 80 μm (t(1430) = 4.472, p < 0.001, PN30 PGE2M = 3.333, PN90 PGE2M = 0.333), 100 μm (t(1430) = 3.744, p < 0.001, PN30 PGE2M = 2.867, PN90 PGE2M = 0.000), 120 μm (t(1430) = 2.912, p < 0.001, PN30 PGE2M = 2.067, PN90 PGE2M = 0.000), 140 μm (t(1430) = 3.068, p = 0.002, PN30 PGE2M = 1.733, PN90 PGE2M = 0.000), 160 μm (t(1430) = 1.299, p = 0.194, PN30 PGE2M = 1.333, PN90 PGE2M = 0.000). However, there is no significant difference between PN90 and PN30 PGE2 males at 0 μm (t(1430) = 0.000, p = 1.000, PN30 PGE2M = 0.000, PN90 PGE2M = 0.000), 180 μm (t(1430) = 1.700, p = 0.077, PN30 PGE2M = 1.000, PN90 PGE2M = 0.000), 200 μm (t(1430) = 0.987, p = 0.324, PN30 PGE2M = 0.533, PN90 PGE2M = 0.000), 220 μm and 240 μm (t(1430) = 0.000, p = 1.000, PN30 PGE2M = 0.000, PN90 PGE2M = 0.000).

In contrast, in females we observe that PN90 PGE2F have significantly lower dendritic arborization than PN30 PGE2F at 20 μm ($t(1430) = 6.012$, $p < 0.001$, PN30 PGE2F = 6.867, PN90 PGE2F = 3.467), 40 μm $t(1430) = 10.053$, $p < 0.001$, PN30 PGE2F = 6.267, PN90 PGE2F = 0.467), 60 μm ($t(1430) = 10.623$, $p < 0.001$, PN30 PGE2F = 6.133, PN90 PGE2F = 0.133), 80 μm ($t(1430) = 9.325$, $p < 0.001$, PN30 PGE2F = 5.333, PN90 PGE2F = 0.067), 100 μm ($t(1430) = 7.908$, $p < 0.001$, PN30 PGE2F = 4.467, PN90 PGE2F = 0.000), 120 μm ($t(1430) = 5.311$, $p < 0.001$, PN30 PGE2F = 3.00, PN90 PGE2F = 0.000) and 140 μm ($t(1430) = 3.00$, $p < 0.003$, PN30 PGE2F = 1.667, PN90 PGE2F = 0.000). However, there was no significant difference in dendritic arborization between P30 PGE2F and P90 PGE2F at 0 μm ($t(1430) = 0.000$, $p = 1.000$, PN30 PGE2F = 0.000, PN90 PGE2F = 0.000), 160 μm ($t(1430) = 1.652$, $p = 0.099$, PN30 PGE2F = 0.933, PN90 PGE2F = 0.000), 180 μm ($t(1430) = 1.062$, $p = 0.288$, PN30 PGE2F = 0.600, PN90 PGE2F = 0.000), 200 μm ($t(1430) = 0.708$, $p = 0.479$, PN30 PGE2F = 0.400, PN90 PGE2F = 0.000), 220 μm ($t(1430) = 0.354$, $p = 0.723$, PN30 PGE2F = 0.200, PN90 PGE2F = 0.000), 240 μm ($t(1430) = 0.118$, $p = 0.906$, PN30 PGE2F = 0.067, PN90 PGE2F = 0.000). Overall, in PGE2-exposed offspring, males at PN90 have increased arborization closer to the cell soma and decreased arborization farther away from the cell soma compared to PN30. However, in PN90 females have consistently low dendritic arborization closer to and farther away from the cell soma.

4.1.4 Summary

We examined 1) sex differences in the healthy and PGE2-exposed brain and 2) the effect of PGE2-exposure in males and female offspring on dendritic arborization at PN30 and PN90 **(Table 1 and 2)**. In early hippocampal development at PN30 saline-exposed females have increased dendritic arborization at an intermediate length from the cell soma compared to PN30

saline-exposed males (40 μm to 100 μm) **(Table 1)**. Similarly, PN30 PGE2-exposed females have increased arborization at an intermediate length compared to PN30 PGE2-exposed males (40 μm to 100 μm). In PGE2-exposed males and females at PN30, we observed increased dendritic arborization at an intermediate range (60 μm to 100 μm).

At PN90 we also observed clear sex differences in the healthy and PGE2-exposed brain. PN90 saline-exposed females had greater arborization closer to the cell soma compared to PN90 males (20 μm). In contrast, PGE2-exposed females had decreased arborization closer to the cell soma compared to PGE2-exposed males (20 μm). Furthermore, PN90 PGE2-exposed males have increased arborization closer to the cell soma (20 μm) compared to saline-exposed males. However, at PN90 PGE2-exposed females had decreased arborization closer to the cell soma (20 μm) compared to saline-exposed females.

Additionally, we also examined the developmental changes in dendritic arborization within each condition (WTM, WTF, PGE2M and PGE2F) **(Table 2)**. In saline-exposed males and females, there was a decrease in dendritic arborization at an intermediate distance (40-80 μm) from the cell soma, however, in females there was an increase in arborization closer to the cell soma (20 μm). Similarly, PN90 PGE2-exposed males had increased arborization closer to the soma and decreased arborization farther from the soma compared to PN30 PGE2-exposed males. However, PN90 PGE2 females have consistently low dendritic arborization closer to and farther away from the cell soma. Overall, we observe differences in dendritic arborization due to sex, PGE2-exposure, and developmental stage.

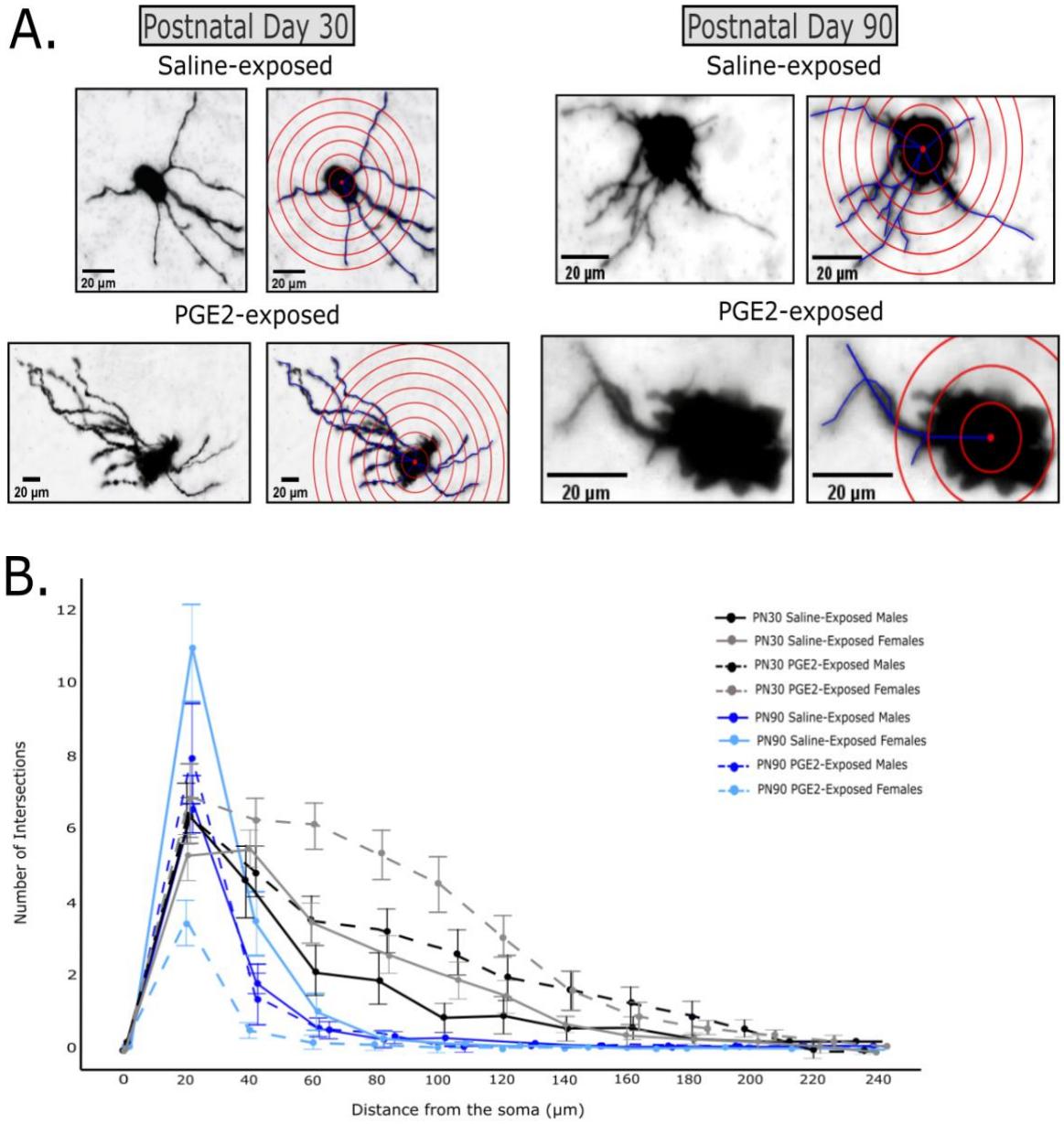

Figure 6. Sholl analysis of saline-exposed and PGE2-exposed offspring at PN30 and PN90. A) Quantification of dendritic arborization every 20 µm from the center of the cell soma. B) The number intersections measured every 20 µm. Data is presented as a mean ± SEM. n = 15 cells per condition from 3 different animals obtained from 3 separate litters.

Table 1: Summary of sex differences and PGE2-exposure on dendritic arborization from the center of the cell soma.

Dendritic arborization findings between 10 to 240 μm is shown. Sex differences in saline and PGE2 offspring are shown, where females are compared to males. The effect of PGE2-exposure is shown in males and females, where they are compared to their saline counterparts. The up and down arrows indicate an increase and decrease in arborization, respectively.

Distance from the cell soma (μm)	**Sex Differences at PN30** *(Compared to the male)*		**Sex Differences at PN90** *(Compared to the male)*		**PGE2-exposure at PN30** *(Compared to saline control)*		**PGE2-exposure at PN90** *(Compared to saline control)*	
	Saline Female	**PGE2 Female**	**Saline Female**	**PGE2 Female**	**PGE2 Male**	**PGE2 Female**	**PGE2 Male**	**PGE2 Female**
0	–	–	–	–	–	–		–
20	–	–	↑	↓	–	–	↑	↓
40	↑	↑	↑	–	–	–	–	↓
60	↑	↑	–	–	↑	↑	–	–
80	–	↑	–	–	↑	↑	–	–
100	↑	↑	–	–	↑	–	–	–
120-240	–	–	–	–	–	–	–	–

Table 2: Summary of the effect of developmental stage on dendritic arborization from the center of the cell soma.

Dendritic arborization findings between 0 to 240 μm is shown. The comparison between PN90 offspring to PN30 offspring is shown for each of the conditions, saline-exposed and PGE2-exposed males and females.

Distance from the cell soma (μm)	**Saline-exposed** *(Compared to PN30)*		**PGE2-exposed** *(Compared to PN30)*	
	PN90 Male	**PN90 Female**	**PN90 Male**	**PN90 Female**
0	–	–	–	–
20	–	↑	↑	↓
40	↓	↓	↓	↓
60	↓	↓	↓	↓
80	↓	↓	↓	↓
100	–	↓	↓	↓
120	–	↓	↓	↓
140	–	–	↓	↓
160	–	–	↓	–
180-240	–	–	–	–

4.2 Branch Order

Neuronal arborization, including the formation of primary, secondary, and tertiary branches, are highly involved in brain connectivity and synapse formation during neurodevelopment (Goikolea-Vives & Stolp, 2021). Morphogens and guidance cues in the brain during critical timepoints contribute to branch complexity (Lu *et al.*, 2013a; Kalil & Dent, 2014). These processes have known to be dysregulated in neurodevelopmental disorder (Goikolea-Vives & Stolp, 2021). We investigated the number of extensions per branch order of hippocampal neuronal cells in saline and PGE2-exposed males and females at PN30 and PN90. The longest neuronal extensions extending from the center of the cell soma was first classified as primary dendrites, the longest dendrites extending out from the primary dendrite was classified as secondary and any dendrites extending from the secondary dendrite was classified as tertiary **(Figure 7A)**. Branch order was fit using a linear mixed effects model, where litter was assigned as a random effect to account for litter-bias. Condition, sex, developmental stage, and branch order were assigned as fixed effects and the interaction between these factors were examined. There was no significant effect of the interaction between condition, sex, stage and branch order ($t(330) = -1.055$, $p = 0.292$). Additionally, there was no significant interaction between condition, sex and branch order ($t(330) = -0.495$, $p = 0.621$), as well as condition, stage and branch order ($t(330) = 1.368$, $p = 0.172$). Based on our model of *best-fit*, we then conducted pairwise comparisons to determine the effect of condition, sex and stage on the number of branches for each branch order.

4.2.1 Postnatal Day 30

Sex Differences in the Healthy Brain

The effect of prenatal PGE2 exposure on the number of primary, secondary and tertiary branches was first determined at PN30 in the healthy brain. **(Figure 7B, Table 3)**. There was no significant difference between WTM and WTF in primary (t(330) = 0.710, p = 0.478, WTM = 5.000, WTF = 4.100), secondary ((t(330) = 0.394, p = 0.693, WTM = 3.100, WTF = 2.600) or tertiary branching (t(330) = 0.237, p = 0.813, WTM = 1.200, WTF = 0.900).

Sex Differences in the PGE2-exposed Brain

We next examined the effect of PGE2 exposure on the number of primary, secondary and tertiary branches at PN30 in the PGE2-exposed brain **(Figure 7B, Table 3)**. Similar to the healthy offspring, there was also no significant difference between PGE2M and PGE2F in primary (t(330) = -0.709, p = 0.479, PGE2M = 5.800, PGE2F = 6.533), secondary (t(330) = -0.258, p = 0.797, PGE2M = 3.133, PGE2F = 3.400) and tertiary branching (t(330) = 0.064, p = 0.949, PGE2M = 0.533, PGE2F = 0.467). Overall, this demonstrates that there are no sex differences in the saline and PGE2-exposed offspring at PN30.

PGE2-exposure in Males and Females

We next examined the effect of PGE2-exposure in males and females at PN30 **(Figure 7B, Table 3)**. There was no significant difference between PGE2M and WTM in primary (t(330) = -0.692, p = 0.490, WTM = 5.000, PGE2M = 5.800), secondary (t(330) = -0.029, p = 0.977, WTM = 3.100, PGE2M = 3.133) and tertiary branching (t(330) = 0.576, p = 0.564, WTM = 1.200, PGE2M = 0.533).

Interestingly, PGE2F had increased primary branching compared to WTF (t(330) = -2.104, p = 0.036, WTF = 4.100, PGE2F = 6.530), however there was no significant difference in

secondary (t(330) = -0.692, p = 0.490, WTF = 2.600, PGE2F = 3.400) or tertiary branching (t(330) = -1.842, p = 0.708, WTF = 0.900, PGE2F = 0.467). This demonstrates that PGE2-exposure has a female specific effect, where PGE2 females have increased primary branching.

4.2.2 Postnatal Day 90

Sex Differences in the Healthy Brain

First, we established the number of primary, secondary and tertiary branches was in the healthy brain at PN90. **(Figure 7B, Table 3)**. WTF had significantly increased secondary branching (t(330) = -3.415, p < 0.001, WTM = 9.260, WTF = 12.800) compared to WTM. However, there was no significant difference between WTM and WTF in primary (t(330) = 0.710, p = 0.478, WTM = 5.933, WTF = 5.600) or tertiary branching (t(330) = -1.482, p = 0.139, WTM = 3.678, WTF = 5.200).

Sex Differences in the PGE2-exposed Brain

We next examined the effect of PGE2-exposure on males and females at PN90 **(Figure 7B, Table 3)**. PGE2F had significantly decreased secondary (t(330) = 4.059, p < 0.001, PGE2M = 12.133, PGE2F = 7.933) and tertiary branching (t(330) = 2.642, p = 0.009, PGE2M = 5.467, PGE2F = 2.733) compared to PGE2M. There were no significant difference between PGE2M and PGE2F in primary branching (t(330) = -0.773, p = 0.440, PGE2M = 5.533, PGE2F = 6.333). Overall, we observe clear sex differences in the healthy and PGE2-exposed brain at PN90. Specifically, in the healthy brain, females have increased secondary branching. In contrast, in the PGE2-exposed brain, females have decreased secondary and tertiary branching.

PGE2-exposure in Males and Females

We next examined the effect of PGE2-exposure in males and females at PN90 **(Figure 7B, Table 3)**. PGE2M had significantly increased secondary branching ($t(330) = -2.771$, $p = 0.006$, WTM = 9.260, PGE2M = 12.133). However, we did not observe any significant difference between WTM and PGE2M in primary ($t(330) = 0.387$, $p = 0.699$, WTM = 5.933, PGE2M = 5.533) and tertiary branching ($t(330) = -1.740$, $p = 0.083$, WTM = 3.670, PGE2M = 5.467)

Furthermore, PGE2F had significantly reduced secondary ($t(330) = 4.704$, $p < 0.001$, WTF = 12.800, PGE2F = 7.933) and tertiary branching ($t(330) = 2.384$, $p = 0.018$, WTF = 5.200, PGE2F = 2.733) compared to WTF. However, we did not observe any significant differences between PGE2F and WTF in primary branching ($t(330) = -0.709$, $p = 0.479$, WTF = 5.600, PGE2F = 6.333). Overall, we observe opposite effects due to PGE2 exposure in males and females, where PGE2-exposed males have increased secondary branching and PGE2-exposed females have decreased secondary and tertiary branching compared to the matched saline controls.

4.2.3 Over Development

Saline-exposed Males and Females

The effect of developmental stage on the number of primary, secondary and tertiary branches was examined within each condition (WTM, WTF, PGE2M, PGE2F) **(Figure 7B, Table 4)**. In saline-exposed males, PN90 WTM had significantly greater secondary ($t(330) = -5.331$, $p < 0.001$, PN30 WTM = 3.100, PN90 WTM = 9.267) and tertiary branching ($t(330) = -2.132$, $p < 0.034$, PN30 WTM = 1.200, PN90 WTM = 3.67). We observed no significant difference in primary branching ($t(330) = -0.807$, $p = 0.420$, PN30 WTM = 5.000, PN90 WTM = 5.933) between PN30 WTM and PN90 WTM.

Furthermore, similar to the males, PN90 WTF had significantly greater secondary ($t(330) = -8.817$, $p < 0.001$, PN30 WTF = 2.600, PN90 WTF = 12.800) and tertiary branching ($t(330) = -2.392$, $p = 0.017$, PN30 WTF = 0.900, PN90 WTF = 5.200) compared to PN30 WTF. There was no significant difference between PN30 WTF and PN90 WTF in primary branching ($t(330) = -1.297$, $p = 0.196$, PN30 WTF = 4.100, PN90 WTF = 5.600). Overall, both PN90 males and females have increased secondary and tertiary branching compared to PN30.

PGE2-exposed Males and Females

We next examined the effect of developmental stage on primary, secondary and tertiary branching in PGE2-exposed males and females **(Figure 7B, Table 4)**. PN90 PGE2M had increased secondary ($t(330) = -8.698$, $p < 0.001$, PN30 PGE2M = 3.133, PN90 PGE2M = 12.133) and tertiary branching ($t(330) = -4.768$, $p < 0.001$, PN30 PGE2M = 0.533, PN90 PGE2M = 5.467) compared to PN30 PGE2M. However, there was no significant difference between PN30 PGE2M and PN90 PGE2M in primary branching ($t(330) = 0.258$, $p = 0.797$, PN30 PGE2M = 5.800, PN90 PGE2M = 5.533).

Additionally, PN90 PGE2F have increased secondary ($t(330) = -4.381$, $p < 0.001$, PN30 PGE2F = 3.400, PN90 PGE2F = 7.933) and tertiary branching ($t(330) = -2.191$, $p = 0.029$, PN30 PGE2F = 0.467, PN90 PGE2F = 2.733) compared to PN30 PGE2F. However, we observed no significant difference between PN30 PGE2F and PN90 PGE2F in primary branching ($t(330) = 0.193$, $p = 0.847$, PN30 PGE2F = 6.533, PN90 PGE2F= 6.333). Overall, similar to the healthy brain, both PGE2-exposed males and females at PN90 have increased secondary and tertiary branching compared to their PN30 counterparts.

4.2.4 Summary

To summarize, we examined 1) sex differences in the healthy and PGE2-exposed brain and 2) the effect of PGE2-exposure in males and females on primary, secondary and tertiary branching at PN30 and PN90 **(Table 3 and 4)**. At PN30, no sex differences were observed in primary, secondary or tertiary branching in both the saline-exposed and PGE2-exposed offspring **(Table 3)**. Additionally, PGE2-exposure had a female specific effect, where only females showed an increase in primary branching compared to saline-exposed females.

Furthermore, at PN90 we also observe contrasting sex differences in the saline-exposed and PGE2-exposed males and females. Saline-exposed females have increased secondary branching, however, in the PGE2-exposed brain, females have decreased secondary and tertiary branching. Furthermore, at PN90, PGE2-exposure increased secondary branching in males and decreased both secondary and tertiary branching in females.

We also observed developmental differences within each of the conditions **(Table 4)**. We determined that PN90 saline-exposed males and females had increased secondary and tertiary branching compared to their PN30 counterparts. In PGE2-exposed males and females, we observed that PN90 males and females also had increased secondary and tertiary branching

compared to their PN30 counterparts. Overall, we have provided evidence that sex, PGE2-exposure and developmental stage impact primary, secondary and tertiary branching.

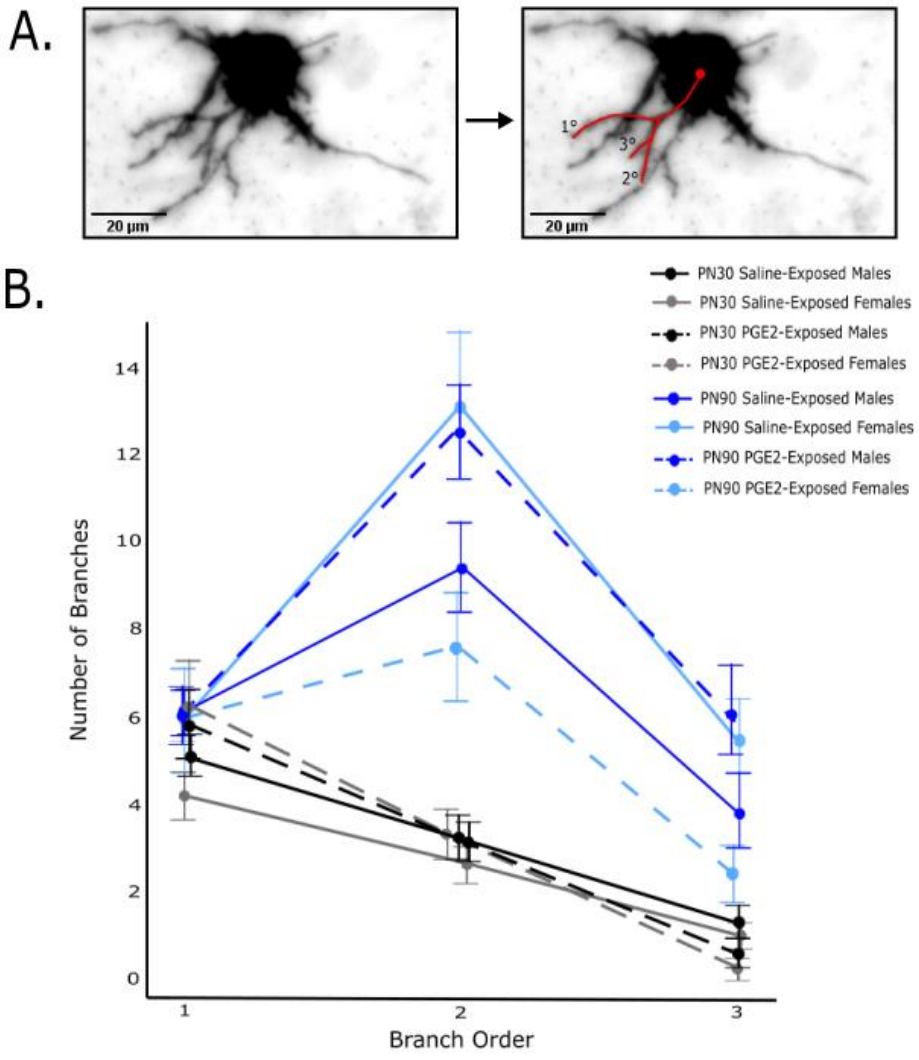

Figure 7. Branch order of saline-exposed and PGE2-exposed offspring at PN30 and PN90. A) Classification of primary, secondary, and tertiary branches. B) The number of primary, secondary, and tertiary branches. Data is presented as a mean ± SEM. n = 15 cells per condition from 3 different animals obtained from 3 separate litters.

Table 3: Summary of sex differences and PGE2-exposure on branch order.

Differences in primary, secondary and tertiary branching in saline and PGE2 male and female offspring is shown. Sex differences in saline and PGE2 offspring are shown, where females are compared to males. The effect of PGE2-exposure is shown in males and females, where they are compared to their saline counterparts. The up and down arrows indicate an increase and decrease in the corresponding branch order, respectively.

Branch Order	**Sex Differences at PN30** *(Compared to the male)*		**Sex Differences at PN90** *(Compared to the male)*		**PGE2-exposure at PN30** *(Compared to saline control)*		**PGE2-exposure at PN90** *(Compared to saline control)*	
	Saline Female	**PGE2 Female**	**Saline Female**	**PGE2 Female**	**PGE2 Male**	**PGE2 Female**	**PGE2 Male**	**PGE2 Female**
1	–	–	–	–	–	↑	–	–
2	–	–	↑	↓	–	–	↑	↓
3	–	–	–	↓	–	–	–	↓

Table 4: Summary of the effect of developmental stage on branch order.

Primary, secondary and tertiary branching of PN90 offspring is compared to PN30 offspring for each of the conditions, saline-exposed and PGE2-exposed males and females.

Branch Order	**Saline Exposed** *(Compared to PN30)*		**PGE2-exposed** *(Compared to PN30)*	
	PN90 Male	**PN90 Female**	**PN90 Male**	**PN90 Female**
1	–	–	–	–
2	↑	↑	↑	↑
3	↑	↑	↑	↑

4.3 Primary Branch Length

Our lab has previously shown that PGE2-exposure increases neurite length *in-vitro* in differentiating NE4C cells and results in the loss of sex-differences observed in saline-exposed mice in the cerebellum (Kissoondoyal *et al.*, 2021; Kissondoyal *et al.*, Unpublished). Based on previous findings we investigated the average primary dendrite length of hippocampal neuronal cells in Saline and PGE2-exposed males and females at PN30 and PN90. The neuronal extensions originating from the center of the cell soma were measured and an average was computed per cell, higher order extensions were not included **(Figure 8A).** Primary branch length was fit using a linear mixed effects model, where litter was assigned as a random effect to account for litter-bias. Condition, sex and developmental stage, were assigned as fixed effects and the interaction between these factors were examined. There was a significant interaction between condition and sex ($t(110) = -2.449$, $p = 0.016$), as well as condition and stage ($t(110) = -2.706$, $p = 0.008$). However, the interaction between condition, sex and stage was not significant ($t(110) = 0.573$, $p = 0.568$). Based on the *model of best-fit* we conducted pairwise comparisons.

4.3.1 Postnatal Day 30

Sex Differences in the Healthy and PGE2-exposed Brain

First, we examined sex differences in the primary branch length in the healthy and PGE2-exposed brain at PN30 **(Figure 8B, Table 5)**. WTF had significantly greater primary branch length compared to WTM ($t(110) = -4.049$, $p = 0.478$, WTM = 62.904, WTF = 112.739). However, there was no significant difference observed between PGE2M and PGE2F ($t(110) = -1.087$, $p = 0.279$, PGE2M = 111.644, PGE2F = 122.566). This suggests that PGE2-exposure results in the loss of innate sex differences observed in the healthy brain.

PGE2-exposed Males and Females

We next examined the effect of PGE2-exposure on primary branch length in males and females **(Figure 8B, Table 5)**. PGE2M had significantly greater branch length ($t(110) = -4.339$, $p < 0.001$, WTM = 62.904, PGE2M = 111.644), while PGE2F ($t(110) = -0.875$, $p = 0.384$, WTF = 112.739, PGE2F = 122.566) did not significantly differ compared to their matched WTF. Overall, we observe a male specific effect of PGE2-exposure on primary branch length.

4.3.2 Postnatal Day 90

Sex Differences in the Healthy and PGE2-exposed Brain

At PN90 sex differences of primary branch length in the healthy and PGE2-exposed brain was studied **(Figure 8B, Table 5).** There was no significant difference in primary branch length between WTF and WTM ($t(110) = -1.423$, $p = 0.158$, WTM = 29.399, WTF = 43.696). There was also no significant difference observed between PGE2F and PGE2M ($t(110) = 1.235$, $p = 0.219$, PGE2M =37.364, PGE2F = 24.953). Overall, no sex differences were observed in the healthy and PGE2-exposed brain at PN90.

PGE2-exposed Males and Females

We also examined the effect of PGE2-exposure on males and females at PN90 **(Figure 8B, Table 5)**. There was no significant difference between PGE2M and WTM ($t(110) = -0.7928$, $p = 0.430$, WTM = 29.399, PGE2M = 37.364), as well as, PGE2F and WTF (110) = 1.866, $p = 0.0648$, WTF = 43.696, PGE2F = 24.953). Overall, there is no effect of PGE2-exposure on primary branch length in males and females at PN90.

4.3.3 Over Development

The effect of developmental stage was also examined on primary branch length within each condition (WTM, WTF, PGE2M and PGE2F) **(Figure 8B, Table 6)**. PN90 WTM had significantly reduced primary branching length compared to PN30 WTM ($t(110) = 2.983$, $p = 0.004$, PN30 WTM = 62.904, PN90 WTM = 29.399). Similarly, we observed that PN90 WTF ($t(110) = 6.146$, $p < 0.001$, PN30 WTF = 112.738, PN90 WTF = 43.696), PN90 PGE2M ($t(110) = 7.393$, $p < 0.001$, PN30 PGE2M = 111.644, PN90 PGE2M = 37.364) and PN90 PGE2F ($t(110) = 9.716$, $p < 0.001$, PN30 PGE2F = 122.566, PN90 PGE2F = 24.953) had significantly reduced primary dendrite length compared to their matched controls at PN30. Overall, over development each of the conditions experience a reduction in primary branch length.

4.3.4 Summary

To summarize, we investigated sex differences, the effect of PGE2-exposure and developmental stage on primary branch length **(Table 5 and 6)**. Saline-exposed females had increased branch length compared to saline-exposed males at PN30 **(Table 5)**. At PN30 we observed a male-specific effect due to PGE2-exposure, where PGE2 males had significantly greater branching compared to saline males. Interestingly, at PN90 there was no sex difference observed between saline-exposed mice. There were also no differences observed due to PGE2-exposure at PN90. When compared over development, PN90 saline-exposed males and females, as well as, PN90 PGE2-exposed males and females have reduced branch length compared to their matched controls at PN30 **(Table 6)**. Overall, we see a loss of innate sex-differences due to PGE2-exposure at PN30, a male specific effect of PGE2-exposure and reduced branch length over development.

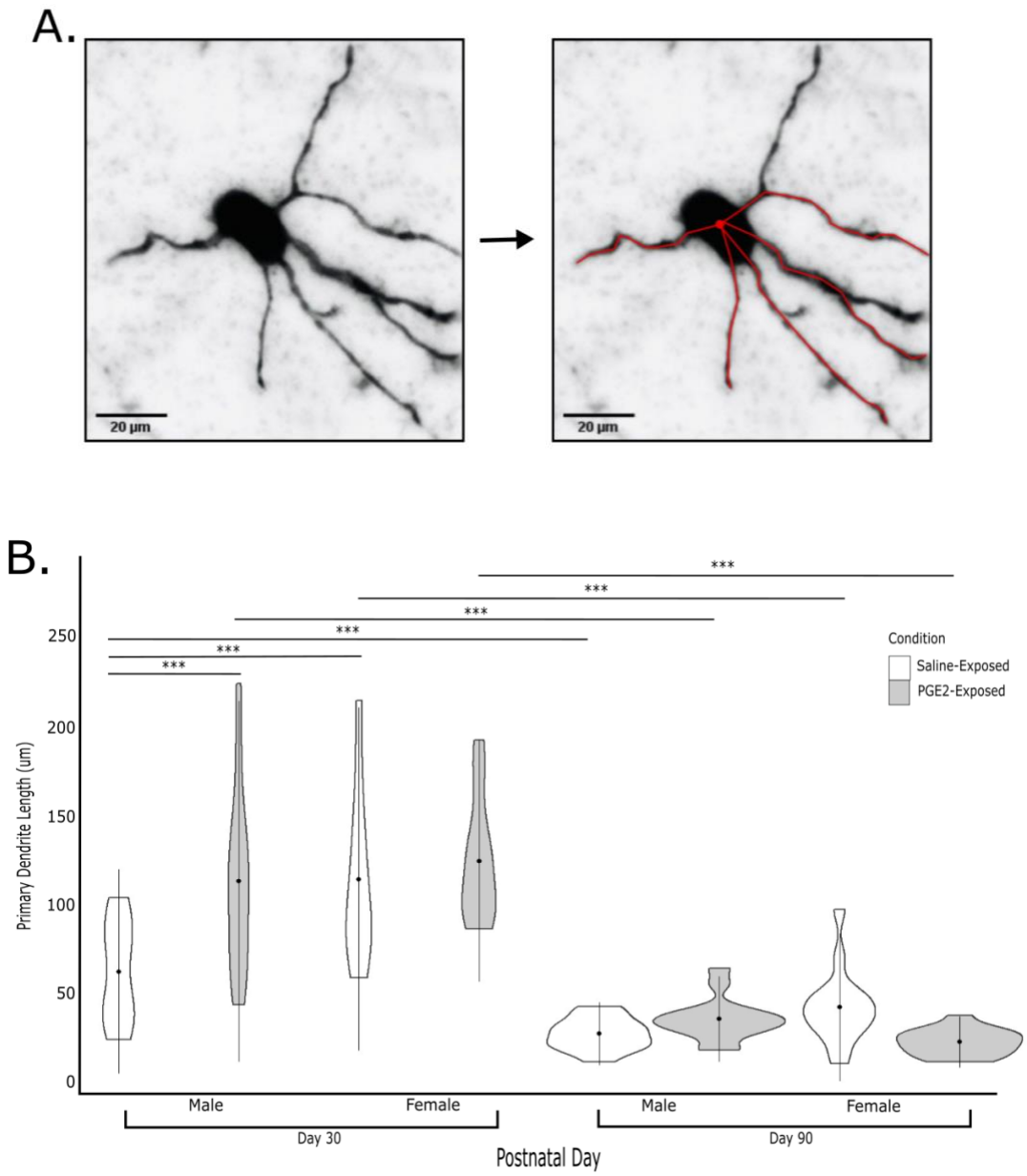

Figure 8. Dendrite length of saline-exposed and PGE2-exposed offspring at PN30 and PN90. A) Quantification of primary dendrite length in hippocampal cells. B) Violin plot of primary dendrite length of each condition. Data is presented as a mean ± SD. n = 15 cells per condition from 3 different animals obtained from 3 separate litters.

Table 5: Summary of sex differences and PGE2-exposure on primary branch length at PN30 and PN90.

Sex differences in saline and PGE2 offspring are shown, where females are compared to males. The effect of PGE2-exposure is shown in males and females, where they are compared to their saline counterparts. The up and down arrows indicate an increase and decrease in primary branch length, respectively.

Primary Branch Length	**Sex Differences at PN30** *(Compared to the male)*		**Sex Differences at PN90** *(Compared to the male)*		**PGE2-exposure at PN30** *(Compared to saline control)*		**PGE2-exposure at PN90** *(Compared to saline control)*	
	Saline Female	**PGE2 Female**	**Saline Female**	**PGE2 Female**	**PGE2 Male**	**PGE2 Female**	**PGE2 Male**	**PGE2 Female**
	↑	–	–	–	↑	–	–	–

Table 6: Summary of the effect of developmental stage on primary branch length.

Primary branch length of PN90 offspring is compared to PN30 offspring for each of the conditions, Saline-exposed and PGE2-exposed males and females.

Branch Order	**Saline-exposed** *(Compared to PN30)*		**PGE2-exposed** *(Compared to PN30)*	
	PN90 Male	**PN90 Female**	**PN90 Male**	**PN90 Female**
	↓	↓	↓	↓

4.4 Cross-sectional Area of the Neuronal Soma

Recent research has provided evidence of deficits in neuronal soma size and volume in individuals with ASD in both different layers and regions of the brain (Wegiel *et al.*, 2014, 2015). The cross-sectional area of the soma of hippocampal neuronal cells in saline and PGE2-exposed males and females at PN30 and PN90 was examined **(Figure 9A)**. Neuronal cross-sectional area was fit using a linear mixed effects model, where litter was assigned as a random effect to account for litter-bias. The model of *best-fit* determined that sex was to be excluded as a factor and as such, sex was removed from the analysis of the neuronal cross-sectional area. Condition and developmental stage were assigned as fixed effects and the interaction between these factors were examined. There was no significant effect of condition ($t(110) = 0.278$, $p = 0.785$), however stage had a significant effect ($t(110) = 4.458$, $p < 0.001$) on neuronal cross-sectional area. In addition, there was a significant interaction between condition and stage ($t(110) = -2.424$, $p = 0.018$). Based on the model of *best-fit*, we conducted pairwise comparisons.

4.4.1 Postnatal Day 30 and Postnatal Day 90

The neuronal cross-sectional area of saline and PGE2-exposed males and females combined, was examined at PN30 and PN90 **(Figure 9B, Table 7)**. There was no significant difference in the cross sectional area of the neuronal soma between PN30 WT and PN30 PGE2 animals ($t(110) = -0.278$, $p = 0.785$, PN30 WT = 216.130 , PN30 PGE2 = 236.694). However, PGE2 animals at PN90 have significantly decreased cross-sectional area of the neuronal soma compared to PN90 WT animals ($t(110) = 3.274$, $p = 0.006$, PN90 WT = 494.424, PN90 PGE2 = 312.127). Overall, we observe that PGE2-exposure has a stage specific effect on the cross-sectional area of the neuronal soma, where there is a reduction in soma size at PN90 due to PGE2-exposure.

4.4.2 Over Development

The neuronal cross-sectional area was examined over development within each condition (WT and PGE2). WT animals at PN90 had significantly larger neuronal cross-sectional areas compared to WT animals at PN30 ($t(110) = -4.458$, $p < 0.001$, PN30 WT = 216.130, PN90 WT =494.424). However, there was no significant difference between PN30 PGE2 and PN90 PGE2 animals ($t(110) = -1.386$, $p = 0.169$, PN30 PGE2 = 236.694, PN90 PGE2 = 312.127). This demonstrates that PGE2-exposure impacts the innate differences of soma size observed over development in the healthy brain.

4.4.3 Summary

To summarize, we examined the effect of PGE2-exposure and developmental stage on the cross-sectional area of the soma. We observe no difference in neuronal soma size between PGE2- and saline-exposed offspring (males and females combined) at PN30, but there was a significant reduction in soma size in PGE2-exposed offspring at PN90 **(Table 7)**. Moreover, we provide evidence that the neuronal soma size increases over development, from PN30 to PN90 in the healthy brain, but was lost due to PGE2-exposure **(Table 8)**. To conclude, we provide evidence that PGE2-exposure has a stage-specific effect.

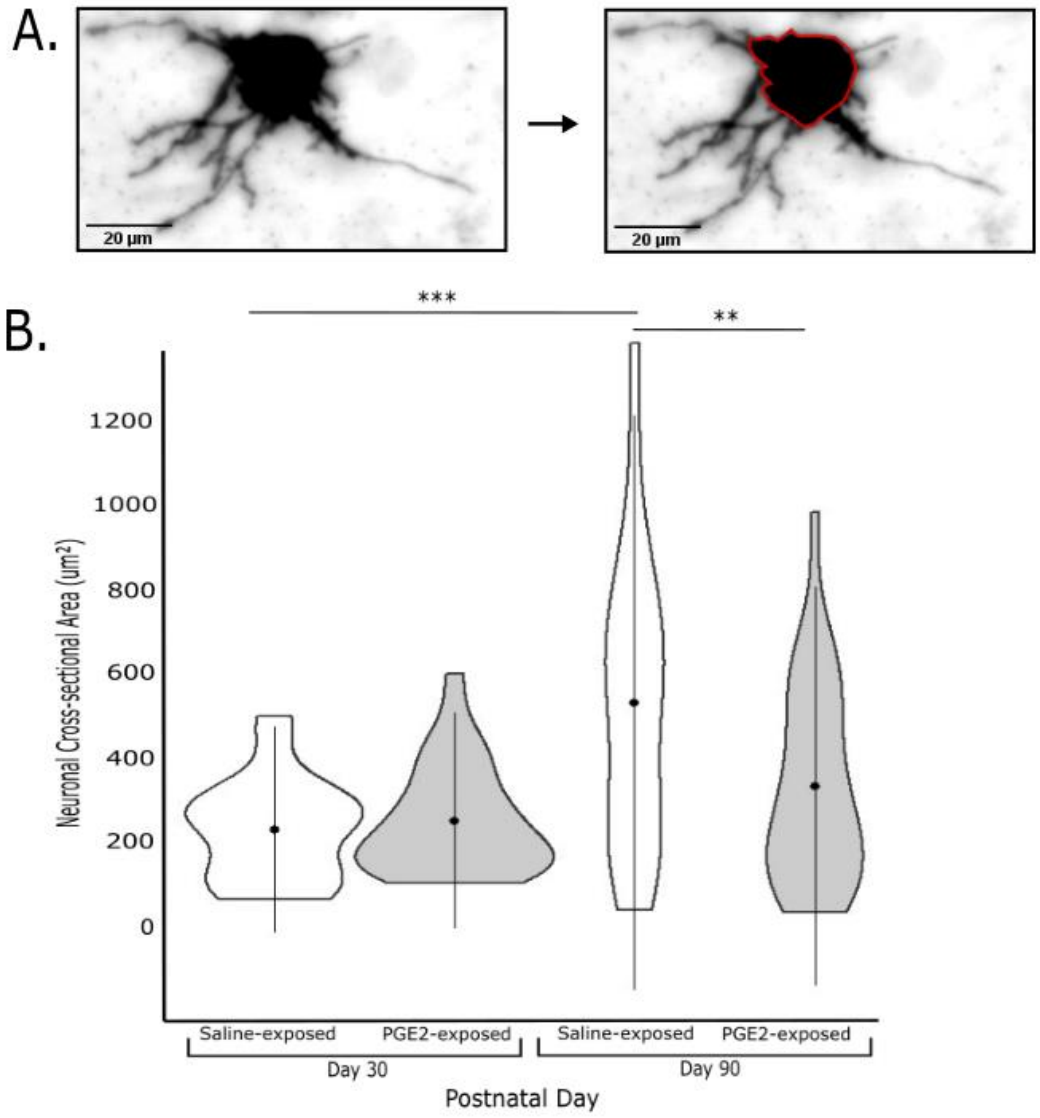

Figure 9. Neuronal soma area of saline- and PGE2-exposed offspring at PN30 and PN90. A) Quantification of cell soma area. B) Violin plot of neuronal cross-sectional area (μm^2). Data is presented as a mean ± SD. n = 15 cells per condition from 3 different animals obtained from 3 separate litters.

Table 7: Summary of PGE2-exposure on the cross-sectional area of the soma at PN30 and PN90.

The effect of PGE2-exposure is shown in males and females combined, where they are compared to their saline counterparts. The up and down arrows indicate an increase and decrease in primary branch length, respectively.

Cross-Sectional Area of the Soma	**PGE2-exposure at PN30** *(Compared to saline control)*	**PGE2-exposure at PN90** *(Compared to saline control)*
	PGE2 Males and Females	**PGE2 Males and Females**
	–	↓

Table 8: Summary of the effect of developmental stage on the cross-sectional area of the neuronal soma.

Primary branch length of PN90 offspring is compared to PN30 offspring for each of the conditions, saline-exposed and PGE2-exposed males and females.

Cross-Sectional Area of the Soma	**Saline-exposed** *(Compared to PN30)*	**PGE2-exposed** *(Compared to PN30)*
	PN90 Males and Females	**PN90 Males and Females**
	↑	–

4.5 Dendritic Looping

In previous studies, our lab has investigated the effect of PGE2 on neurite and dendritic loop formation. Specifically, *in-vitro* studies of PGE2 exposure on differentiating NE4C stem cells provided evidence of increased looping in neurites (Kissoondoyal & Crawford, 2021). Furthermore, *in-vivo* studies in COX-2 KI and PGE2-exposed model demonstrate increased proportion of dendritic loops in the cerebellum (Kissoondoyal *et al.*, 2021; Kissondoyal *et al.*, Unpublished). Here, we investigated whether sex (male or female), postnatal stage (PN30 or PN90) and condition (saline-exposed or PGE2-exposed) affects the odds of observing a dendritic loop in the hippocampus. The maximum exterior turning angle of all dendrites was measured, where a turning angle greater than 270° was classified as a loop **(Figure 10A)**. An odds ratio (OR) above 1, indicates a greater likelihood of observing a dendritic loop, while an OR less than 1, indicates a decreased likelihood of observing a dendritic loop.

Binomial logistical regression was used to determine the odds of observing a dendritic loop at the baseline intercept (PN30 saline-exposed male) for comparisons. A significant OR of 0.034 in the PN30 saline male control intercept ($p<0.001$), indicating that it is less likely to observe a dendritic loop **(Figure 10B and Table 9)**. Next, we examined whether sex (animal was a female) affects the odds of observing a dendritic loop. Sex does not affect the likelihood of observing a dendritic loop compared baseline model, the PN30 saline control male (OR = 0.831, $p = 0.529$). Interestingly, postnatal stage (animal was from PN90) significantly decreased the odds of observing a dendritic loop (OR = 0.504, $p = 0.020$) and condition (animal was PGE2 exposed) increased the odds of observing a dendritic loop (OR = 1.974, $p = 0.035$). Overall, we determined that sex did not significantly affect the likelihood of observing a dendritic loop, however, stage and condition significantly affect the likelihood of observing a loop.

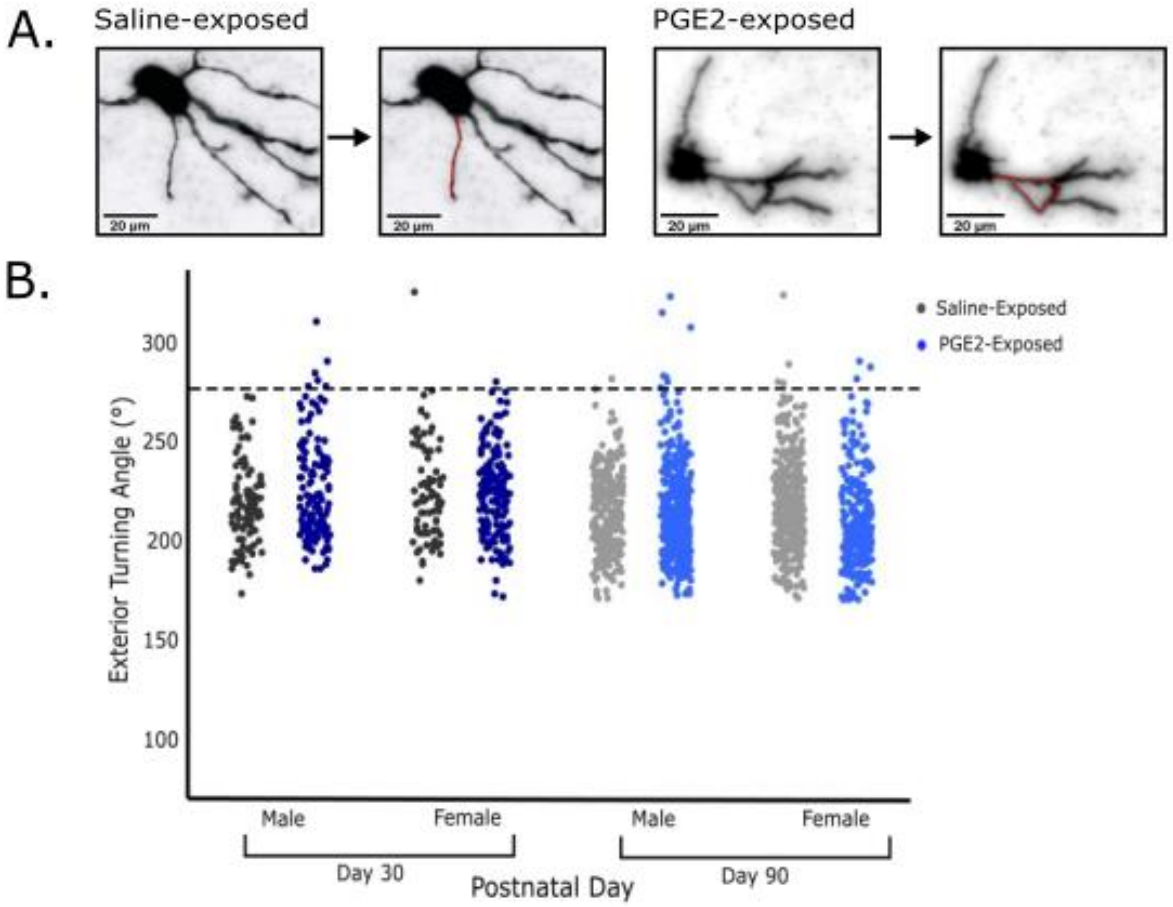

Figure 10. Dendritic exterior angles of saline- and PGE2-exposed animals.
A) Quantification dendritic looping, the exterior turning angle of each dendrite was measured. B) Graph showing the distribution of exterior turning angles for each condition. Each dot represents the exterior turning angle of a single dendrite. Any dendrite with an exterior turning angle greater than 270° was considered a loop, indicated by the dotted line. n = 15 cells per condition from 3 different animals obtained from 3 separate litters.

Table 9: Odds of observing dendritic loops in the hippocampus of PGE2-exposed at PN90.

Data is presented as odds ratios (95% confidence intervals) for the baseline (PN30 saline-exposed male) and factors, which includes sex, stage, and PGE2-exposure. A total of 3 animals obtained from 3 separate litters were used per condition.

Factor	OR (95% CI)	p-value	Likelihood of observing a dendritic loop
Baseline *(PN30 saline-exposed Male)*	0.034 (0.023-0.049)	8.65E-21	———
Sex *(Female)*	0.831 (0.620-1.115)	0.529	Decreased *(Non-significant)*
Stage *(PN90)*	0.504 (0.375-0.677)	**0.020**	Decreased *(Significant)*
Condition *(PGE2-exposed)*	1.974 (1.430-2.725)	**0.035**	Increased *(Significant)*

4.6 Dendritic Spine Density

Dendritic spines are small protrusions found on the dendrite and play a critical role in the strength and stability of synapses in the brain (Martínez-Cerdeño, 2017). We have previously provided evidence that changes in PGE2 levels impacts dendritic spine density in the cerebellum. Specifically, in the COX2-KI model we observed a loss of sex-differences in spine density and in PGE2-exposed animals we observed an increased spine density compared to saline controls (Kissoondoyal *et al.*, 2021; Kissondoyal *et al.*, Unpublished). In this study, we investigated dendritic spine density of hippocampal neuronal cells in saline and PGE2-exposed males and females at PN30 and PN90. Dendritic spine density was calculated as the number of spines per μm **(Figure 11A)**.

Dendritic spine density (spines/μm) was fit using a linear mixed effects model, where litter was assigned as a random effect to account for litter-bias. The model of *best-fit* determined that sex was to be excluded as a factor and as such, sex was removed from the analysis of dendritic spine density. Condition and developmental stage were assigned as fixed effects and the interaction between these factors were examined. There was no significant effect of condition ($t(110) = 0.612$, $p = 0.542$), however stage had a significant ($t(110) = 3.106$, $p = 0.002$) effect on spine density. In addition, there was no significant interaction between condition and stage ($t(110) = -1.036$, $p = 0.303$). Based on the model of *best fit*, we conducted pairwise comparisons.

4.6.1 Postnatal Day 30 and Postnatal Day 90

The dendritic spine density of saline and PGE2-exposed males and females combined, was examined at PN30 and PN90 **(Figure 11B)**. There was no significant difference in spine density between PN30 WT and PN30 PGE2 animals ($t(110) = -0.612$, $p = 0.542$, PN30 WT = 0.433 , PN30 PGE2 = 0.486), as well as, PN90 WT and PN90 PGE2 animals ($t(110) = 0.855$, $p =$

0.394, PN90 WT = 0.704, PN90 PGE2 = 0.632). Overall, there was no effect of PGE2-exposure on spine density at PN30 and PN90.

4.6.2 Over Development

Dendritic spine density was examined over development within each condition (WT and PGE2) **(Figure 11B).** WT animals at PN90 had significantly increased spine density compared to WT animals at PN30 ($t(110) = -3.106$, $p = 0.002$, PN30 WT = 0.433, PN90 WT = 0.704). However, there was no significant difference between PN30 PGE2 and PN90 PGE2 animals ($t(110) = -1.733$, $p = 0.394$, PN30 PGE2 = 0.486, PN90 PGE2 = 0.632). Overall, we observed an increase in spine density over development.

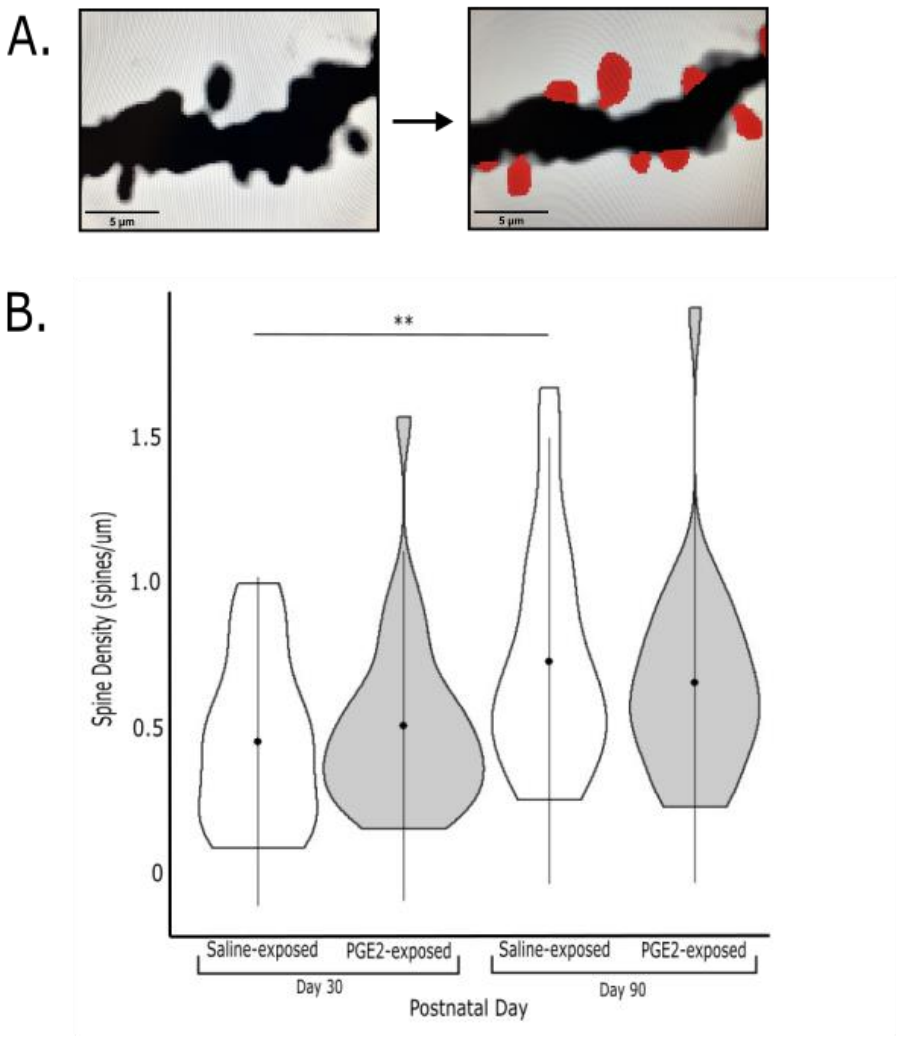

Figure 11. Dendritic spine density in saline and PGE2-exposed animals.
A) Detection of dendritic spines using the NIS-Elements Artificial Intelligence software. B) Violin plot showing the dendritic spine density (spines/µm) in males and females of saline and PGE2-exposed. Data is presented as a mean ± SD. n = 15 cells per condition from 3 different animals obtained from 3 separate litters.

4.7 Dendritic Spine Morphologies

Dendric spine morphology is also another factor that is involved in synaptic transmission, and stability (Martínez-Cerdeño, 2017). There are three major morphologies in the brain, both thin and stubby shaped spines are more immature spines and found in the developing brain and are short-lived. However, mushroom shaped spines are prominent in the developed brain and stronger synapses (Nimchinsky *et al.*, 2002; Risher *et al.*, 2014). We investigated the odds of observing mature dendritic spines in the hippocampus of saline control and PGE2 exposed males and females was investigated at P30 and PN90. We investigated whether sex (male or female), postnatal stage (PN30 or PN90) and condition (saline-exposed or PGE2-exposed) affects the odds of observing a mature dendritic spine. Dendritic spine classification was conducted using previously established guidelines (Risher *et al.*, 2014; Kissoondoyal *et al.*, 2021). We used the NIS-Elements artificial intelligence software to detect dendritic spine morphologies and obtain width and length measurements. We used a top-down sequential approach to classify them into their corresponding morphologies. Dendritic spines with a length > 1.4 µm were first classified as thin. Subsequently, in the remaining pool of dendritic spines, those with a width > length was classified as stubby, and the remaining were classified as mushroom shaped. Thin and stubby shaped spines were classified as immature and mushroom shaped spines were classified as mature spines for statistical analyses.

Binomial logistical regression was used to determine the odds of observing a mature dendritic spine at the baseline intercept (PN30 saline-exposed male) for comparisons **(Table 10)**. A significant odds ratio (OR) of 0.434 in the PN30 saline male control intercept ($p<0.001$) was determined, indicating that it is less likely to observe a mature dendritic spine. We found that postnatal stage (if the animal was from PN90), significantly increased the likelihood of observing

a mature dendritic spine (OR = 1.444, $p < 0.001$). However, sex (if the animal was female) did not significantly affect the likelihood of observing a mature dendritic spine compared to the baseline (OR = 0.907, $p = 0.188$). Additionally, condition (if the animal was PGE2-exposed) did not significantly affect the likelihood of observing a mature dendritic spine compared to the baseline (OR = 1.036, $p = 0.636$). Overall, we have provided evidence that postnatal stage affects the likelihood of observing a mature dendritic spine, however both sex and condition do not.

Table 10: Odds of observing mature dendritic spines in the hippocampus of PGE2-exposed at PN90.

Data is presented as odds ratios (95% confidence intervals) for the baseline (PN30 saline Control Male) and factors, which includes sex, stage, and PGE2-exposure. A total of 3 animals obtained from 3 separate litters were used per condition.

Factor	OR (95% CI)	p-value	Likelihood of observing a mature spine
Baseline *(PN30 saline Control Male)*	0.434 (0.400-0.471)	2.13E-24	———
Sex *(Female)*	0.907 (0.842-0.977)	0.188	Decreased *(Non-significant)*
Stage *(PN90)*	1.444 (1.343-1.552)	**3.97E-07**	Increased *(Significant)*
Condition *(PGE2-exposed)*	1.036 (0.962-1.115)	0.636	Increased *(Non-Significant)*

4.8 Hippocampal Protein Expression

In this study we provided evidence that a single maternal injection at G11 contributes to abnormal dendritic morphology in the developing hippocampus of male and female offpsring. We further examined the expression of proteins that are involved in cytoskeletal architecture and hippocampal function. Our lab has previously determined that atypical dendritic morphology in the cerebellum of COX2-KI and PGE2-exposed offspring, may be due to changes in the expression of, ß-actin, a protein critical for cytoskeletal structure and spinophilin (SPN), a protein enriched in dendritic spines (Kissoondoyal *et al.*, 2021; Kissondoyal *et al.*, Unpublished). Furthermore, previously in our COX2-KI model it was determined that ASD-risk genes involved in synaptic transmission were impacted (Rai-Bhogal, Ahmad, Li, & Crawford, 2018). Two receptors critical for hippocampal function and long-term potentiation is NMDA2A, an isoform of NMDA highly expressed later in development and AMPA (Lee *et al.*, 2003; Sanderson *et al.*, 2008; Lujan *et al.*, 2012; Shipton & Paulsen, 2014; Cercato *et al.*, 2016). Both these receptors have also been highly implicated in autism (Blundell *et al.*, 2010; Won *et al.*, 2012; Choi *et al.*, 2016).

Based on our lab's studies and previous research, we examined the effect of PGE2 exposure on ß-actin, spinophilin, NMDA2A and AMPA (GluR1). The fold change of protein expression relative to saline-exposed males was fit using linear mixed effects modeling, where condition and sex were assigned as fixed effects. Technical replicate was assigned as a random effect to account for confounding differences due to experimental conditions.

4.8.1 Protein Expression of ß-actin

For ß-actin, the model of *best-fit* determined that sex was to be excluded as a factor and as such, sex was removed from the analysis of ß-actin protein expression **(Figure 12A and B)**.

Condition was assigned as a fixed-effect and it has a significant effect on the expression of ß-actin ($t(9.00) = -3.093$, $p = 0.013$). Based on the model of *best-fit*, further pairwise comparisons were conducted. We determined that PGE2-exposed offspring (males and females combined) have significantly reduced ß-actin protein expression compared to saline-exposed offspring (males and females) ($t(9.00) = 3.093$, $p = 0.013$).

4.8.2 Protein Expression of Spinophilin

For spinophilin, there was no model of *best-fit* and as such, pairwise comparisons could not be conducted. The model of *best-fit* was determined based on the AIC value and p-value (refer to the methods). All comparisons were made to the baseline model, model 0 (M0), where no fixed effects were assigned, and technical replicate was assigned as the random effect. In model 1 (M1), we assigned condition and sex as fixed effects, compared to the baseline model (M0), M1 was not a representative model (AIC = 13.186, $p = 0.1613$). In model 2 (M2), we assigned condition as the fixed effect, excluding sex. Compared to M0, M2 was not a representative model (AIC = 14.714, $p = 0.161$). Although there was no model of *best-fit*, we observed slight trends in the fold-change of spinophilin expression, where the fold-change was determined relative to saline-exposed males (WTM = 1). We observed a slight upward trend in the fold-change of spinophilin expression in saline-exposed females, compared to saline-exposed males with an average of 1.231 (SEM = 0.276). Similarly, a slight upward trend is observed in PGE2-exposed males compared to saline-exposed males, with an average fold-change of 1.360 (SEM = 0.330). We also observed a slight decrease in the fold-change of PGE2-exposed females with an average of 1.188 (SEM = 0.229), compared to both saline-exposed females and PGE2-exposed males. Although we observed slight trends in the average fold-change of spinophilin, there was no model of *best-fit* and further pairwise comparisons could not be conducted.

4.8.3 Protein Expression of NMDA2A

For NMDA2A, there was no model of *best-fit* and as such, pairwise comparisons could not be conducted. The model of *best-fit* was determined based on the AIC value and p-value (refer to the methods). All comparisons were made to the baseline model, model 0 (M0), where no fixed effects were assigned, and technical replicate was assigned as the random effect. In model 1 (M1), we assigned condition and sex as fixed effects, compared to the baseline model (M0), M1 was not a representative model (AIC = 6.089, p = 0.284). In model 2 (M2), we assigned condition as the fixed effect, excluding sex. Compared to M0, M2 was not a representative model (AIC = 7.146, p = 0.686). Although there was no model of *best-fit*, we observed slight trends in the fold-change of NMDA2A expression, where the fold-change was determined relative to saline-exposed males (WTM = 1). The average fold-change of NMDA2A in saline-exposed females compared to saline-exposed males, with an average of 1.316 (SEM = 0.243). We also observed a slight upward trend in the average fold-change of both PGE2-exposed males and females, with an average of 1.186 (SEM = 0.165) and 1.222 (SEM = 0.143), respectively, compared to saline-exposed males. In addition, we observed a slight downward trend in the average fold-change of NMDA2A expression in PGE2-exposed females, with an average of 1.222 (SEM = 0.143), compared to saline-exposed females. Although we observed slight trends, there was no model of *best-fit* and further pairwise comparisons could not be conducted.

4.8.4 Protein Expression of AMPA

For AMPA, the model of *best-fit* determined that sex was to be excluded as a factor and as such, sex was removed from the analysis of AMPA protein expression **(Figure 12A and C)**. Condition was assigned as a fixed-effect and there was no significant effect on the expression of

AMPA ($t(9.00) = 1.769$, $p = 0.111$). Based on the model of *best-fit*, further pairwise comparisons were conducted. We determined that there was no significant difference between PGE2-exposed offspring (males and females) and saline-exposed offspring (males and females) ($t(9.00) = -1.769$, $p = 0.111$).

Overall, our western blot data shows that PGE2-exposure results in a significant reduction in ß-actin and has no effect on the expression of AMPA. Further analysis would need to be conducted to further elucidate whether PGE2-exposure impacts spinophilin and NMDA expression in the hippocampus at PN90 (see Future Directions below).

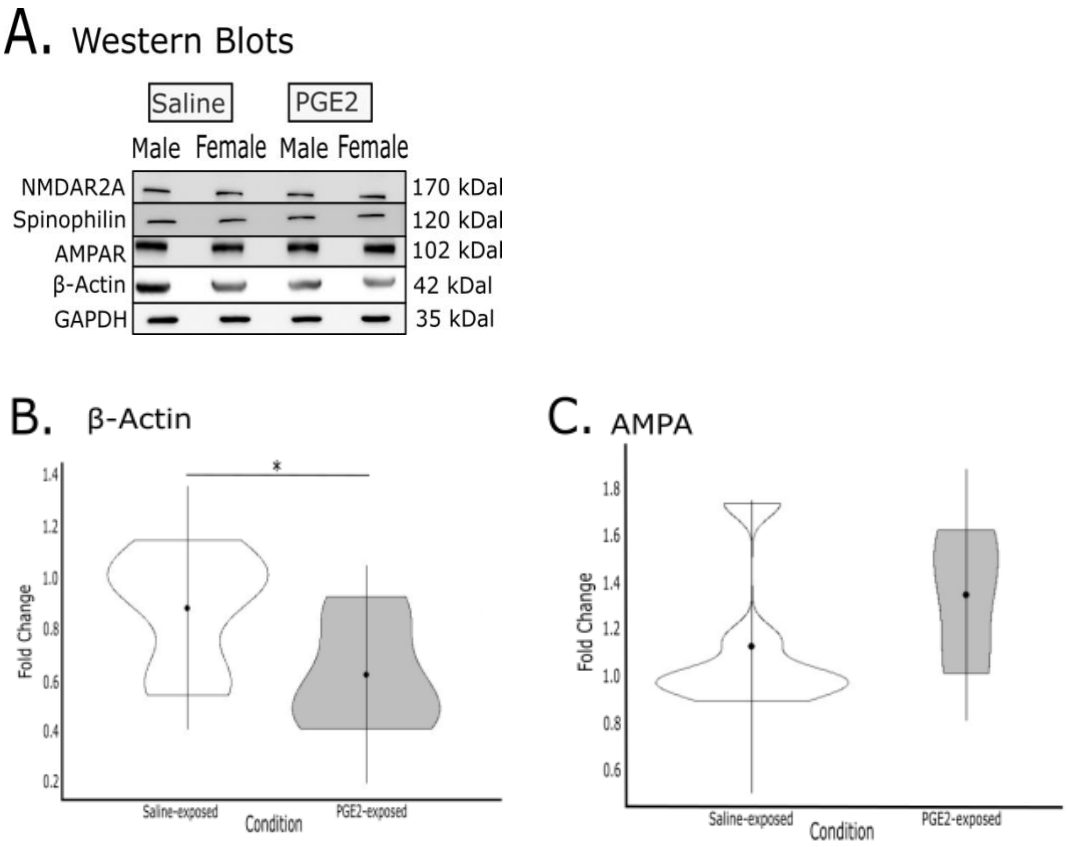

Figure 12. Protein expression of B-actin and AMPA in the hippocampus at PN90. A) Western blot of pooled hippocampal isolates of saline- and PGE2-exposed males and females at PN90. B) ß-actin expression. C) AMPA expression. Protein expression was first quantified relative to GAPDH (control), followed by the fold-change relative to saline-exposed males. Data is presented as a mean ± SD. n = 3 technical replicates, each pooled sample consists of 5 animals obtained from 3 separate litters.

CHAPTER 5: DISCUSSION

5.1 Overview

In the last decades the prevalence of autism has been drastically increasing (Zablotsky *et al.*, 2014; CDC, 2018). Research has shown that although there are improved diagnostic tools allowing better detection, increased awareness of the disorder and women are having children at a later age; these factors only account for approximately 50% of the increase in ASD prevalence. The remaining contributing factors remains largely unclear (Hertz-Picciotto & Delwiche, 2009; Weintraub, 2011). However, in recent years there has been increasing evidence from both clinical and epidemiological studies that various environmental risk factors influence neurodevelopment, contributing to disorders such as ASD (Hinz *et al.*, 2008; Tamiji & Crawford, 2010a, 2010b; Liew *et al.*, 2016; Hajisoltani *et al.*, 2019). Specifically, prenatal exposure to environmental risk factors, including drugs such as misoprostol and acetaminophen, pollution/toxins, infection and inflammation are known to impact the levels of lipid signalling such as the bioactive lipid signalling molecule, prostaglandin E2 (PGE2), which is critical for healthy brain development and has been implicated in autism (Bandim *et al.*, 2003; Tamiji & Crawford, 2010a, 2010b; Brandlistuen *et al.*, 2013; Wong & Crawford, 2014). Additionally, various brain regions have been implicated in ASD including the prefrontal cortex, amygdala, cerebellum and hippocampus (Wegiel *et al.*, 2014; Ha *et al.*, 2015; Reinhardt *et al.*, 2020b; Richards, Greimel, *et al.*, 2020b). Ultimately, it is becoming increasingly critical to understand the contributing factors to the pathophysiology of ASD.

Our lab has recently determined that PGE2 exposure contributes to abnormalities in dendritic formation, differential expression of actin-dependent proteins in the developing cerebellum and associated motor deficits (Kissondoyal *et al.*, Unpublished). The implications of

PGE2 exposure on the developing hippocampus is less understood. In this study we provide evidence that a single maternal injection of PGE2 during a critical developmental window in pregnancy affects the developing hippocampus in a sex-dependent manner. In aim 1, we investigated the effect of prenatal PGE2 exposure on dendritic arborization, branch order, primary branch length, cell soma size, dendritic looping, spine morphology in males and females at two critical stages in hippocampal development, PN30 and PN90. In aim 2, we investigated the impact of PGE2 exposure on proteins critical for hippocampal function. Our study provides evidence that PGE2 exposure contributes to impaired hippocampal development, specifically abnormal dendritic morphology and expression of proteins involved in cytoskeletal architecture.

5.2 The effect of PGE2 on Dendritic Morphology

5.2.1 Dendritic Arborization and Branch Order

Sex Differences in the healthy vs. PGE2-exposed brain

In the hippocampus, we observed distinct sex differences in the healthy brain and PGE2-exposed brain at both PN30 and PN90. Specifically, at PN30 in saline and PGE2-exposed offspring, females had increased arborization at an intermediate length (40-100 μm) from the center of the cell soma compared to males **(Fig. 6, Table 1)**. Interestingly, there was no significant changes in overall primary, secondary or tertiary branching in saline and PGE2 females compared to their male counterparts at PN30 **(Fig. 7, Table 3)**. Although there were no significant sex-differences in overall branch order, the increase in dendritic arborization observed at an intermediate length in saline and PGE2 females may be attributed to increased secondary or tertiary branching at an intermediate length specifically. However, corresponding changes in secondary or tertiary branches along specific distances from the center of the neuronal soma would need to be elucidated to fully consolidate this. Studies have also examined differences in

apical and basal dendrites in hippocampal pyramidal cells (Cheng *et al.*, 2017; Barón-Mendoza *et al.*, 2021), which may also account for increases in arborization observed in PN30 saline and PGE2 females. However, this would need to be further investigated in our study. Interestingly, later in development at PN90, saline females had increased arborization closer to the cell soma, while PGE2 females had decreased arborization closer to the soma compared to males. This may be linked to corresponding changes in higher order branching. Specifically, in PN90 saline females there was a significant increase in secondary branching, while in PGE2 females there was a decrease in secondary and tertiary branching compared to their male counterparts. This indicates that saline females maintain high dendritic arborization throughout development compared to males and at PN90, PGE2 exposure disrupts this innate sex difference.

Similar to our findings, in earlier studies on rats, it was found that females had increased dendritic branching compared to males in the CA3 (CA; Cornu Ammonis) region of the hippocampus (Gould *et al.*, 1990). However, in the CA1 region of rats it was determined that males have increased dendritic branching compared to females (Markham *et al.*, 2005). Additionally, a study examining sex differences of dendritic arborization at PN28 in pyramidal cells of the CA1 region in the hippocampus, found that males had increased arborization distally, compared to females (Keil *et al.*, 2017). This potentially suggests that sex differences in dendritic arborization may be specific to the hippocampal region and cell-type, which may account for the contrasting results. Furthermore, previous studies indicate that sexually dimorphic characteristics observed during development of specific brain regions, including the hippocampus, may be attributed to the influence of estradiol and androgens during the perinatal period (Isgor & Sengelaub, 2003; Arnold, 2009; Lenz *et al.*, 2012). One study demonstrated that androgen exposure in females during early postnatal development contributes to increase

dendritic arbor and dendrite length in CA3 pyramidal cells of the hippocampus (Isgor & Sengelaub, 2003). In contrast, another study demonstrated that the loss of androgens by conducting an orchidectomy in adult male rats, contributed to an increase in mossy fibers, apical and basal dendritic branching of pyramidal cells in the CA3 region of the hippocampus. This suggests that the lack of androgen contributes to an increase in dendritic arborization in adulthood (Mendell *et al.*, 2017). These contrasting findings suggest that changes in androgen and estradiol levels during critical timepoints in perinatal and postnatal development may contribute to differences in sexually dimorphic characteristics across hippocampal development.

Furthermore, studies have also found sex differences in various factors related to hippocampal function that may contribute to sex differences in dendritic arborization observed in our study, including neuronal proliferation (Tanapat *et al.*, 1999; Rummel *et al.*, 2010), hippocampal volume over development (Qiu *et al.*, 2013), long-term potentiation (Warren *et al.*, 1995; Tada *et al.*, 2015) and GABAergic signaling (GABA; Gamma aminobutyric acid). GABAergic signaling has been of particular interest, as the switch from $GABA_A$- mediated excitation to inhibition in regions of the hippocampus during development occurs earlier in female rats contributing to differences in arborization. The developmental switch from $GABA_A$-mediated excitation to inhibition occurs in the first week of postnatal development for females, while in males it occurs within the first two weeks of postnatal development (Nuñez *et al.*, 2003; Perrot-Sinal *et al.*, 2003; Nuñez & McCarthy, 2007, 2008; Murguía-Castillo *et al.*, 2013). This suggests that males experience a longer time window of $GABA_A$- mediated excitation during development compared to females. Furthermore, studies have also shown that GABAergic signaling is influenced by hormones. Specifically, newborn male rats have presented more robust and greater $GABA_A$- mediated excitation compared to females and this response has been

exacerbated with estradiol or testosterone treatment. Interestingly, chronic estradiol exposure in males' results in an extended period of $GABA_A$- mediated excitation in hippocampal pyramidal cells (Nuñez *et al.*, 2005; Nuñez & McCarthy, 2008). This suggests that estradiol in males may contribute to a longer developmental window of $GABA_A$- mediated excitation compared to females, thereby contributing to sex differences in dendritic arborization.

To summarize, our results provide evidence of distinct sex differences in early and late hippocampal development. These sexually dimorphic characteristics of dendritic arborization in the developing hippocampus may be attributed to various influences during critical timepoints in development, including region and cell-type specificity (Keil *et al.*, 2017), susceptibility to hormonal changes (Isgor & Sengelaub, 2003; Mendell *et al.*, 2017) and the developmental transition of GABAergic signaling (Nuñez *et al.*, 2005; Nuñez & McCarthy, 2007). Additionally, our results show that innate sex-differences are maintained in PGE2-exposed males and females at PN30, however at PN90 there is a reverse in these innate sex differences. This suggests prenatal PGE2 exposure has prolonged effects later into development and may potentially dysregulate factors involved in hippocampal development mentioned above, however this would need to be further elucidated.

PGE2 Exposure in Males and Females

In the hippocampus, PGE2-exposure in male and female offspring, resulted in increased dendritic arborization at an intermediate distance (60-80) from the cell soma compared to the saline counterparts at PN30 **(Fig. 6, Table 1)**. However, at PN90 we observed an increase in arborization closer to the soma in the PGE2 male, while a decrease in arborization closer to the soma in the PGE2 female compared to their saline counterparts. There have been similar findings in the other models of ASD, such as the BTBR model. In the BTBR model of autism, it was

found that there was increased dendritic arbor in pyramidal cells of the CA1 region of the hippocampus at an intermediate length from the cell soma (Cheng *et al.*, 2017). This is similar to the finding in our PGE2-exposed male and female offspring at PN30. Additionally, in the VPA model, a well-established model of ASD, prenatal VPA exposure contributed to increased embryonic neurogenesis, however it was observed that in adult mice there was decreased dendritic processes in the dentate gyrus of the hippocampus (Juliandi *et al.*, 2015). Although this study did not specifically examine sex differences (Juliandi *et al.*, 2015), it is similar to the findings we observed in PGE2-exposed female offspring later in development at PN90. Our study suggests that there may be an overgrowth in dendritic arborization early in development due to PGE2-exposure in PN30 males and females, however this only persists in males later in development, where PN90 females experience a reduction in dendritic arbor. Ultimately, our findings suggest that PGE2-exposure has both a sex and stage specific effect.

Furthermore, there is evidence of a positive feedback loop between PGE2 and estradiol first identified in the endometrium (Waclawik *et al.*, 2009), which may potentially explain the findings of our study. The positive feedback loop in the central nervous system (CNS), was first reported in the developing cerebellum (Dean, Wright, *et al.*, 2012). During the first two weeks of postnatal development, a study provided evidence that postnatal PGE2 exposure via intracranial injections contributes to enhanced aromatase activity, subsequently increasing estradiol synthesis in Purkinje cells of the cerebellum (Dean, Wright, *et al.*, 2012). Interestingly, another study provided further evidence that inflammation in the cerebellum contributes to increased PGE2 levels due to increased aromatase activity and subsequent estradiol synthesis, resulting in reduced dendrite length and dendritic arborization of Purkinje cells during the second week of postnatal development. Inhibition of the aromatase enzyme, reduced PGE2 and estradiol levels,

reversing the effects observed on dendrite length and arborization. This was not observed during the first or third week of postnatal development of the cerebellum (Hoffman *et al.*, 2016). Furthermore, these studies have only examined the effects of cerebellar dendritic arborization by directly administering PGE2 injections postnatally (Dean, Wright, *et al.*, 2012; Hoffman *et al.*, 2016), however additional studies would need to be conducted if similar findings are observed due to prenatal PGE2 exposure. Although the impact of the PGE2-estradiol feedback loop on hippocampal dendritic arborization needs to be investigated, there is evidence that aromatase is expressed in the male and female rodent hippocampus (Hojo *et al.*, 2004; Prange-Kiel *et al.*, 2006). *In-vivo* studies also provide evidence that aromatase inhibition in hippocampal neurons leads to impairments in LTP and the expression of proteins involved in cytoskeletal structure in females, compared to males (Vierk *et al.*, 2012). This suggests aromatase is a key regulator of dendritic branching (Vierk *et al.*, 2012) and may be dysregulated by PGE2 exposure in our rodent model. Ultimately, based on recent studies, dysregulation of the PGE2-estradiol feedback loop during a critical time period in development may be a contributing factor to dendritic abnormalities in the hippocampus (Hojo *et al.*, 2004; Dean, Wright, *et al.*, 2012; Vierk *et al.*, 2012; Hoffman *et al.*, 2016).

Developmental Differences

In addition to examining the effect of and PGE2-exposure on dendritic arborization and branch order, we also investigated the effect of developmental stage **(Fig. 6, Table 2)**. We found that PN90 saline males and females have decreased branching at an intermediate length (40-80 μm) compared to their counterparts at PN30. PN90 saline females also have increased arborization closer to the soma (20 μm) compared to PN30 saline females. This indicates that there are clear sex differences during hippocampal development. Additionally, PN90 PGE2

exposed males and females had decreased dendritic arborization at an intermediate length (40-100 μm) and farther away from the soma (120-140 μm), compared to PN30 saline males and females, respectively. Additionally, PN90 PGE2 males have increased arborization closer to the soma compared to PN30 PGE2 males (20 μm). This suggests that PGE2-exposure results in a change of innate developmental differences, observed in saline offspring. Furthermore, we determined that PN90 saline males and females have increased secondary and tertiary branching compared to their counterparts at PN30 **(Fig. 7, Table 4)**. A similar trend was observed in the PGE2 males and females. This suggests the formation of secondary and tertiary branching observed over development in control males and females, is also maintained in PGE2-exposed males and females.

There are three major phases of dendritic development: an initial growth phase of dendritic branches, followed by a period of elongation and retraction and completing with dendritic stabilization (Goikolea-Vives & Stolp, 2021). The rates of each of these phases differ based on factors such as region of the brain and cell type. In humans, there is an outgrowth of dendritic branching during gestational weeks 16 to 26 and up to 36 weeks. Basal dendrites experience stabilization, with no new formation of dendritic extensions early in development compared to apical dendrites (Walkley *et al.,* 2000; Lu *et al.*, 2013a). In comparison, the mouse brain faces this significant growth in dendrites within the first week of postnatal development (PN7-PN10), which is similar to the timeline observed in humans (Clifford *et al.*, 2014; Hoshiba *et al.*, 2016; Ka *et al.*, 2016; Viale *et al.*, 2019). In the mouse visual cortex, it was shown that there was significant growth in basal arborization between PN7 and PN30. Interestingly, they determined that the number of basal dendrites was mainly established by PN7, however the length of the segments continued to significantly grow well into PN30 (Richards *et al.*, 2020).

This may potentially explain the findings of our study. In our study, we found that saline-exposed males and females later in development had reduced dendritic branching at an intermediate length, but an overall increase in higher order branching compared to their saline counterparts. This could potentially indicate that although there was an increase in higher order branching, the lengths of the higher order branches may be shorter contributing to a decrease in the number of intersecting branches at an intermediate length later in development. Furthermore, additional factors may influence the differences observed in dendritic arborization and branch order over development, including the rate or time interval of outgrowth/extension and pruning/retraction (Goikolea-Vives & Stolp, 2021).

5.2.2 Dendrite length

Sex Differences in the healthy vs. PGE2-exposed brain

In the hippocampus, we observed distinct sex differences in saline-exposed offspring at PN30, specifically females had increased primary dendrite length compared to males (**Fig. 8, Table 5)**. There were no sex differences observed in the PGE2-exposed brain at PN30, which indicates PGE2-exposure eliminates the innate sex differences that are observed. Furthermore, there were no sex differences in saline-exposed and PGE2-exposed offspring at PN90. In the human brain, neuronal growth stabilizes early in development, specifically 30-55% of cortical neurons reach their maximum length early in neurodevelopment (Becker *et al.*, 1984; Walkley *et al.*, 2000; Lu *et al.*, 2013b). A similar pattern has been observed in the mouse, where the length of the dendrite stabilizes during a specific time interval depending on the region of the brain (Clifford et al., 2014; Hoshiba et al., 2016; Ka, Chopra, Dravid, & Kim, 2016; Viale et al., 2019). The innate sex difference observed in our study is supported by other studies examining sex differences, where female rats have longer dendrite lengths compared to males in specific brain

regions, such as the locus coeruleus (Bangasser *et al.*, 2011) and CA3 region of the hippocampus (McEwen *et al.*, 1997). In contrast, a study examining dendritic length of primary and non-primary dendrites at PN0 hippocampal neurons *in-vitro* found no sex differences in the average primary dendrite length and non-primary dendrite length. However, in cortical neurons they provided evidence of increased primary dendrite length in females and no difference in non-primary dendrite length compared to males (Keil *et al.*, 2017). This suggests that sex differences observed in dendrite length is dependent on both the region of the brain, cell-type, and developmental stage.

PGE2 exposure in Males and Females

We further examined the effect of PGE2 exposure on average primary dendrite length **(Fig. 8, Table 5)**. At PN30, PGE2 males had increased dendrite length compared to saline males. PGE2 exposure did not significantly affect females. Additionally, there was no effect of PGE2-exposure on males and females at PN90. This suggests PGE2 exposure has a sex and stage specific effect. In line with our study, other research studies examining dendrite length in rodent models of ASD have found increased dendrite lengths. Specifically in the BTBR model, the lengths of the apical, basal and total dendritic arbor of hippocampal pyramidal cells was increased (Cheng *et al.*, 2017). Similarly, in MECP2 male mice, there was an increase in dendritic arborization length of pyramidal cells (Jiang *et al.*, 2013). Interestingly, prenatal exposure to Bisphenol A in rats resulted in an increase in dendrite length of primary hippocampal cells in both males and females (Thongkorn *et al.*, 2021). Although other studies have also found evidence of increased dendrite lengths in models of ASD, our study provides evidence that prenatal PGE2 exposure is sex- and stage-dependent.

Developmental Differences

In our study, we provide evidence that PN90 saline males and females have reduced dendrite length compared PN30 saline males and females **(Fig. 8, Table 6)**. A similar pattern was observed in PN90 PGE2 males and females. This suggests that in the developing brain, PGE2 exposure may not impact dendritic length. The extension of dendrites is a highly dynamic process, where in one study examining dendritic pruning and maturation of cerebellar granule cells found there was an increased rate of dendritic extension early in development, followed by stabilization and pruning of the extensions (Dhar *et al.*, 2018). Similarly, in PN0-7 hippocampal neurons *in-vitro* found that there was increased growth of dendrites during the early days *in-vitro*, followed by stabilization and retraction later *in-vitro* (Dailey & Smith, 1996). Ultimately, this suggests that in our study, the reduction in dendrite length at PN90 compared to PN30 in saline and PGE2 males, is due to stabilization and pruning mechanisms that occur over development.

5.2.3 Cross-sectional Area of the Soma

PGE2 exposure in males and females

In our study we observed that at PN30, PGE2-exposed offspring (males and females) had no significant difference compared to saline-exposed offspring (males and females) in cell soma size **(Fig. 9, Table 7)**. In contrast, at PN90 PGE2 exposed offspring had reduced cross-sectional area of the neuronal soma, compared to saline-exposed offspring. This suggests that PGE2 exposure has a stage specific effect on neuronal cross-sectional soma. In contrast to what we observed, in mature mice prenatally exposed to VPA, it was found that there was an increase in soma size of microglial cells in the hippocampus (Lucchina & Depino, 2014). In Pten mutated mice, another model of ASD, there was an increase in soma size in 1 month, 2-3 month and 4-6

month old mice in granule cells of the dentate gyrus and CA3 regions of the hippocampus (Kwon *et al.*, 2006). In contrast, in the BTBR model of ASD there was a significant reduction in soma size of CA1 pyramidal neurons (Cheng *et al.*, 2017). Similar findings have been discovered in post-mortem brains of individuals with ASD, where a decrease in neuronal soma volume was found in various regions of the brain, including CA1-CA4 region of the hippocampus, thalamus, amygdala, entorhinal cortex and nucleus accumbens (Wegiel *et al.*, 2015). These studies suggest that neuronal soma size may be dependent on region of the hippocampus, cell-type and developmental stage. In our study, PGE2 exposure has a stage-specific effect on neuronal soma size, where hypotrophy of the neuronal soma was observed in PN90 PGE2-exposed mice.

Developmental Differences

In this study, we observed an innate increase in neuronal soma size from PN30 to PN90 in saline-exposed offspring (males and females) **(Fig. 9, Table 8)**. However, there was a loss in innate differences in PGE2-exposed offspring from PN30 to PN90. Although there is a lack of longitudinal studies investigating the cross-sectional area or volume of the neuronal soma, studies have examined changes in volume of the hippocampus over development, which can be attributed to changes in factors such as the area or volume of the cell soma. One study examining hippocampal volume in mice found there was a significant in increase in the volume of both hippocampal hemispheres at 4 weeks of age, which further increased at 24 weeks of age and persisted at 36 weeks of age (Brait *et al.*, 2021). The growth of the hippocampus is known to be perturbed in ASD (Schumann *et al.*, 2004; Barnea-Goraly *et al.*, 2014; Reinhardt *et al.*, 2020a; Richards, Greimel, *et al.*, 2020a). In one study examining volume deficits in individuals with ASD between 11-23 years old, found corresponding neuronal volume deficits in specific regions

of the brain (Wegiel *et al.*, 2014). Similarly, in our model, we show that the innate growth of neuronal soma size in the hippocampus is disturbed by PGE2-exposure.

5.2.4 Dendritic Looping

In this study, we observed an increase in odds of observing a dendritic loop in PGE2-exposed offspring and a decrease in dendritic loops observed in PN90 offspring, compared to the baseline model (PN30 saline-exposed males) **(Fig. 10, Table 9)**. Interestingly, there was no impact of sex on the odds of observing dendritic loops. Self-avoidance is a critical mechanism involved in synaptogenesis to ensure appropriate dendritic growth and prevent self-fasciculation of neuronal extensions. Abnormalities have been observed in axon pathfinding and circuit formation contributing to deficits in the nervous system and disorders including, retinal dysplasia and autism (Minshew & Williams, 2007; McFadden & Minshew, 2013). Previously our lab has provided evidence that an increase in PGE2 exposure contributes to neurite looping in differentiating NE4C stem cells (Kissoondoyal & Crawford, 2021) and in the cerebellum (Kissondoyal *et al.*, Unpublished) . Although there is a lack of research examining self-fasciculation of dendrites in other models of ASD, one study examining overlapping copy number variants in autism patients found 21 overlapping genes associated with neuronal outgrowth and pathfinding, indicating one of the contributing factors to the pathophysiology of ASD is impaired neuronal pathfinding (Sbacchi *et al.*, 2010). Furthermore, we also observed a decrease of dendritic looping over development, from PN30 to PN90. Further studies across developmental timepoints would need to be conducted to examine whether self-fasciculation is an innate phenomenon during dendritic growth and neuronal pathfinding in the developing brain. However, one study provided evidence of naturally occurring loops of varying radii in rat cortical neurons, suggesting that loop formation and size of the radii may be specific to the

region of the brain and neural type (Mondal *et al.*, 2014). Overall, our results suggest dendritic looping is a naturally occurring phenomenon in the developing brain, which is increased due to PGE2-exposure.

5.2.5 Dendritic Spine Density

We observed a significant increase in dendritic spine density in PN90 saline-exposed offspring (males and females combined) compared to PN30 saline-exposed offspring, which suggests there is an increase in dendritic spines over development **(Fig. 11)**. However, PGE2-exposure did not influence dendritic spine density at PN30 and PN90, suggesting that the innate developmental difference observed in saline-exposed offspring was lost due to PGE2 exposure. In contrast to our findings, other studies have provided evidence of changes in dendritic spine density in models of ASD. Previously, in our lab we found an increase in dendritic spine density in the cerebellum of one-month old PGE2-exposed offspring (Kissondoyal *et al.,* Unpublished). Similarly, in post-mortem brains of individuals with ASD a significant increase in spine density was found in apical dendrites of pyramidal cells (Hutsler & Zhang, 2010). However, in 9 week old VPA-exposed offspring, a decrease in dendritic spine density in the CA1 hippocampal region of has been observed (Takuma *et al.*, 2014). Similarly, a decrease in dendritic spine density in the CA1 region of the hippocampus has been observed in Shank1 mutated ASD mice (Qin *et al.*, 2022). Similar to our findings, C58/J autistic-like male mice had no changes in dendritic spine density in apical and basal dendrites of pyramidal neurons from the hippocampus, however they found decreased dendritic spine density in the prefrontal cortex of apical dendrites (Barón-Mendoza *et al.*, 2021). Overall, the contrasting findings regarding spine density suggests that changes in dendritic spine density is highly dynamic and may be regionally and cell-type specific, as well as, specific to the orientation of the dendrite itself.

During development, dendritic spine density is known to drastically increase during early postnatal stages, followed by a significant reduction later in development due to pruning mechanisms (Rakic *et al.*, 1986). In contrast to our findings, one study using in-*vivo* imaging to track dendritic spine turnover during development, found there was a 25% net loss of dendritic spines between one to four-months in the cerebral cortex of mice and follow 4 months, the number of spines remained stable (Zuo, Lin, *et al.*, 2005). Previous studies have also found an increase rate of spine elimination in neocortical pyramidal cells of adolescent mice (Holtmaat *et al.*, 2005; Zuo, Yang, *et al.*, 2005). Interestingly, a recent study examining spine turnover in the CA1 region of the hippocampus using *in-vivo* imaging found that adult hippocampal neurons have largely distinct spine dynamics compared to the neocortex, including percentage of impermanent spines and turnover time, which suggests spine dynamics is specific to the brain region and timepoint in development (Attardo *et al.*, 2015). Although in our study sex was found not to impact dendritic spine density, studies in the past few decades have suggested that hippocampal spine dynamics is highly impacted by hormonal changes over development (Murphy & Segal, 1996; Murphy *et al.*, 1998; Leranth *et al.*, 2003; Jacome *et al.*, 2016). One study examining the impact of estradiol rat hippocampal neurons in-vitro, found estradiol reduces GABAergic inhibition thereby increasing dendritic spine density (Murphy *et al.*, 1998). Similarly, in female and male rodents both estradiol and testosterone increase spine density in the CA1 region (Jacome *et al.*, 2016). Thus, hippocampal spine dynamics is highly sensitive to hormonal changes, which may also be a contributing to factor to an increase in spine density observed in our results. However, further studies would need to be conducted to fully understand the relationship between hormonal changes and link to spine density dynamics over development.

5.2.6 Dendritic Spine Morphologies

Dendritic spines are small protrusions found along the dendrite itself, highly involved in excitatory and inhibitory synapses in the brain (Peters & Kaiserman-Abramof, 1970; Tønnesen *et al.*, 2014). Synaptic activity is highly regulated by the morphology of dendritic spines during development, where thin and stubby shaped spines (*immature spines*) are transient and highly expressed in the developing brain, whereas mushroom shaped spines (*mature spines*) are stable and found in the developed brain (Peters & Kaiserman-Abramof, 1970; Grutzendler *et al.*, 2002a; Holtmaat *et al.*, 2005; Tønnesen *et al.*, 2014). We examined the effect of sex, developmental stage and PGE2-exposure on the likelihood of observing mature dendritic spines **(Table 10)**. Interestingly, we found no effect of sex or PGE2-exposure on the likelihood of observing mature spines, however stage increased the odds of observing mature spines in the hippocampus. In contrast to what we found in the hippocampus, our lab previously found an increased likelihood of observing mature spines in the cerebellum of one-month old PGE2-exposed males and females (Kissondoyal *et al.*, Unpublished). Similarily, in the cerebral cortex of VPA-exposed offspring a decrease in immature spines and an increase in mushroom shaped spines were found (Mahmood *et al.*, 2018). In the hippocampus of C58/J autistic-like mice, they found changes in spine morphology according to their dendrite location. In apical and basal dendrites, there was an increase in stubby (*immature*) spines, however, in basal dendrites there was an increase in filipodia/thin (*highly transient and immature*) spines (Barón-Mendoza *et al.*, 2021). This indicates that differences in dendtitic spine morphology may be regionally specific and specific relative to the dendritic location. Although we did not observe any overall differences in spine morphology due to PGE2-exposure, there may be differences based on dendrite location and further analysis would need to be conducted.

Although we did not fnd sex differences in the likelihood of observing mature dendritic spines, some studies have found regionally specific sex-differences in the brain. Previously, our lab has found that PN30 females have decreased mushroom-shaped spines compared to males in the cerebellum (Kissondoyal *et al.,* Unpublished). In the auditory and visual cortex of mice, females had reduced stubby and mushroom shaped spines compared to males during adolescence, with no signifcant age-sex interactions (Parker *et al.*, 2020). Similar to our findings in the hippocampus, one study examining sex differences of CA1 hippocampal neurons *in-vitro* found no overall differences in the number of mature spines. However, when taking stages of the estrus cycle into account they found a decrease in mature spines in females compared to males (Brandt *et al.*, 2020). Thus, sex differences in dendritic spine morphologies may differ based on the region of the brain, as well as, the stage of estrus cycle.

In addition, we found a significant increase in mushroom-shaped spines over development, which is highly consistent with findings across various brain regions, as mushroom-shaped spines are highly present in stable synapses and the developed brain (Peters & Kaiserman-Abramof, 1970; Grutzendler *et al.*, 2002a; Holtmaat *et al.,* 2005; Tønnesen *et al.,* 2014). In the visual cortex of male and female mice, PN84 male and female mice had an increase of short mushroom-shaped spine density (Parker *et al.,* 2020). Similarily, using two-photo *in-vivo* imaging of layer-5 pyramidal neurons in the cortex, they observed a high turnover of fliipodia-like spines during 2-4 weeks postnatally, which either led to the formation of mature dendritic spines or the elimination of the filipodia-like spines altogether (Grutzendler *et al.,* 2002a). Similar findings have been determined in other regions of the brain in rodents, including the olfactory bulb (Mizrahi & Katz, 2003), amygdala (Ryan *et al.*, 2016) and hippocampus

(Mizrahi *et al.*, 2004). Thus, consistent with our findings, there is a significant formation of mature dendritic spines contributing to stable synapses in the developed brain.

5.3 The effect of PGE2 on Hippocampal Protein Expression

We observed distinct changes in dendritic morphology, which could potentially be due to aberrant expression of proteins responsible for cytoskeletal architecture and axon guidance during neurodevelopment. We analyzed the expression of ß-actin, spinophilin, NMDA2A receptor (N-methyl-D-aspartate 2A subunit) and AMPA (Alpha-amino-3-hydroxy-5-methyl-4-isoxazole propionic acid) receptor, which are all critical for hippocampal functions including dendritic growth and long-term potentiation. We were only able to determine a model of *best-fit* for ß-actin and AMPA, which excluded sex as a factor. Based on this, we determined that PGE2-exposed offspring (males and females) have decreased expression of ß-actin. We found no significant difference in AMPA expression between PGE2-exposed and saline-exposed offspring.

5.3.1 ß-actin and Spinophilin Expression

ß-actin plays a pivotal role in dendritic spine morphogenesis, neuronal migration, axonal growth and guidance during neurodevelopment which is regulated by polymerization/depolymerization of actin filaments (Cheever *et al.*, 2012; Cheever & Ervasti, 2013). Spinophilin is an actin-scaffolding protein that is involved in regulating actin dynamics, contributing to changes in spine density and morphology during neurodevelopment, as well as synaptic plasticity (Allen *et al.*, 1997; Feng *et al.*, 2000). In our study, in PGE2-exposed males and females we observed sex- and stage-specific changes in dendritic morphology, including dendritic arborization, branch order and primary dendrite length, which may be associated with a corresponding decrease in ß-actin **(Fig. 12)**. In one study examining the role of ß-actin in the

hippocampus, found ß-actin ablation resulted in drastic changes in the morphology of the pyramidal cell layers in the CA1 and dentate gyrus, as well as, behavioral manifestations such as hyperactivity, reduced spatial reasoning, learning and memory (Cheever *et al.*, 2012), suggesting ß -actin plays an essential role in driving hippocampal functions. Previously, our lab has found that impaired dendritic growth may be associated with a decrease in ß-actin levels, in PGE2-exposed differentiating NE4C stem cells (Kissoondoyal & Crawford, 2021) and the cerebellum of male and female offspring (Kissondoyal *et al.*, Unpublished). We also observed similar changes due to a decrease in PGE2 levels in the cerebellum of COX2-KI mice (Kissoondoyal *et al.*, 2021). Other studies examining actin dynamics have found similar results, Shank3-deficient mice have decreased actin filament expression in the prefrontal cortex, associated with increased expression of actin depolymerizing factors (Duffney *et al.*, 2015). Impaired actin dynamics has also been implicated in clinical studies of ASD and neurodevelopmental disorder. Stem cells from exfoliated deciduous teeth of ASD patients demonstrated aberrant actin filament reconstruction (Griesi-Oliveira *et al.*, 2018). Additionally, one of the patients in the study had previously shown altered neurite growth and morphology in induced-pluripotent stem cells (iPSC) derived neuronal cells in a previous study by the same group (Griesi-Oliveira *et al.*, 2015, 2018). In individuals with Rett syndrome, a neurodevelopmental disorder that also falls on the spectrum, red bloods had decreased ß -actin levels (Cortelazzo *et al.*, 2014). Both animal and clinical studies support our findings, indicating that impaired actin dynamics may be linked to abnormal dendritic morphology, contributing to ASD-related symptoms.

We also examined the effect of PGE2-exposure on spinophilin, where we observed sex-specific trends due to PGE2-exposre on the fold-change of spinophilin expression (Fig. 12). Although we were unable to conduct further analysis on spinophilin expression in PGE2-exposed

male and female offspring, it has been implicated in other studies that have found abnormal dendritic growth. In our study we found no effect of PGE2-exposure on spine density and dendritic spine morphology, which may indicate that the expression of spinophilin may not be impacted. However, further analysis examining biological replicates would need to be conducted to fully elucidate this (see future directions). In contrast to what we found in the hippocampus, our lab has found an increase and decrease expression of spinophilin in the cerebellum of COX-KI and PGE2-exposed males and females, respectively. The changes in spinophilin expression were associated with an increase spine density of mature dendritic spines (Kissoondoyal *et al.*, 2021; Kissoondoyal *et al.*, Unpublished). Similarly, in rats administered a direct PGE2-injection into the cerebellum during postnatal stages demonstrated decreased levels of spinophilin (Dean, Knutson, *et al.*, 2012). In contrast, in the BTBR model of autism there was an increase in hippocampal spinophilin levels associated with ASD-behavioral symptoms, suggesting aberrant spinophilin expression one of the contributing factors to impaired hippocampal functions associated with ASD (Jasien *et al.*, 2014). Interestingly, in the hippocampus of spinophilin knockout mice there was a reduction in the overall volume of the hippocampus, thickness of the hippocampal layers and increased number of dendritic spines, suggesting that spinophilin is highly involved in regulating dendritic morphological changes (Feng *et al.*, 2000). Thus, spinophilin, a protein highly expressed in dendritic spines is critical for hippocampal driven functions and may potentially be impacted by PGE2-exposure during hippocampal development, however this would need to be further examined in future studies, as mentioned below.

5.3.2 NMDA2A and AMPA Receptor Expression

In the hippocampus, both NMDA and AMPA receptors are involved in driving a mechanism known as long-term potentiation (LTP), which is responsible for hippocampal learning and memory. During LTP, the binding of the neurotransmitter glutamate to NMDA results in downstream signaling cascades, followed by an induction of AMPA expression in the neuronal membrane, which regulates dendritic spine dynamics (Lynch *et al.*, 1990; Sumi & Harada, 2020). In our study, we were unable to conduct further analysis on the expression of NMDA2A due to non-significant modelling of the data **(Fig. 12)**. Although this was the case, we observed sex-specific trends due to PGE2-exposre on the fold-change of NMDA2A expression. However, further analysis using biological replicates would need to be conducted to fully understand whether PGE2-exposure impacts NMDA expression in male and female offspring. Our lab has previously found genes associated with glutamate signaling and synaptic plasticity perturbed in COX2-KI mice in early embryonic stages (Rai-Bhogal, Ahmad, *et al.*, 2018). One of the proteins affected was calmodulin-kinase 2b (CAMK2b), a downstream enzyme involved in long-term potentiation and regulated by NMDA receptor expression (Rai-Bhogal, Ahmad, *et al.*, 2018). One study using cultured mice cortical neurons inhibited NMDA2A expression, which resulted in reduced expression of inflammation-induced PLA2 and COX2, which subsequently reduced PGE2 levels (Rajagopal *et al.*, 2019). Additionally, hippocampal rat slices exposed to COX2 inhibitors have reduced post-synaptic membrane excitability, which is tightly regulated by NMDA2A expression. Subsequent exposure to PGE2 rescued impaired membrane excitability caused by COX2 inhibitors (Chen *et al.*, 2002). This suggests that there is a strong relationship between COX2/PGE2 signaling and NMDA-induced long-term potentiation in the brain. Additionally, NMDA has been highly implicated in models of ASD, including increased

expression in cortical neurons of VPA-exposed offspring (Rinaldi *et al.*, 2007) and reduced NMDA-dependent LTP in the CA1 region of Fmr1 mice (Yau *et al.*, 2016). Additionally, NMDA inhibition in fragile-x-syndrome (FXS) mice rescued impaired long-term depression (LTD), a learning and memory mechanism also regulated by NMDA (Hugger Toft *et al.*, 2016). Although we unable to determine whether PGE2-exposure impacts NMDA protein expression, previous studies suggest a relationship between NMDA and COX2/PGE2 signaling, as well as impaired NMDA expression is observed in models of autism. As such, additional studies would need to be conducted to fully elucidate whether PGE2-exposure impacts NMDA-induced LTP at the circuit and behavioural level.

In our study, we found no significant effect of PGE2-exposure on hippocampal AMPA receptor expression (Fig. 12). In contrast to our study, previous research indicates PGE2 signaling regulates AMPA function. In female rats administered a direct PGE2 injection into the preoptic area, experienced masculinization of behaviors, which was reversed by an inhibitor of AMPA (Wright & McCarthy, 2009). The same group provided evidence that increased PGE2 levels in the preoptic area induces phosphorylation of AMPA, thereby increasing AMPA insertion in the neuronal membrane (Lenz *et al.*, 2011). However, in contrast to our study, McCarthy and colleagues administer PGE2 postnatally and conduct subsequent tests during early postnatal development which may explain the different findings. Impaired AMPA function has been implicated in autism and neurodevelopmental disorder, where in neural progenitor cells derived from males with FXS (Fragile X syndrome), there was an increased expression of AMPA, contributing to enhanced neuronal differentiation, altered morphology and circuit formation, which was ameliorated via AMPA inhibition (Achuta *et al.*, 2018). Similar findings have been identified in Fmr1 knockout mice, where behavioural deficits in spatial patterning was

associated with reduced AMPA-induced excitatory-post synaptic potentials (EPSPs) (Yau *et al.*, 2016). In Cntnap2 knockout and VPA-exposed mice, social deficits, a symptom of ASD, was found to be ameliorated following administration of an AMPA antagonist (Kim *et al.*, 2018). Overall, dysregulation of both NMDA and AMPA receptors has been implicated in autism, however, these studies often focus on juvenile or adolescent mice. In our study, we examined NMDA and AMPA expression in mature mice, which may explain the opposing results. We observed that PGE2-exposure had a sex- and stage-specific effect on hippocampal dendritic morphology and as such, AMPA and NMDA expression may be impacted during early postnatal development, which needs to be investigated. Additionally, further analysis examining biological replicates to account for differences between male and female offspring would need to be conducted.

5.4 Implications of Abnormal Cytoskeletal Dynamics

In our study, we observed distinct sex-dependent changes in dendritic morphology due to PGE2 exposure over hippocampal development, with a corresponding change in ß-actin expression, which can ultimately impact synaptic transmission in the brain. Dendrites are highly polarized, and their primary function is processing neuronal information, where the organization of dendritic arborization dictates the synaptic input field. Factors such as dendritic volume, length, width and surface area ultimately determine the size of the receptive field, thereby influencing synaptic inputs (Spruston, 2008; Salazar *et al.*, 2016). Thus, during development it is crucial that the dendritic size directly corresponds to the size of presynaptic terminals for appropriate neuronal processing (Salazar *et al.*, 2016). Hippocampal arbours are uniquely organized and receive input from distinct regions. Neurons located in the CA1 region of the hippocampus, consist of apical and basal dendrites, where apical dendrites receive their input

from the entorhinal cortex, while basal dendrites receive their input from the CA3 region (Spruston, 2008). In our study, we found abnormal growth of hippocampal dendritic arborization, which could largely alter synaptic inputs in hippocampal regions, thereby impacting hippocampal functions. Synaptic integration is highly dependent on distance, the extent of arborization and length of the primary dendrites from the center of the cell soma. Synapses occurring at a greater distance would not highly influence the stimulation of an action potential due to the dissipation of the signal across a large distance (Williams & Stuart, 2003). One study found that excitatory post-synaptic current (EPSC) was inversely related to total dendritic branch length in hippocampal neurons, suggesting that increased branch length would contribute to the dissipation of EPSCs along the dendrite (Peng *et al.*, 2009). In our study we found there was a sex- and stage-dependent effect on dendrite length, as such, changes in dendrite length may contribute to corresponding changes in EPSCs in the hippocampus. However, neurons may compensate for larger dendritic distances by altering the conductance (Williams & Stuart, 2003). In apical dendrites of CA1 pyramidal neurons, they found a direct relationship between EPSP amplitudes and distance of the dendrite from the soma, where increased EPSP amplitudes were observed at greater dendritic distances (Magee & Cook, 2000). Similarly, another study found that signal propagation due to larger dendritic distances may be compensated for by increased AMPA receptor expression at distal regions on the dendrite (Nicholson *et al.*, 2006). Although we found aberrant dendritic growth in PGE2-exposed male and female offspring during hippocampal development, the brain may compensate for these changes by altering conductance at the circuit level or the expression of proteins involved in synaptic input at the molecular level. Thus, it is also critical to obtain an understanding of the effect of PGE2-exposure on synaptic input/output currents and conductance.

Furthermore, during neurodevelopment differentiated neurons migrate to their specific location and form specific connections with neighboring neurons directed by both intrinsic and extrinsic cues (Marín *et al.*, 2010). Dendritic growth is restricted to a distinct spatial region, guided by a combination of attractive and repulsive cues. Specifically, dendrites extending from the same soma are directed by repulsive cues which results in self-avoidance or fasciculation. Dendrites from neurons that perform the same function are also guided by attractive and repulsive cues to prevent overlap, known as dendritic tiling. Ultimately, these factors contribute to dendritic arbor maximizing the area they cover and prevent redundancy (Grueber & Sagasti, 2010). In our study, we found increased dendritic loops in the hippocampus due to PGE2 exposure, suggesting that PGE2-exposure interferes with critical steps in neuronal pathfinding and guidance during development. Overall, we determined that prenatal PGE2 exposure impacts dendritic morphology during hippocampal development in a sex-dependent manner, which can contribute to deficits in synaptic transmission and axon guidance.

5.5 The Pathophysiology of Autism

The prevalence of ASD has been exponentially increasing over the past several decades, impacting 1-2% Canadians (Anagnostou *et al.*, 2014; Zablotsky *et al.*, 2014). With the rising prevalence of ASD, the social cost and financial burden is also drastically increasing (Cakir *et al.*, 2020). As such, there is an urgent need to address the increasing prevalence and rising socioeconomic impact of ASD by investigating contributing factors to the etiology of ASD. The heterogeneity of autism is reflected by various contributing factors and deformities in a multitude of brain regions (Bandim *et al.*, 2003; Rossignol, Genuis and Frye, 2014; Liew *et al.*, 2016; R. Richards *et al.*, 2020b; Reinhardt *et al.*, 2020). There has been growing evidence of atypical dendritic growth contributing to the pathophysiology of ASD in both animal and human studies

in various brain regions. In addition, the relationship between the hippocampus and ASD was previously overlooked, as it was originally believed that hippocampal deficits were not a major contributing factor to the major behavioural domains that characterize ASD. However, recent research suggests hippocampal impairments may contribute to deficits in social communication, cognition and lead to restricted/repetitive behaviours (Banker *et al.*, 2021). Thus, our study focused on understanding the sex-dependent consequences of PGE2-exposure on cytoskeletal dynamics and how it could contribute to hippocampal-dependent learning, memory and spatial reasoning deficits over development.

In this study, we observed distinct morphological changes in dendritic arbor during hippocampal development in PGE2-exposed males and females, which may be driven by atypical expression of proteins involved in cytoskeletal architecture and contribute to hippocampal relate behavioral deficits. Previously, in our COX2-KI and PGE2-exposed offspring, we also observed abnormal dendritic morphology and spine density in the cerebellum, which contributed to atypical motor behaviours early in development (Kissoondoyal *et al.*, 2021). Similarly, in PN70 VPA-exposed offspring, there was an increase in neuronal arborization in the nucleus accumbens, prefrontal cortex, amygdala and decreased arborization in the hippocampus, contributing various behavioural deficits including locomotion and exploratory behaviour (Bringas *et al.*, 2013). Studies in post-mortem brains of ASD patients have found similar results. In the amygdala of post-mortem brains ranging from early childhood to late adulthood, there was an increase in spine density in young cases of ASD, which decreased over development followed by no significant difference between ASD and healthy individuals later in adulthood (Weir *et al.*, 2018). This is one of the major studies that examines the trajectory of dendritic growth over development in humans, providing evidence that ASD-related symptoms

in early childhood may be related to aberrant dendritic growth in the amygdala, one of the many regions implicated in autism (Weir *et al.*, 2018). Similarly, Hutsler and Zhang (2010) found increased spine densities in the superficial layers of the frontal, temporal, and parietal lobe regions of post-mortem brains from ASD individuals. Interestingly, they found that high dendritic spine densities was correlated with ASD patients would had decreased levels of cognitive functioning (Hutsler & Zhang, 2010). Ultimately, both animal and human studies have found aberrant growth of dendritic arbor in brain regions implicated in ASD, including the hippocampus, which leads to changes in synaptic transmission and ultimately contributing to ASD-related behavioral symptoms.

5.6 Study limitations and Future Directions

In the first aim of our study, we examined dendritic arborization of cells across the whole hippocampus using Golgi-Cox staining, followed by confocal microscopy. The hippocampus consists of various regions (e.g. CA1-CA3 and dentate gyrus) and cell-types (e.g. pyramidal, granule) which all have different functions and can potentially be affected by PGE2-exposure differently. Our study did not take hippocampal-regions and cell-types into account. However, future studies can examine specific cell-types within hippocampal regions using techniques such as primary cell culture or two-photo *in-vivo* microscopy (Grutzendler, Kasthuri and Gan, 2002; Traetta *et al.*, 2021). In the second aim of our study, we investigated the effect of PGE2-exposure on hippocampal cytoskeletal proteins using western blotting analysis. For each of the saline- and PGE2-exposed groups, we pooled samples from five different males and females obtained from three separate litters to obtain a global perspective of protein expression for each of the conditions, as previously conducted in our lab (Kissoondoyal & Crawford, 2021; Kissoondoyal *et al.*, 2021). We also pooled samples due to the limited protein aliquots from hippocampal

samples. In addition, due to limitations caused by the pandemic our breeding protocols were delayed, and we were unable to examine stage-specific effects of protein expression. Thus, we focused on protein expression in the mature brain at PN90. However, future work in our lab will focus on conducting western blot analysis at both PN30 and PN90 using biological replicates, instead of pooled samples. Our second aim also does not consider differences in expression in hippocampal regions and cell-types, as such, future work in the lab will use immunohistochemistry to complement my data. Furthermore, additional proteins highly involved in hippocampal cytoskeletal dynamics could be examined, such as neurotrophic factors which have been perturbed due to environmental risk factors in the hippocampus of ASD models (Juliandi *et al.*, 2015). My study provides us with a preliminary understanding of hippocampal impairments due to PGE2-exposure may be driven by abnormal dendritic growth over development. However, it is critical to obtain a holistic perspective of deficits, including at the circuit and behavioral level. Currently, future studies in the lab are focusing on circuit level deficits in the dorsal and ventral regions of the hippocampus by examining input/output current, paired-pulse facilitation and LTP. Additionally, behavioral tests using the Morris water maze and Barnes maze test will be conducted to investigate whether these morphological, molecular and potential circuit level deficits contribute to learning, memory and spatial reasoning deficits at the behavioural level.

5.7 Concluding Remarks

This study examined the role of prenatal PGE2-exposure on dendritic morphology in the hippocampus of male and female offspring. We provided evidence that disruption of COX2/PGE2 signaling has sex-dependent consequences on cytoskeletal dynamics in the developing hippocampus. In our first aim, we used Golgi-Cox staining, followed by confocal

microscopy and we observed distinct changes in dendritic arborization, length, branch order, cross-sectional area of the soma and looping in both males and females. In our second aim, we identified that these morphological changes may be driven by changes in the expression of proteins critical for cytoskeletal architecture, such as ß-actin. Disruption of cytoskeletal architecture may disrupt hippocampal circuit level dynamics, contributing to learning, memory and spatial reasoning deficits, which would need to be elucidated in future studies. Ultimately, our study provides strong evidence of the importance of COX2/PGE2 signaling in the developing hippocampus in males and females and how it may contribute to the pathophysiology of ASD.

REFERENCES

Aarum, J., Sandberg, K., Haeberlein, S.L.B., & Persson, M.A.A. (2003) Migration and differentiation of neural precursor cells can be directed by microglia. *Proc. Natl. Acad. Sci. U. S. A.*, **100**, 15983–15988.

Abu-Khaklil, A., Fu, L., Grove, E.A., Zecevic, N., & Geschwind, D.H. (2004) Wnt genes define distinct boundaries in the developing human brain: Implications for human forebrain patterning. *J. Comp. Neurol.*, **474**, 276–288.

Achuta, V.S., Möykkynen, T., Peteri, U.K., Turconi, G., Rivera, C., Keinänen, K., & Castrén, M.L. (2018) Functional changes of AMPA responses in human induced pluripotent stem cell-derived neural progenitors in fragile X syndrome. *Sci. Signal.*, **11**.

Alebouyeh, M., Takeda, M., Onozato, M.L., Tojo, A., Noshiro, R., Hasannejad, H., Inatomi, J., Narikawa, S., Huang, X.L., Khamdang, S., Anzai, N., & Endou, H. (2003) Expression of human organic anion transporters in the choroid plexus and their interactions with neurotransmitter metabolites. *J. Pharmacol. Sci.*, **93**, 430–436.

Allen, P.B., Ouimet, C.C., & Greengard, P. (1997) Spinophilin, a novel protein phosphatase 1 binding protein localized to dendritic spines. *Proc. Natl. Acad. Sci. U. S. A.*, **94**, 9956.

Amateau, S.K. & McCarthy, M.M. (2004) Induction of PGE2 by estradiol mediates developmental masculinization of sex behavior. *Nat. Neurosci.*, **7**, 643–650.

American Psychiatric Association (2014) What Is Autism Spectrum Disorder? [WWW Document]. URL https://www.psychiatry.org/patients-families/autism/what-is-autism-spectrum-disorder

Anagnostou, E., Zwaigenbaum, L., Szatmari, P., Fombonne, E., Fernandez, B.A., Woodbury-

Smith, M., Brian, J., Bryson, S., Smith, I.M., Drmic, I., Buchanan, J.A., Roberts, W., & Scherer, S.W. (2014) Autism spectrum disorder: Advances in evidence-based practice. *CMAJ*,.

Andrade, C. (2016) Use of acetaminophen (paracetamol) during pregnancy and the risk of autism spectrum disorder in the offspring. *J. Clin. Psychiatry*, **77**, e152–e154.

Andreasson, K. (2010) Emerging roles of PGE2 receptors in models of neurological disease. *Prostaglandins Other Lipid Mediat.*,.

Anna, X., Toft, K.H., Lundbye, C.J., Tue, X., & Banke, G. (2016) Neurobiology of Disease Dysregulated NMDA-Receptor Signaling Inhibits Long-Term Depression in a Mouse Model of Fragile X Syndrome.

Arnold, A.P. (2009) The organizational-activational hypothesis as the foundation for a unified theory of sexual differentiation of all mammalian tissues. *Horm. Behav.*, **55**, 570–578.

Atladóttir, H.Ó., Thorsen, P., Østergaard, L., Schendel, D.E., Lemcke, S., Abdallah, M., & Parner, E.T. (2010) Maternal infection requiring hospitalization during pregnancy and autism spectrum disorders. *J. Autism Dev. Disord.*, **40**, 1423–1430.

Attardo, A., Fitzgerald, J.E., & Schnitzer, M.J. (2015) Impermanence of dendritic spines in live adult CA1 hippocampus. *Nat. 2015 5237562*, **523**, 592–596.

Aylward, E.H., Minshew, N.J., Goldstein, G., Honeycutt, N.A., Augustine, A.M., Yates, K.O., Barta, P.E., & Pearlson, G.D. (1999) MRI volumes of amygdala and hippocampus in non-mentally retarded autistic adolescents and adults. *Neurology*, **53**, 2145–2150.

Bahn, A., Ljubojević, M., Lorenz, H., Schultz, C., Ghebremedhin, E., Ugele, B., Sabolić, I., Burckhardt, G., & Hagos, Y. (2005) Murine renal organic anion transporters mOAT1 and mOAT3 facilitate the transport of neuroactive tryptophan metabolites. *Am. J. Physiol. - Cell*

Physiol., **289**.

Bandim, J., Ventura, L., Miller, M., Almeida, H., & Costa, A. (2003) Autism and Möbius sequence: an exploratory study of children in northeastern Brazil. *Arq. Neuropsiquiatr.*, **61**, 181–185.

Bangasser, D.A., Zhang, X., Garachh, V., Hanhauser, E., & Valentino, R.J. (2011) Sexual dimorphism in locus coeruleus dendritic morphology: a structural basis for sex differences in emotional arousal. *Physiol. Behav.*, **103**, 342–351.

Banker, S.M., Gu, X., Schiller, D., & Foss-Feig, J.H. (2021) Hippocampal contributions to social and cognitive deficits in autism spectrum disorder. *Trends Neurosci.*, **44**, 793–807.

Barnea-Goraly, N., Frazier, T.W., Piacenza, L., Minshew, N.J., Keshavan, M.S., Reiss, A.L., & Hardan, A.Y. (2014) A preliminary longitudinal volumetric MRI study of amygdala and hippocampal volumes in autism. *Prog. Neuro-Psychopharmacology Biol. Psychiatry*, **48**, 124–128.

Barón-Mendoza, I., Maqueda-Martínez, E., Martínez-Marcial, M., De la Fuente-Granada, M., Gómez-Chavarin, M., & González-Arenas, A. (2021) Changes in the Number and Morphology of Dendritic Spines in the Hippocampus and Prefrontal Cortex of the C58/J Mouse Model of Autism. *Front. Cell. Neurosci.*, **15**, 370.

Bates, D., Mächler, M., Bolker, B.M., & Walker, S.C. (2015) Fitting linear mixed-effects models using lme4. *J. Stat. Softw.*, **67**.

Becker, L.E., Armstrong, D.L., Chan, F., & Wood, M.M. (1984) Dendritic development in human occipital cortical neurons. *Brain Res.*, **315**, 117–124.

Bennett, C.N. & Horrobin, D.F. (2000) Gene targets related to phospholipid and fatty acid metabolism in schizophrenia and other psychiatric disorders: an update. *Prostaglandins.*

Leukot. Essent. Fatty Acids, **63**, 47–59.

Blundell, J., Blaiss, C.A., Etherton, M.R., Espinosa, F., Tabuchi, K., Walz, C., Bolliger, M.F., Südhof, T.C., & Powell, C.M. (2010) Neuroligin-1 Deletion Results in Impaired Spatial Memory and Increased Repetitive Behavior. *J. Neurosci.*, **30**, 2115–2129.

Boland, L.M., Drzewiecki, M.M., Timoney, G., & Casey, E. (2009) Inhibitory effects of polyunsaturated fatty acids on Kv4/KChIP potassium channels. *Am. J. Physiol. - Cell Physiol.*, **296**, 1003–1014.

Bosetti, F., Weerasinghe, G.R., Rosenberger, T.A., & Rapoport, S.I. (2003) Valproic acid down-regulates the conversion of arachidonic acid to eicosanoids via cyclooxygenase-1 and -2 in rat brain. *J. Neurochem.*, **85**, 690–696.

Bozdagi, O., Sakurai, T., Papapetrou, D., Wang, X., Dickstein, D.L., Takahashi, N., Kajiwara, Y., Yang, M., Katz, A.M., Scattoni, M.L., Harris, M.J., Saxena, R., Silverman, J.L., Crawley, J.N., Zhou, Q., Hof, P.R., & Buxbaum, J.D. (2010) Haploinsufficiency of the autism-associated Shank3 gene leads to deficits in synaptic function, social interaction, and social communication.

Brait, V.H., Wright, D.K., Nategh, M., Oman, A., Syeda, W.T., Ermine, C.M., O'Brien, K.R., Werden, E., Churilov, L., Johnston, L.A., Thompson, L.H., Nithianantharajah, J., Jackman, K.A., & Brodtmann, A. (2021) Longitudinal hippocampal volumetric changes in mice following brain infarction. *Sci. Reports 2021 111*, **11**, 1–13.

Brandlistuen, R.E., Ystrom, E., Nulman, I., Koren, G., & Nordeng, H. (2013) Prenatal paracetamol exposure and child neurodevelopment: A sibling-controlled cohort study. *Int. J. Epidemiol.*, **42**, 1702–1713.

Brandt, N., Löffler, T., Fester, L., & Rune, G.M. (2020) Sex-specific features of spine densities

in the hippocampus. *Sci. Reports 2020 101*, **10**, 1–12.

Bringas, M.E., Carvajal-Flores, F.N., López-Ramírez, T.A., Atzori, M., & Flores, G. (2013) Rearrangement of the dendritic morphology in limbic regions and altered exploratory behavior in a rat model of autism spectrum disorder. *Neuroscience*, **241**, 170–187.

Brown, T.I., Whiteman, A.S., Aselcioglu, I., & Stern, C.E. (2014) Structural differences in hippocampal and prefrontal gray matter volume support flexible context-dependent navigation ability. *J. Neurosci.*, **34**, 2314–2320.

Cakir, J., Frye, R.E., & Walker, S.J. (2020) The lifetime social cost of autism: 1990–2029. *Res. Autism Spectr. Disord.*, **72**, 101502.

Calderón-Garcidueñas, L., Franco-Lira, M., Torres-Jardón, R., Henriquez-Roldán, C., Barragán-Mejía, G., Valencia-Salazar, G., Gonzaléz-Maciel, A., Reynoso-Robles, R., Villarreal-Calderón, R., & Reed, W. (2007) Pediatric Respiratory and Systemic Effects of Chronic Air Pollution Exposure: Nose, Lung, Heart, and Brain Pathology. *Toxicol. Pathol.*, **35**, 154–162.

Calderón-Garcidueñas, L., Kulesza, R.J., Doty, R.L., D'Angiulli, A., & Torres-Jardón, R. (2015) Megacities air pollution problems: Mexico City Metropolitan Area critical issues on the central nervous system pediatric impact. *Environ. Res.*,.

CDC (2018) Data & Statistics on Autism Spectrum Disorder [WWW Document]. URL https://www.cdc.gov/ncbddd/autism/data.html

Cercato, M.C., Vázquez, C.A., Kornisiuk, E., Aguirre, A.I., Colettis, N., Snitcofsky, M., Jerusalinsky, D.A., & Baez, M. V. (2016) GluN1 and GluN2A NMDA Receptor Subunits Increase in the Hippocampus during Memory Consolidation in the Rat. *Front. Behav. Neurosci.*, **10**.

Chaddad, A., Desrosiers, C., Hassan, L., & Tanougast, C. (2017) Hippocampus and amygdala

radiomic biomarkers for the study of autism spectrum disorder. *BMC Neurosci.*, **18**, 1–12.

Cheever, T.R. & Ervasti, J.M. (2013) Actin isoforms in neuronal development and function. *Int. Rev. Cell Mol. Biol.*, **301**, 157–213.

Cheever, T.R., Li, B., & Ervasti, J.M. (2012) Restricted morphological and behavioral abnormalities following ablation of β-actin in the brain. *PLoS One*, **7**.

Chen, C. & Bazan, N.G. (2005) Endogenous PGE2 regulates membrane excitability and synaptic transmission in hippocampal CA1 pyramidal neurons. *J. Neurophysiol.*, **93**, 929–941.

Chen, C., Magee, J.C., & Bazan, N.G. (2002) Cyclooxygenase-2 regulates prostaglandin E2 signaling in hippocampal long-term synaptic plasticity. *J. Neurophysiol.*, **87**, 2851–2857.

Cheng, N., Alshammari, F., Hughes, E., Khanbabaei, M., & Rho, J.M. (2017) Dendritic overgrowth and elevated ERK signaling during neonatal development in a mouse model of autism.

Choi, C.S., Gonzales, E.L., Kim, K.C., Yang, S.M., Kim, J.W., Mabunga, D.F., Cheong, J.H., Han, S.H., Bahn, G.H., & Shin, C.Y. (2016) The transgenerational inheritance of autism-like phenotypes in mice exposed to valproic acid during pregnancy. *Sci. Reports 2016*, **6**, 1–11.

Christensen, J., Grnøborg, T.K., Srøensen, M.J., Schendel, D., Parner, E.T., Pedersen, L.H., & Vestergaard, M. (2013) Prenatal valproate exposure and risk of autism spectrum disorders and childhood autism. *JAMA*, **309**, 1696–1703.

Clancy, B., Finlay, B., Darlington, R., & Anand, K. (2007) Extrapolating brain development from experimental species to humans. *Neurotoxicology*, **28**, 931–937.

Clifford, M.A., Athar, W., Leonard, C.E., Russo, A., Sampognaro, P.J., Van Der Goes, M.S., Burton, D.A., Zhao, X., Lalchandani, R.R., Sahin, M., Vicini, S., & Donoghue, M.J. (2014)

EphA7 signaling guides cortical dendritic development and spine maturation. *Proc. Natl. Acad. Sci. U. S. A.*, **111**, 4994–4999.

Cooper, R.A., Richter, F.R., Bays, P.M., Plaisted-Grant, K.C., Baron-Cohen, S., & Simons, J.S. (2017a) Reduced Hippocampal Functional Connectivity During Episodic Memory Retrieval in Autism. *Cereb. Cortex*, **27**, 888–902.

Cooper, R.A., Richter, F.R., Bays, P.M., Plaisted-Grant, K.C., Baron-Cohen, S., & Simons, J.S. (2017b) Reduced Hippocampal Functional Connectivity During Episodic Memory Retrieval in Autism. *Cereb. Cortex*, **27**, 888–902.

Cortelazzo, A., De Felice, C., Pecorelli, A., Belmonte, G., Signorini, C., Leoncini, S., Zollo, G., Capone, A., Della Giovampaola, C., Sticozzi, C., Valacchi, G., Ciccoli, L., Guerranti, R., & Hayek, J. (2014) Beta-Actin Deficiency with Oxidative Posttranslational Modifications in Rett Syndrome Erythrocytes: Insights into an Altered Cytoskeletal Organization. *PLoS One*, **9**, e93181.

Croissant, Y. (2020) Mlogit: Random utility models in r. *J. Stat. Softw.*, **95**, 1–41.

Dailey, M.E. & Smith, S.J. (1996) The Dynamics of Dendritic Structure in Developing Hippocampal Slices. *J. Neurosci.*, **76**, 2983–2994.

Danesi, C., Keinänen, K., & Castrén, M.L. (2019) Dysregulated Ca2+-permeable AMPA receptor signaling in neural progenitors modeling fragile X syndrome. *Front. Synaptic Neurosci.*, **11**, 2.

Davidson, P.S.R., Drouin, H., Kwan, D., Moscovitch, M., & Rosenbaum, R.S. (2012) Memory as social glue: Close interpersonal relationships in amnesic patients. *Front. Psychol.*, **3**, 531.

Dawson, G., Toth, K., Abbott, R., Osterling, J., Munson, J., Estes, A., & Liaw, J. (2004) Early Social Attention Impairments in Autism: Social Orienting, Joint Attention, and Attention to

Distress. *Dev. Psychol.*, **40**, 271–283.

Dean, S.L., Knutson, J.F., Krebs-Kraft, D.L., & Mccarthy, M.M. (2012) Prostaglandin E2 is an endogenous modulator of cerebellar development and complex behavior during a sensitive postnatal period. *Eur. J. Neurosci.*, **35**, 1218.

Dean, S.L., Wright, C.L., Hoffman, J.F., Wang, M., Alger, B.E., & McCarthy, M.M. (2012) Prostaglandin E2 stimulates estradiol synthesis in the cerebellum postnatally with associated effects on Purkinje neuron dendritic arbor and electrophysiological properties. *Endocrinology*, **153**, 5415–5427.

Dhar, M., Hantman, A.W., & Nishiyama, H. (2018) Developmental pattern and structural factors of dendritic survival in cerebellar granule cells in vivo. *Sci. Reports 2018 81*, **8**, 1–14.

Duffney, L.J., Zhong, P., Wei, J., Matas, E., Cheng, J., Qin, L., Ma, K., Dietz, D.M., Kajiwara, Y., Buxbaum, J.D., & Yan, Z. (2015) Autism-like Deficits in Shank3-Deficient Mice Are Rescued by Targeting Actin Regulators. *Cell Rep.*, **11**, 1400–1413.

El-Ansary, A., Alhakbany, M., Aldbass, A., Qasem, H., Al-Mazidi, S., Bhat, R.S., & Al-Ayadhi, L. (2021) Alpha-Synuclein, cyclooxygenase-2 and prostaglandins-EP2 receptors as neuroinflammatory biomarkers of autism spectrum disorders: Use of combined ROC curves to increase their diagnostic values. *Lipids Health Dis.*, **20**.

Espinosa, J.S., Wheeler, D.G., Tsien, R.W., & Luo, L. (2009) Uncoupling dendrite growth and patterning: single-cell knockout analysis of NMDA receptor 2B. *Neuron*, **62**, 205–217.

Esplugues, J. V (2002a) NO as a signalling molecule in the nervous system. *Br. J. Pharmacol.*, **135**, 1079–1095.

Esplugues, J. V (2002b) NO as a signalling molecule in the nervous system. *Br. J. Pharmacol.*, **135**, 1079–1095.

Evseenko, D., Paxton, J.W., & Keelan, J.A. (2006) Active transport across the human placenta: Impact on drug efficacy and toxicity. *Expert Opin. Drug Metab. Toxicol.*,.

Faul, F., Erdfelder, E., Lang, A., & Buchner, A. (2007) G*Power 3: a flexible statistical power analysis program for the social, behavioral, and biomedical sciences. *Behav. Res. Methods*, **39**, 175–191.

Feng, J., Yan, Z., Ferreira, A., Tomizawa, K., Liauw, J.A., Zhuo, M., Allen, P.B., Ouimet, C.C., & Greengard, P. (2000) Spinophilin regulates the formation and function of dendritic spines. *PNAS August 1*, **97**.

Ferrucci, L., Cherubini, A., Bandinelli, S., Bartali, B., Corsi, A., Lauretani, F., Martin, A., Andres-Lacueva, C., Senin, U., & Guralnik, J.M. (2006) Relationship of plasma polyunsaturated fatty acids to circulating inflammatory markers. *J. Clin. Endocrinol. Metab.*, **91**, 439–446.

Gao, J., Wang, X., Sun, H., Cao, Y., Liang, S., Wang, H., Wang, Y., Yang, F., Zhang, F., & Wu, L. (2016) Neuroprotective effects of docosahexaenoic acid on hippocampal cell death and learning and memory impairments in a valproic acid-induced rat autism model. *Int. J. Dev. Neurosci.*, **49**, 67–78.

Gąssowska-Dobrowolska, M., Cieślik, M., Czapski, G.A., Jęśko, H., Frontczak-Baniewicz, M., Gewartowska, M., Dominiak, A., Polowy, R., Filipkowski, R.K., Babiec, L., & Adamczyk, A. (2020) Prenatal Exposure to Valproic Acid Affects Microglia and Synaptic Ultrastructure in a Brain-Region-Specific Manner in Young-Adult Male Rats: Relevance to Autism Spectrum Disorders. *Int. J. Mol. Sci.*, **21**, 3576.

Gervin, K., Nordeng, H., Ystrom, E., Reichborn-Kjennerud, T., & Lyle, R. (2017) Long-term prenatal exposure to paracetamol is associated with DNA methylation differences in

children diagnosed with ADHD. *Clin. Epigenetics*, **9**, 77.

Goikolea-Vives, A. & Stolp, H.B. (2021) Connecting the Neurobiology of Developmental Brain Injury: Neuronal Arborisation as a Regulator of Dysfunction and Potential Therapeutic Target. *Int. J. Mol. Sci.*, **22**.

Gonzalez, C.H., Marques-Dias, M.J., Kim, C.A., Sugayama, S.M.M., Da Paz, J.A., Huson, S.M., & Holmes, L.B. (1998) Congenital abnormalities in Brazilian children associated with misoprostol misuse in first trimester of pregnancy. *Lancet (London, England)*, **351**, 1624–1627.

Gould, E., Westlind-Danielsson, A., Frankfurt, M., & McEwen, B.S. (1990) Sex differences and thyroid hormone sensitivity of hippocampal pyramidal cells. *J. Neurosci.*, **10**, 996–1003.

Griesi-Oliveira, K., Acab, A., Gupta, A.R., Sunaga, D.Y., Chailangkarn, T., Nicol, X., Nunez, Y., Walker, M.F., Murdoch, J.D., Sanders, S.J., Fernandez, T. V., Ji, W., Lifton, R.P., Vadasz, E., Dietrich, A., Pradhan, D., Song, H., Ming, G.L., Gu, X., Haddad, G., Marchetto, M.C.N., Spitzer, N., Passos-Bueno, M.R., State, M.W., & Muotri, A.R. (2015) Modeling non-syndromic autism and the impact of TRPC6 disruption in human neurons. *Mol. Psychiatry*, **20**, 1350–1365.

Griesi-Oliveira, K., Suzuki, A.M., Alves, A.Y., Mafra, A.C.C.N., Yamamoto, G.L., Ezquina, S., Magalhães, Y.T., Forti, F.L., Sertie, A.L., Zachi, E.C., Vadasz, E., & Passos-Bueno, M.R. (2018) Actin cytoskeleton dynamics in stem cells from autistic individuals. *Sci. Reports 2018 81*, **8**, 1–10.

Grueber, W.B. & Sagasti, A. (2010) Self-avoidance and tiling: Mechanisms of dendrite and axon spacing. *Cold Spring Harb. Perspect. Biol.*, **2**.

Grutzendler, J., Kasthuri, N., & Gan, W.B. (2002a) Long-term dendritic spine stability in the

adult cortex. *Nature*, **420**, 812–816.

Grutzendler, J., Kasthuri, N., & Gan, W.B. (2002b) Long-term dendritic spine stability in the adult cortex. *Nat. 2003 4206917*, **420**, 812–816.

Ha, S., Sohn, I.-J., Kim, N., Sim, H.J., & Cheon, K.-A. (2015) Characteristics of Brains in Autism Spectrum Disorder: Structure, Function and Connectivity across the Lifespan. *Exp. Neurobiol.*, **24**, 273.

Haag, M. (2003) Essential fatty acids and the brain. *Can. J. Psychiatry*, **48**, 195–203.

Hajisoltani, R., Karimi, S.A., Rahdar, M., Davoudi, S., Borjkhani, M., Hosseinmardi, N., Behzadi, G., & Janahmadi, M. (2019) Hyperexcitability of hippocampal CA1 pyramidal neurons in male offspring of a rat model of autism spectrum disorder (ASD) induced by prenatal exposure to valproic acid: A possible involvement of Ih channel current. *Brain Res.*, **1708**, 188–199.

Hartley, T., Lever, C., Burgess, N., & O'Keefe, J. (2014) Space in the brain: how the hippocampal formation supports spatial cognition. *Philos. Trans. R. Soc. B Biol. Sci.*, **369**.

Hertz-Picciotto, I. & Delwiche, L. (2009) The rise in autism and the role of age at diagnosis. *Epidemiology*, **20**, 84–90.

Hinz, B., Cheremina, O., & Brune, K. (2008) Acetaminophen (paracetamol) is a selective cyclooxygenase-2 inhibitor in man. *FASEB J.*, **22**, 383–390.

Hoffman, D.R., Boettcher, J.A., & Diersen-Schade, D.A. (2009) Toward optimizing vision and cognition in term infants by dietary docosahexaenoic and arachidonic acid supplementation: A review of randomized controlled trials. *Prostaglandins Leukot. Essent. Fat. Acids*, **81**, 151–158.

Hoffman, J.F., Christopher, X., Wright, L., & Mccarthy, M.M. (2016) A Critical Period in

Purkinje Cell Development Is Mediated by Local Estradiol Synthesis, Disrupted by Inflammation, and Has Enduring Consequences Only for Males.

Hojo, Y., Hattori, T.A., Enami, T., Furukawa, A., Suzuki, K., Ishii, H.T., Mukai, H., Morrison, J.H., Janssen, W.G.M., Kominami, S., Harada, N., Kimoto, T., & Kawato, S. (2004) Adult male rat hippocampus synthesizes estradiol from pregnenolone by cytochromes P45017alpha and P450 aromatase localized in neurons. *Proc. Natl. Acad. Sci. U. S. A.*, **101**, 865–870.

Holtmaat, A.J.G.D., Trachtenberg, J.T., Wilbrecht, L., Shepherd, G.M., Zhang, X., Knott, G.W., & Svoboda, K. (2005) Transient and persistent dendritic spines in the neocortex in vivo. *Neuron*, **45**, 279–291.

Hoozemans, J.J.M., Rozemuller, A.J.M., Janssen, I., De Groot, C.J.A., Veerhuis, R., & Eikelenboom, P. (2001) Cyclooxygenase expression in microglia and neurons in Alzheimer's disease and control brain. *Acta Neuropathol. 2000 1011*, **101**, 2–8.

Hoshiba, Y., Toda, T., Ebisu, H., Wakimoto, M., Yanagi, S., & Kawasaki, H. (2016) Sox11 Balances Dendritic Morphogenesis with Neuronal Migration in the Developing Cerebral Cortex. *J. Neurosci.*, **36**, 5775–5784.

Hou, Q., Wang, Y., Li, Y., Chen, D., Yang, F., & Wang, S. (2018) A developmental study of abnormal behaviors and altered GABAergic signaling in the VPA-treated rat model of autism. *Front. Behav. Neurosci.*, **12**, 182.

Hu, X., Viesselmann, C., Nam, S., Merriam, E., & Dent, E.W. (2008) Activity-dependent dynamic microtubule invasion of dendritic spines. *J. Neurosci.*, **28**, 13094–13105.

Hugger Toft, A.K., Lundbye, C.J., & Banke, T.G. (2016) Dysregulated NMDA-Receptor Signaling Inhibits Long-Term Depression in a Mouse Model of Fragile X Syndrome. *J.*

Neurosci., **36**, 9817–9827.

Hutsler, J.J. & Zhang, H. (2010) Increased dendritic spine densities on cortical projection neurons in autism spectrum disorders. *Brain Res.*, **1309**, 83–94.

Immordino-Yang, M.H. & Singh, V. (2013) Hippocampal contributions to the processing of social emotions. *Hum. Brain Mapp.*, **34**, 945–955.

Isgor, C. & Sengelaub, D.R. (2003) Effects of neonatal gonadal steroids on adult CA3 pyramidal neuron dendritic morphology and spatial memory in rats. *J. Neurobiol.*, **55**, 179–190.

Jacome, L.F., Barateli, K., Buitrago, D., Lema, F., Frankfurt, M., & Luine, V.N. (2016) Gonadal Hormones Rapidly Enhance Spatial Memory and Increase Hippocampal Spine Density in Male Rats. *Endocrinology*, **157**, 1357–1362.

Jasien, J.M., Daimon, C.M., Wang, R., Shapiro, B.K., Martin, B., & Maudsley, S. (2014) The effects of aging on the BTBR mouse model of autism spectrum disorder. *Front. Aging Neurosci.*, **6**, 225.

Jiang, H. yin, Xu, L. lian, Shao, L., Xia, R. man, Yu, Z. he, Ling, Z. xin, Yang, F., Deng, M., & Ruan, B. (2016) Maternal infection during pregnancy and risk of autism spectrum disorders: A systematic review and meta-analysis. *Brain. Behav. Immun.*, **58**, 165–172.

Jiang, M., Ash, R.T., Baker, S.A., Suter, B., Ferguson, A., Park, J., Rudy, J., Torsky, S.P., Chao, H.T., Zoghbi, H.Y., & Smirnakis, S.M. (2013) Dendritic arborization and spine dynamics are abnormal in the mouse model of MECP2 duplication syndrome. *J. Neurosci.*, **33**, 19518–19533.

Jiang, N.M., Cowan, M., Moonah, S.N., & Petri, W.A. (2018) The Impact of Systemic Inflammation on Neurodevelopment. *Trends Mol. Med.*,.

Juliandi, B., Tanemura, K., Igarashi, K., Tominaga, T., Furukawa, Y., Otsuka, M., Moriyama,

N., Ikegami, D., Abematsu, M., Sanosaka, T., Tsujimura, K., Narita, M., Kanno, J., & Nakashima, K. (2015) Reduced Adult Hippocampal Neurogenesis and Cognitive Impairments following Prenatal Treatment of the Antiepileptic Drug Valproic Acid. *Stem Cell Reports*, **5**, 996–1009.

Ka, M., Chopra, D.A., Dravid, S.M., & Kim, W.Y. (2016) Essential Roles for ARID1B in Dendritic Arborization and Spine Morphology of Developing Pyramidal Neurons. *J. Neurosci.*, **36**, 2723–2742.

Kalil, K. & Dent, E.W. (2014) Branch management: mechanisms of axon branching in the developing vertebrate CNS. *Nat. Rev. Neurosci.*, **15**, 7.

Kane, M.J., Angoa-Peréz, M., Briggs, D.I., Sykes, C.E., Francescutti, D.M., Rosenberg, D.R., & Kuhn, D.M. (2012) Mice Genetically Depleted of Brain Serotonin Display Social Impairments, Communication Deficits and Repetitive Behaviors: Possible Relevance to Autism. *PLoS One*, **7**, 48975.

Kataoka, S., Takuma, K., Hara, Y., Maeda, Y., Ago, Y., & Matsuda, T. (2013) Autism-like behaviours with transient histone hyperacetylation in mice treated prenatally with valproic acid. *Int. J. Neuropsychopharmacol.*, **16**, 91–103.

Kawa, R. & Pisula, E. (2010) Locomotor activity, object exploration and space preference in children with autism and Down syndrome. *undefined*,.

Keil, K.P., Sethi, S., Wilson, M.D., Chen, H., & Lein, P.J. (2017) In vivo and in vitro sex differences in the dendritic morphology of developing murine hippocampal and cortical neurons. *Sci. Rep.*, **7**.

Kennedy, D.P. & Adolphs, R. (2014) Violations of Personal Space by Individuals with Autism Spectrum Disorder. *PLoS One*, **9**, e103369.

Kim, J.W., Park, K., Kang, R.J., Gonzales, E.L.T., Kim, D.G., Oh, H.A., Seung, H., Ko, M.J., Kwon, K.J., Kim, K.C., Lee, S.H., Chung, C.H., & Shin, C.Y. (2018) Pharmacological modulation of AMPA receptor rescues social impairments in animal models of autism. *Neuropsychopharmacol. 2018 442*, **44**, 314–323.

Kim, K.C., Kim, P., Go, H.S., Choi, C.S., Park, J.H., Kim, H.J., Jeon, S.J., Dela Pena, I.C., Han, S.H., Cheong, J.H., Ryu, J.H., & Shin, C.Y. (2013) Male-specific alteration in excitatory post-synaptic development and social interaction in pre-natal valproic acid exposure model of autism spectrum disorder. *J. Neurochem.*, **124**, 832–843.

Kim, K.C., Kim, P., Go, H.S., Choi, C.S., Yang, S. Il, Cheong, J.H., Shin, C.Y., & Ko, K.H. (2011) The critical period of valproate exposure to induce autistic symptoms in Sprague–Dawley rats. *Toxicol. Lett.*, **201**, 137–142.

Kirkby, N.S., Chan, M. V., Zaiss, A.K., Garcia-Vaz, E., Jiao, J., Berglund, L.M., Verdu, E.F., Ahmetaj-Shala, B., Wallace, J.L., Herschman, H.R., Gomez, M.F., & Mitchell, J.A. (2016) Systematic study of constitutive cyclooxygenase-2 expression: Role of NF-κB and NFAT transcriptional pathways. *Proc. Natl. Acad. Sci. U. S. A.*, **113**, 434–439.

Kissoondoyal, A. & Crawford, D. (2021) Prostaglandin E2 Increases Neurite Length and the Formation of Axonal Loops, and Regulates Cone Turning in Differentiating NE4C Cells Via PKA. *Cell. Mol. Neurobiol.*,.

Kissoondoyal, A., Rai-Bhogal, R., & Crawford, D.A. (2021) Abnormal dendritic morphology in the cerebellum of cyclooxygenase-2− knockin mice. *Eur. J. Neurosci.*, **54**, 6355–6373.

Knopf, A. (2020) Autism prevalence increases from 1 in 60 to 1 in 54: CDC. *Brown Univ. Child Adolesc. Behav. Lett.*, **36**, 4–4.

Koehn, L.M., Huang, Y., Habgood, M.D., Kysenius, K., Crouch, P.J., Dziegielewska, K.M., &

Saunders, N.R. (2020) Effects of paracetamol (acetaminophen) on gene expression and permeability properties of the rat placenta and fetal brain. *F1000Research*, **9**.

Koepsell, H. (2013) The SLC22 family with transporters of organic cations, anions and zwitterions. *Mol. Aspects Med.*,.

Kojima, H., Katsura, E., Takeuchi, S., Niiyama, K., & Kobayashi, K. (2004) Screening for estrogen and androgen receptor activities in 200 pesticides by in vitro reporter gene assays using Chinese hamster ovary cells. *Environ. Health Perspect.*, **112**, 524–531.

Korbecki, J., Baranowska-Bosiacka, I., Gutowska, I., & Chlubek, D. (2013) The effect of reactive oxygen species on the synthesis of prostanoids from arachidonic acid. *J. Physiol. Pharmacol.*,.

Kordulewska, N.K., Kostyra, E., Chwała, B., Moszyńska, M., Cieślińska, A., Fiedorowicz, E., & Jarmołowska, B. (2019) A novel concept of immunological and allergy interactions in autism spectrum disorders: Molecular, anti-inflammatory effect of osthole. *Int. Immunopharmacol.*, **72**, 1–11.

Kwon, C.H., Luikart, B.W., Powell, C.M., Zhou, J., Matheny, S.A., Zhang, W., Li, Y., Baker, S.J., & Parada, L.F. (2006) Pten Regulates Neuronal Arborization and Social Interaction in Mice. *Neuron*, **50**, 377–388.

Ladesich, J.B., Pottala, J. V., Romaker, A., & Harris, W.S. (2011) Membrane level of omega-3 docosahexaenoic acid is associated with severity of obstructive sleep apnea. *J. Clin. Sleep Med.*, **7**, 391–396.

Lan, J., Hu, Y., Wang, X., Zheng, W., Liao, A., Wang, S., Li, Y., Wang, Y., Yang, F., & Chen, D. (2021) Abnormal spatiotemporal expression pattern of progranulin and neurodevelopment impairment in VPA-induced ASD rat model. *Neuropharmacology*, **196**,

108689.

Lee, H.K., Takamiya, K., Han, J.S., Man, H., Kim, C.H., Rumbaugh, G., Yu, S., Ding, L., He, C., Petralia, R.S., Wenthold, R.J., Gallagher, M., & Huganir, R.L. (2003) Phosphorylation of the AMPA Receptor GluR1 Subunit Is Required for Synaptic Plasticity and Retention of Spatial Memory. *Cell*, **112**, 631–643.

Lee, J., Chung, C., Ha, S., Lee, D., Kim, D.Y., Kim, H., & Kim, E. (2015) Shank3-mutant mice lacking exon 9 show altered excitation/inhibition balance, enhanced rearing, and spatial memory deficit. *Front. Cell. Neurosci.*, **9**, 94.

Lenz, K.M., Nugent, B.M., & McCarthy, M.M. (2012) Sexual differentiation of the rodent brain: dogma and beyond. *Front. Neurosci.*, **6**.

Lenz, K.M., Wright, C.L., Martin, R.C., & McCarthy, M.M. (2011) Prostaglandin E2 Regulates AMPA Receptor Phosphorylation and Promotes Membrane Insertion in Preoptic Area Neurons and Glia during Sexual Differentiation. *PLoS One*, **6**, e18500.

Leranth, C., Petnehazy, O., & MacLusky, N.J. (2003) Gonadal Hormones Affect Spine Synaptic Density in the CA1 Hippocampal Subfield of Male Rats. *J. Neurosci.*, **23**, 1588–1592.

Li, D.Y., Hardy, P., Abran, D., Martinez-Bermudez, A.K., Guerguerian, A.M., Bhattacharya, M., Almazan, G., Menezes, R., Peri, K.G., Varma, D.R., & Chemtob, S. (1997) Key role for cyclooxygenase-2 in PGE2 and PGF2alpha receptor regulation and cerebral blood flow of the newborn. *Am. J. Physiol.*, **273**.

Liew, Z., Ritz, B., Virk, J., & Olsen, J. (2016) Maternal use of acetaminophen during pregnancy and risk of autism spectrum disorders in childhood: A Danish national birth cohort study. *Autism Res.*, **9**, 951–958.

Lind, S.E., Williams, D.M., Raber, J., Peel, A., & Bowler, D.M. (2013) Spatial navigation

impairments among intellectually high-functioning adults with autism spectrum disorder: Exploring relations with theory of mind, episodic memory, and episodic future thinking. *J. Abnorm. Psychol.*, **122**, 1189.

Longair, M., Baker, D., & Armstrong, J. (2011) Simple Neurite Tracer: open source software for reconstruction, visualization and analysis of neuronal processes. *Bioinformatics*, **27**, 2453–2454.

Losonczy, A., Makara, J.K., & Magee, J.C. (2008) Compartmentalized dendritic plasticity and input feature storage in neurons. *Nature*, **452**, 436–441.

Lu, D., He, L., Xiang, W., Ai, W.M., Cao, Y., Wang, X.S., Pan, A., Luo, X.G., Li, Z., & Yan, X.X. (2013a) Somal and dendritic development of human CA3 pyramidal neurons from midgestation to middle childhood: a quantitative Golgi study. *Anat. Rec. (Hoboken).*, **296**, 123–132.

Lu, D., He, L., Xiang, W., Ai, W.M., Cao, Y., Wang, X.S., Pan, A., Luo, X.G., Li, Z., & Yan, X.X. (2013b) Somal and dendritic development of human CA3 pyramidal neurons from midgestation to middle childhood: a quantitative Golgi study. *Anat. Rec. (Hoboken).*, **296**, 123–132.

Lucchina, L. & Depino, A.M. (2014) Altered Peripheral and Central Inflammatory Responses in a Mouse Model of Autism. *Autism Res.*, **7**, 273–289.

Lujan, B., Liu, X., & Qi, W. (2012) Differential roles of GluN2A- and GluN2B-containing NMDA receptors in neuronal survival and death. *Int. J. Physiol. Pathophysiol. Pharmacol.*, **4**, 211.

Lynch, G., Kessler, M., Arai, A., & Larson, J. (1990) The nature and causes of hippocampal long-term potentiation. *Prog. Brain Res.*, **83**, 233–250.

Magee, J.C. & Cook, E.P. (2000) Somatic EPSP amplitude is independent of synapse location in hippocampal pyramidal neurons. *Nat. Neurosci. 2000 39*, **3**, 895–903.

Maguire, E.A., Gadian, D.G., Johnsrude, I.S., Good, C.D., Ashburner, J., Frackowiak, R.S.J., & Frith, C.D. (2000) Navigation-related structural change in the hippocampi of taxi drivers. *Proc. Natl. Acad. Sci.*, **97**, 4398–4403.

Maher, F.O., Clarke, R.M., Kelly, A., Nally, R.E., & Lynch, M.A. (2006) Interaction between interferon γ and insulin-like growth factor-1 in hippocampus impacts on the ability of rats to sustain long-term potentiation. *J. Neurochem.*, **96**, 1560–1571.

Mahmood, U., Ahn, S., Yang, E.J., Choi, M., Kim, H., Regan, P., Cho, K., & Kim, H.S. (2018) Dendritic spine anomalies and PTEN alterations in a mouse model of VPA-induced autism spectrum disorder. *Pharmacol. Res.*, **128**, 110–121.

Marín, O., Valiente, M., Ge, X., & Tsai, L.H. (2010) Guiding neuronal cell migrations. *Cold Spring Harb. Perspect. Biol.*,.

Markham, J.A., McKian, K.P., Stroup, T.S., & Juraska, J.M. (2005) Sexually dimorphic aging of dendritic morphology in CA1 of hippocampus. *Hippocampus*, **15**, 97–103.

Markram, H., Lübke, J., Frotscher, M., & Sakmann, B. (1997) Regulation of synaptic efficacy by coincidence of postsynaptic APs and EPSPs. *Science (80-.).*, **275**, 213–215.

Markram, K., Rinaldi, T., Mendola, D. La, Sandi, C., & Markram, H. (2007) Abnormal Fear Conditioning and Amygdala Processing in an Animal Model of Autism. *Neuropsychopharmacol. 2008 334*, **33**, 901–912.

Martínez-Cerdeño, V. (2017) Dendrite and spine modifications in autism and related neurodevelopmental disorders in patients and animal models. *Dev. Neurobiol.*, **77**, 393.

McEwen, B.S., Conrad, C.D., Kuroda, Y., Frankfurt, M., Maria Magarinos, A., & McKittrick, C.

(1997) Prevention of stress-induced morphological and cognitive consequences. *Eur. Neuropsychopharmacol.*, **7 Suppl 3**.

McFadden, K. & Minshew, N.J. (2013) Evidence for dysregulation of axonal growth and guidance in the etiology of ASD. *Front. Hum. Neurosci.*, **0**, 671.

Mendell, A.L., Atwi, S., Bailey, C.D.C., McCloskey, D., Scharfman, H.E., & MacLusky, N.J. (2017) Expansion of mossy fibers and CA3 apical dendritic length accompanies the fall in dendritic spine density after gonadectomy in male, but not female, rats. *Brain Struct. Funct.*, **222**, 587.

Meyer, U., Yee, B.K., & Feldon, J. (2007) The Identification of Critical Time Windows by Epidemiological Studies The Neurodevelopmental Impact of Prenatal Infections at Different Times of Pregnancy: The Earlier the Worse?

Minshew, N.J. & Williams, D.L. (2007) The New Neurobiology of Autism: Cortex, Connectivity, and Neuronal Organization. *Arch. Neurol.*, **64**, 945.

Mizrahi, A., Crowley, J.C., Shtoyerman, E., & Katz, L.C. (2004) High-Resolution In Vivo Imaging of Hippocampal Dendrites and Spines. *J. Neurosci.*, **24**, 3147–3151.

Mizrahi, A. & Katz, L.C. (2003) Dendritic stability in the adult olfactory bulb. *Nat. Neurosci.*, **6**, 1201–1207.

Møller, P., Danielsen, P.H., Karottki, D.G., Jantzen, K., Roursgaard, M., Klingberg, H., Jensen, D.M., Christophersen, D.V., Hemmingsen, J.G., Cao, Y., & Loft, S. (2014) Oxidative stress and inflammation generated DNA damage by exposure to air pollution particles. *Mutat. Res. - Rev. Mutat. Res.*,.

Mondal, A., Black, B., Kim, Y.T., & Mohanty, S. (2014) Loop formation and self-fasciculation of cortical axon using photonic guidance at long working distance. *Sci. Rep.*, **4**.

Montagrin, A., Saiote, C., & Schiller, D. (2018) The social hippocampus. *Hippocampus*, **28**, 672–679.

Morgan, L.K., MacEvoy, S.P., Aguirre, G.K., & Epstein, R.A. (2011) Distances between Real-World Locations Are Represented in the Human Hippocampus. *J. Neurosci.*, **31**, 1238–1245.

Mukaetova-Ladinska, E.B., Arnold, H., Jaros, E., Perry, R., & Perry, E. (2004) Depletion of MAP2 expression and laminar cytoarchitectonic changes in dorsolateral prefrontal cortex in adult autistic individuals. *Neuropathol. Appl. Neurobiol.*, **30**, 615–623.

Murguía-Castillo, J., Beas-Zárate, C., Rivera-Cervantes, M.C., Feria-Velasco, A.I., & Ureña-Guerrero, M.E. (2013) NKCC1 and KCC2 protein expression is sexually dimorphic in the hippocampus and entorhinal cortex of neonatal rats. *Neurosci. Lett.*, **552**, 52–57.

Murphy, D.D., Cole, N.B., Greenberger, V., & Segal, M. (1998) Estradiol Increases Dendritic Spine Density by Reducing GABA Neurotransmission in Hippocampal Neurons. *J. Neurosci.*, **18**, 2550–2559.

Murphy, D.D. & Segal, M. (1996) Regulation of Dendritic Spine Density in Cultured Rat Hippocampal Neurons by Steroid Hormones. *J. Neurosci.*, **16**, 4059–4068.

Nicholson, D.A., Trana, R., Katz, Y., Kath, W.L., Spruston, N., & Geinisman, Y. (2006) Distance-dependent differences in synapse number and AMPA receptor expression in hippocampal CA1 pyramidal neurons. *Neuron*, **50**, 431–442.

Nimchinsky, E.A., Sabatini, B.L., & Svoboda, K. (2002) STRUCTURE AND FUNCTION OF DENDRITIC SPINES. *Annu. Rev. Physiol*, **64**, 313–353.

Nørregaard, R., Kwon, T.H., & Frøkiær, J. (2015) Physiology and pathophysiology of cyclooxygenase-2 and prostaglandin E2 in the kidney. *Kidney Res. Clin. Pract.*, **34**, 194.

Nuñez, J.L., Alt, J.J., & McCarthy, M.M. (2003) A new model for prenatal brain damage: I. GABAA receptor activation induces cell death in developing rat hippocampus. *Exp. Neurol.*, **181**, 258–269.

Nuñez, J.L., Bambrick, L.L., Krueger, B.K., & McCarthy, M.M. (2005) Prolongation and enhancement of γ-aminobutyric acidA receptor mediated excitation by chronic treatment with estradiol in developing rat hippocampal neurons. *Eur. J. Neurosci.*, **21**, 3251–3261.

Nuñez, J.L. & McCarthy, M.M. (2007) Evidence for an extended duration of GABA-mediated excitation in the developing male versus female hippocampus. *Dev. Neurobiol.*, **67**, 1879–1890.

Nuñez, J.L. & McCarthy, M.M. (2008) Androgens predispose males to GABAA-mediated excitotoxicity in the developing hippocampus. *Exp. Neurol.*, **210**, 699–708.

Ohno, T., Ohtsuki, H., & Okabe, S. (1985) Effects of 16,16-dimethyl prostaglandin E2 on ethanol-induced and aspirin-induced gastric damage in the rat. Scanning electron microscopic study. *Gastroenterology*, **88**, 353–361.

Parker, E.M., Kindja, N.L., Cheetham, C.E.J., & Sweet, R.A. (2020) Sex differences in dendritic spine density and morphology in auditory and visual cortices in adolescence and adulthood. *Sci. Reports 2020 101*, **10**, 1–11.

Pastuszak, A., Schüler, L., Speck-Martins, C., Coelho, K., Cordello, S., Vargas, F., Brunoni, D., Schwarz, I., Larrandaburu, M., Safattle, H., Meloni, V., & Koren, G. (1998) Use of misoprostol during pregnancy and Möbius' syndrome in infants. *N. Engl. J. Med.*, **338**, 1881–1885.

Peng, Y.R., He, S., Marie, H., Zeng, S.Y., Ma, J., Tan, Z.J., Lee, S.Y., Malenka, R.C., & Yu, X. (2009) Coordinated Changes in Dendritic Arborization and Synaptic Strength during Neural

Circuit Development. *Neuron*, **61**, 71–84.

Peri, K.G., Hardy, P., Ding You Li, Varma, D.R., & Chemtob, S. (1995) Prostaglandin G/H Synthase-2 Is a Major Contributor of Brain Prostaglandins in the Newborn (∗). *J. Biol. Chem.*, **270**, 24615–24620.

Perrot-Sinal, T.S., Auger, A.P., & McCarthy, M.M. (2003) Excitatory actions of GABA in developing brain are mediated by l-type Ca2+ channels and dependent on age, sex, and brain region. *Neuroscience*, **116**, 995–1003.

Perry, D., Hendler, T., & Shamay-Tsoory, S.G. (2011) Projecting memories: The role of the hippocampus in emotional mentalizing. *Neuroimage*, **54**, 1669–1676.

Peters, A. & Kaiserman-Abramof, I.R. (1970) The small pyramidal neuron of the rat cerebral cortex. The perikaryon, dendrites and spines. *Am. J. Anat.*, **127**, 321–355.

Posar, A. & Visconti, P. (2018) Sensory abnormalities in children with autism spectrum disorder. *J. Pediatr. (Rio. J).*,.

Prange-Kiel, J., Fester, L., Zhou, L., Lauke, H., Carrétero, J., & Rune, G.M. (2006) Inhibition of hippocampal estrogen synthesis causes region-specific downregulation of synaptic protein expression in hippocampal neurons. *Hippocampus*, **16**, 464–471.

Public Health Agency of Canada (2018) Autism spectrum disorder among children and youth in Canada 2018: A report of the national autism spectrum disorder surveillance system URL https://www.canada.ca/en/public-health/services/publications/diseases-conditions/autism-spectrum-disorder-children-youth-canada-2018.html

Qasem, H., Al-Ayadhi, L., Bjørklund, G., Chirumbolo, S., & El-Ansary, A. (2018) Impaired lipid metabolism markers to assess the risk of neuroinflammation in autism spectrum disorder. *Metab. Brain Dis.*, **33**, 1141–1153.

Qin, Y., Du, Y., Chen, L., Liu, Y., Xu, W., Liu, Y., Li, Y., Leng, J., Wang, Y., Zhang, X.-Y., Feng, J., Zhang, F., Jin, L., Qiu, Z., Gong, X., & Wang, H. (2022) A recurrent SHANK1 mutation implicated in autism spectrum disorder causes autistic-like core behaviors in mice via downregulation of mGluR1-IP3R1-calcium signaling. *Mol. Psychiatry 2022*, 1–14.

Qiu, L.R., Germann, J., Spring, S., Alm, C., Vousden, D.A., Palmert, M.R., & Lerch, J.P. (2013) Hippocampal volumes differ across the mouse estrous cycle, can change within 24 hours, and associate with cognitive strategies. *Neuroimage*, **83**, 593–598.

Rai-Bhogal, R., Ahmad, E., Li, H., & Crawford, D.A. (2018a) Microarray analysis of gene expression in the cyclooxygenase knockout mice – a connection to autism spectrum disorder. *Eur. J. Neurosci.*, **47**, 750–766.

Rai-Bhogal, R., Ahmad, E., Li, H., & Crawford, D.A. (2018b) Microarray analysis of gene expression in the cyclooxygenase knockout mice – a connection to autism spectrum disorder. *Eur. J. Neurosci.*, **47**, 750–766.

Rai-Bhogal, R., Wong, C., Kissoondoyal, A., Davidson, J., Li, H., & Crawford, D.A. (2018) Maternal exposure to prostaglandin E2 modifies expression of Wnt genes in mouse brain – An autism connection. *Biochem. Biophys. Reports*, **14**, 43–53.

Rajagopal, S., Fitzgerald, A.A., Deep, S.N., Paul, S., & Poddar, R. (2019) Role of GluN2A NMDA receptor in homocysteine-induced prostaglandin E2 release from neurons. *J. Neurochem.*, **150**, 44–55.

Rakic, P., Bourgeois, J.P., Eckenhoff, M.F., Zecevic, N., & Goldman-Rakic, P.S. (1986) Concurrent overproduction of synapses in diverse regions of the primate cerebral cortex. *Science*, **232**, 232–235.

Rasalam, A.D., Hailey, H., Williams, J.H.G., Moore, S.J., Turnpenny, P.D., Lloyd, D.J., & Dean,

J.C.S. (2005) Characteristics of fetal anticonvulsant syndrome associated autistic disorder. *Dev. Med. Child Neurol.*, **47**, 551–555.

Raymond, G. V., Bauman, M.L., & Kemper, T.L. (1996) Hippocampus in autism: a Golgi analysis. *Acta Neuropathol.*, **91**, 117–119.

Reichova, A., Bacova, Z., Bukatova, S., Kokavcova, M., Meliskova, V., Frimmel, K., Ostatnikova, D., & Bakos, J. (2020) Abnormal neuronal morphology and altered synaptic proteins are restored by oxytocin in autism-related SHANK3 deficient model. *Mol. Cell. Endocrinol.*, **518**, 110924.

Reinhardt, V.P., Iosif, A.M., Libero, L., Heath, B., Rogers, S.J., Ferrer, E., Nordahl, C., Ghetti, S., Amaral, D., & Solomon, M. (2020a) Understanding Hippocampal Development in Young Children With Autism Spectrum Disorder. In *Journal of the American Academy of Child and Adolescent Psychiatry*. Elsevier Inc., pp. 1069–1079.

Reinhardt, V.P., Iosif, A.M., Libero, L., Heath, B., Rogers, S.J., Ferrer, E., Nordahl, C., Ghetti, S., Amaral, D., & Solomon, M. (2020b) Understanding Hippocampal Development in Young Children With Autism Spectrum Disorder. *J. Am. Acad. Child Adolesc. Psychiatry*, **59**, 1069–1079.

Riccomagno, M.M. & Kolodkin, A.L. (2015) Sculpting Neural Circuits by Axon and Dendrite Pruning. *Annu. Rev. Cell Dev. Biol.*, **31**, 779–805.

Richards, R., Greimel, E., Kliemann, D., Koerte, I.K., Schulte-Körne, G., Reuter, M., & Wachinger, C. (2020a) Increased hippocampal shape asymmetry and volumetric ventricular asymmetry in autism spectrum disorder. *NeuroImage Clin.*, **26**.

Richards, R., Greimel, E., Kliemann, D., Koerte, I.K., Schulte-Körne, G., Reuter, M., & Wachinger, C. (2020b) Increased hippocampal shape asymmetry and volumetric ventricular

asymmetry in autism spectrum disorder. *Neuroimage (Amst).*, **26**.

Richards, S.E.V., Moore, A.R., Nam, A.Y., Saxena, S., Paradis, S., & van Hooser, S.D. (2020) Experience-Dependent Development of Dendritic Arbors in Mouse Visual Cortex. *J. Neurosci.*, **40**, 6536–6556.

Rinaldi, T., Kulangara, K., Antoniello, K., & Markram, H. (2007) Elevated NMDA receptor levels and enhanced postsynaptic long-term potentiation induced by prenatal exposure to valproic acid. *Proc. Natl. Acad. Sci. U. S. A.*, **104**, 13501–13506.

Ring, M., Gaigg, S.B., de Condappa, O., Wiener, J.M., & Bowler, D.M. (2018) Spatial navigation from same and different directions: The role of executive functions, memory and attention in adults with autism spectrum disorder. *Autism Res.*, **11**, 798–810.

Risher, W., Ustunkaya, T., Singh Alvarado, J., & Eroglu, C. (2014) Rapid Golgi analysis method for efficient and unbiased classification of dendritic spines. *PLoS One*, **9**.

Rodier, P. (1980) Chronology of neuron development: animal studies and their clinical implications. *Dev. Med. Child Neurol.*, **22**, 525–545.

Rossignol, D.A., Genuis, S.J., & Frye, R.E. (2014) Environmental toxicants and autism spectrum disorders: a systematic review. *Transl. Psychiatry*, **4**, e360.

Roullet, F.I., Wollaston, L., deCatanzaro, D., & Foster, J.A. (2010) Behavioral and molecular changes in the mouse in response to prenatal exposure to the anti-epileptic drug valproic acid. *Neuroscience*, **170**, 514–522.

Rueden, C.T., Schindelin, J., Hiner, M.C., DeZonia, B.E., Walter, A.E., Arena, E.T., & Eliceiri, K.W. (2017) ImageJ2: ImageJ for the next generation of scientific image data. *BMC Bioinforma. 2017 181*, **18**, 1–26.

Rummel, J., Epp, J.R., & Galea, L.A.M. (2010) Estradiol does not influence strategy choice but

place strategy choice is associated with increased cell proliferation in the hippocampus of female rats. *Horm. Behav.*, **58**, 582–590.

Ryan, S.J., Ehrlich, D.E., & Rainnie, D.G. (2016) Morphology and dendritic maturation of developing principal neurons in the rat basolateral amygdala. *Brain Struct. Funct.*, **221**, 839–854.

Salazar, F.R., D'Avila, F.B., de Oliveira, M.H., Ferreira, P.L., & Bergold, A.M. (2016) Development and validation of a bioanalytical method for five antidepressants in human milk by LC-MS. *J. Pharm. Biomed. Anal.*, **129**, 502–508.

Samuelsson, A.M., Jennische, E., Hansson, H.A., & Holmäng, A. (2006) Prenatal exposure to interleukin-6 results in inflammatory neurodegeneration in hippocampus with NMDA/GABAA dysregulation and impaired spatial learning. *Am. J. Physiol. - Regul. Integr. Comp. Physiol.*, **290**.

Sanderson, D.J., Good, M.A., Seeburg, P.H., Sprengel, R., Rawlins, J.N.P., & Bannerman, D.M. (2008) Chapter 9 The role of the GluR-A (GluR1) AMPA receptor subunit in learning and memory. *Prog. Brain Res.*, **169**, 159–178.

Sang, N., Zhang, J., Marcheselli, V., Bazan, N.G., & Chen, C. (2005) Postsynaptically Synthesized Prostaglandin E2 (PGE2) Modulates Hippocampal Synaptic Transmission via a Presynaptic PGE2 EP2 Receptor. *J. Neurosci.*, **25**, 9858.

Sastry, P.S. (1985) Lipids of nervous tissue: composition and metabolism. *Prog. Lipid Res.*, **24**, 69–176.

Sbacchi, S., Acquadro, F., Calo, I., Cali, F., & Romano, V. (2010) Functional Annotation of Genes Overlapping Copy Number Variants in Autistic Patients: Focus on Axon Pathfinding. *Curr. Genomics*, **11**, 136–145.

Schafer, M. & Schiller, D. (2018) Navigating Social Space. *Neuron*, **100**, 476–489.

Schiavi, S., Carbone, E., Melancia, F., Buzzelli, V., Manduca, A., Campolongo, P., Pallottini, V., & Trezza, V. (2020) Perinatal supplementation with omega-3 fatty acids corrects the aberrant social and cognitive traits observed in a genetic model of autism based on FMR1 deletion in rats. *Nutr. Neurosci.*,.

Schindelin, J., Arganda-Carreras, I., Frise, E., Kaynig, V., Longair, M., Pietzsch, T., Preibisch, S., Rueden, C., Saalfeld, S., Schmid, B., Tinevez, J.-Y., White, D.J., Hartenstein, V., Eliceiri, K., Tomancak, P., & Cardona, A. (2012) Fiji: an open-source platform for biological-image analysis. *Nat. Methods 2012 97*, **9**, 676–682.

Schneider, T. & Przewłocki, R. (2005) Behavioral Alterations in Rats Prenatally Exposed to Valproic Acid: Animal Model of Autism. *Neuropsychopharmacology*, **30**, 80–89.

Schumann, C.M., Hamstra, J., Goodlin-Jones, B.L., Lotspeich, L.J., Kwon, H., Buonocore, M.H., Lammers, C.R., Reiss, A.L., & Amaral, D.G. (2004) The amygdala is enlarged in children but not adolescents with autism; the hippocampus is enlarged at all ages. *J. Neurosci.*, **24**, 6392–6401.

Semple, B.D., Blomgren, K., Gimlin, K., Ferriero, D.M., & Noble-Haeusslein, L.J. (2013) Brain development in rodents and humans: Identifying benchmarks of maturation and vulnerability to injury across species. *Prog. Neurobiol.*, **106**–**107**, 1–16.

Shepherd, G.M.G., Stepanyants, A., Bureau, I., Chklovskii, D., & Svoboda, K. (2005) Geometric and functional organization of cortical circuits. *Nat. Neurosci.*, **8**, 782–790.

Shipton, O.A. & Paulsen, O. (2014) GluN2A and GluN2B subunit-containing NMDA receptors in hippocampal plasticity. *Philos. Trans. R. Soc. B Biol. Sci.*, **369**.

Song, T.J., Lan, X.Y., Wei, M.P., Zhai, F.J., Boeckers, T.M., Wang, J.N., Yuan, S., Jin, M.Y.,

Xie, Y.F., Dang, W.W., Zhang, C., Schön, M., Song, P.W., Qiu, M.H., Song, Y.Y., Han, S.P., Han, J.S., & Zhang, R. (2019) Altered behaviors and impaired synaptic function in a novel rat model with a complete Shank3 deletion. *Front. Cell. Neurosci.*, **13**, 111.

Soto, A.M., Chung, K.L., & Sonnenschein, C. (1994) The pesticides endosulfan, toxaphene, and dieldrin have estrogenic effects on human estrogen-sensitive cells. *Environ. Health Perspect.*, **102**, 380–383.

Spencer, C.M., Alekseyenko, O., Serysheva, E., Yuva-Paylor, L.A., & Paylor, R. (2005) Altered anxiety-related and social behaviors in the Fmr1 knockout mouse model of fragile X syndrome. *Genes, Brain Behav.*, **4**, 420–430.

Spruston, N. (2008) Pyramidal neurons: dendritic structure and synaptic integration. *Nat. Rev. Neurosci.*, **9**, 206–221.

Steffenrud, S. (1980) Metabolism of 16, 16-dimethyl-prostaglandin E2 in the human female. *Biochem. Med.*, **24**, 274–292.

Su, H.M. (2010) Mechanisms of n-3 fatty acid-mediated development and maintenance of learning memory performance. *J. Nutr. Biochem.*,.

Sumi, T. & Harada, K. (2020) Mechanism underlying hippocampal long-term potentiation and depression based on competition between endocytosis and exocytosis of AMPA receptors. *Sci. Reports 2020 101*, **10**, 1–14.

T Schultz, S. & G Gould, G. (2016) Acetaminophen Use for Fever in Children Associated with Autism Spectrum Disorder. *Autism. Open. Access*, **06**.

Tada, H., Koide, M., Ara, W., Shibata, Y., Funabashi, T., Suyama, K., Goto, T., & Takahashi, T. (2015) Estrous Cycle-Dependent Phasic Changes in the Stoichiometry of Hippocampal Synaptic AMPA Receptors in Rats. *PLoS One*, **10**.

Takahashi, T., Nowakowski, R., & Caviness, V. (1995) The cell cycle of the pseudostratified ventricular epithelium of the embryonic murine cerebral wall. *J. Neurosci.*, **15**, 6046–6057.

Takuma, K., Hara, Y., Kataoka, S., Kawanai, T., Maeda, Y., Watanabe, R., Takano, E., Hayata-Takano, A., Hashimoto, H., Ago, Y., & Matsuda, T. (2014) Chronic treatment with valproic acid or sodium butyrate attenuates novel object recognition deficits and hippocampal dendritic spine loss in a mouse model of autism. *Pharmacol. Biochem. Behav.*, **126**, 43–49.

Tamiji, J. & Crawford, D.A. (2010a) Misoprostol elevates intracellular calcium in Neuro-2a cells via protein kinase A. *Biochem. Biophys. Res. Commun.*, **399**, 565–570.

Tamiji, J. & Crawford, D.A. (2010b) Prostaglandin E2 and misoprostol induce neurite retraction in Neuro-2a cells. *Biochem. Biophys. Res. Commun.*, **398**, 450–456.

Tanapat, P., Hastings, N.B., Reeves, A.J., & Gould, E. (1999) Estrogen stimulates a transient increase in the number of new neurons in the dentate gyrus of the adult female rat. *J. Neurosci.*, **19**, 5792–5801.

Tang, G., Gudsnuk, K., Kuo, S.H., Cotrina, M.L., Rosoklija, G., Sosunov, A., Sonders, M.S., Kanter, E., Castagna, C., Yamamoto, A., Yue, Z., Arancio, O., Peterson, B.S., Champagne, F., Dwork, A.J., Goldman, J., & Sulzer, D. (2014) Loss of mTOR-Dependent Macroautophagy Causes Autistic-like Synaptic Pruning Deficits. *Neuron*, **83**, 1131–1143.

Thongkorn, S., Kanlayaprasit, S., Panjabud, P., Saeliw, T., Jantheang, T., Kasitipradit, K., Sarobol, S., Jindatip, D., Hu, V.W., Tencomnao, T., Kikkawa, T., Sato, T., Osumi, N., & Sarachana, T. (2021) Sex differences in the effects of prenatal bisphenol A exposure on autism-related genes and their relationships with the hippocampus functions. *Sci. Reports 2021 111*, **11**, 1–19.

Tian, J., Kim, S.F., Hester, L., & Snyder, S.H. (2008) S-nitrosylation/activation of COX-2

mediates NMDA neurotoxicity. *Proc. Natl. Acad. Sci. U. S. A.*, **105**, 10537–10540.

Tian, Y., Yang, C., Shang, S., Cai, Y., Deng, X., Zhang, J., Shao, F., Zhu, D., Liu, Y., Chen, G., Liang, J., Sun, Q., Qiu, Z., & Zhang, C. (2017) Loss of FMRP impaired hippocampal long-term plasticity and spatial learning in rats. *Front. Mol. Neurosci.*, **10**, 269.

Tong, L., Aleph Prieto, G., Kramár, E.A., Smith, E.D., Cribbs, D.H., Lynch, G., & Cotman, C.W. (2012) Brain-derived neurotrophic factor-dependent synaptic plasticity is suppressed by interleukin-1β via p38 mitogen-activated protein kinase. *J. Neurosci.*, **32**, 17714–17724.

Tønnesen, J., Katona, G., Rózsa, B., & Nägerl, U.V. (2014) Spine neck plasticity regulates compartmentalization of synapses. *Nat. Neurosci.*, **17**, 678–685.

Traetta, M.E., Codagnone, M.G., Uccelli, N.A., Ramos, A.J., Zárate, S., & Reinés, A. (2021) Hippocampal neurons isolated from rats subjected to the valproic acid model mimic in vivo synaptic pattern: evidence of neuronal priming during early development in autism spectrum disorders. *Mol. Autism*, **12**.

Travers, B.G., Bigler, E.D., Duffield, T.C., Prigge, M.D.B., Froehlich, A.L., Lange, N., Alexander, A.L., & Lainhart, J.E. (2018) Longitudinal development of manual motor ability in autism spectrum disorder from childhood to mid-adulthood relates to adaptive daily living skills. *Dev. Sci.*, **20**.

Vereker, E., O'Donnell, E., & Lynch, M.A. (2000) The inhibitory effect of interleukin-1β on long-term potentiation is coupled with increased activity of stress-activated protein kinases. *J. Neurosci.*, **20**, 6811–6819.

Viale, B., Song, L., Petrenko, V., Wenger Combremont, A.L., Contestabile, A., Bocchi, R., Salmon, P., Carleton, A., An, L., Vutskits, L., & Kiss, J.Z. (2019) Transient Deregulation of Canonical Wnt Signaling in Developing Pyramidal Neurons Leads to Dendritic Defects and

Impaired Behavior. *Cell Rep.*, **27**, 1487-1502.e6.

Vierk, R., Glassmeier, G., Zhou, L., Brandt, N., Fester, L., Dudzinski, D., Wilkars, W., Bender, R.A., Lewerenz, M., Gloger, S., Graser, L., Schwarz, J., & Rune, G.M. (2012) Aromatase Inhibition Abolishes LTP Generation in Female But Not in Male Mice. *J. Neurosci.*, **32**, 8116–8126.

Waclawik, A., Jabbour, H.N., Blitek, A., & Ziecik, A.J. (2009) Estradiol-17β, Prostaglandin E2 (PGE2), and the PGE2 Receptor Are Involved in PGE2 Positive Feedback Loop in the Porcine Endometrium. *Endocrinology*, **150**, 3823–3832.

Walkley, S.U., Zervas, M., & Wiseman, S. (2000) Gangliosides as modulators of dendritogenesis in normal and storage disease-affected pyramidal neurons. *Cereb. Cortex*, **10**, 1028–1037.

Warren, S.G., Humphreys, A.G., Juraska, J.M., & Greenough, W.T. (1995) LTP varies across the estrous cycle: enhanced synaptic plasticity in proestrus rats. *Brain Res.*, **703**, 26–30.

Wegiel, J., Flory, M., Kuchna, I., Nowicki, K., Ma, S.Y., Imaki, H., Wegiel, J., Cohen, I.L., London, E., Brown, W.T., & Wisniewski, T. (2014) Brain-region-specific alterations of the trajectories of neuronal volume growth throughout the lifespan in autism. *Acta Neuropathol. Commun.*, **2**, 1–18.

Wegiel, J., Flory, M., Schanen, N.C., Cook, E.H., Nowicki, K., Kuchna, I., Imaki, H., Ma, S.Y., Wegiel, J., London, E., Casanova, M.F., Wisniewski, T., & Brown, W.T. (2015) Significant neuronal soma volume deficit in the limbic system in subjects with 15q11.2-q13 duplications. *Acta Neuropathol. Commun.*, **3**, 63.

Wei, H., Alberts, I., & Li, X. (2013) Brain IL-6 and autism. *Neuroscience*,.

Wei, H., Chadman, K.K., McCloskey, D.P., Sheikh, A.M., Malik, M., Brown, W.T., & Li, X. (2012) Brain IL-6 elevation causes neuronal circuitry imbalances and mediates autism-like

behaviors. *Biochim. Biophys. Acta - Mol. Basis Dis.*, **1822**, 831–842.

Wei, H., Zou, H., Sheikh, A.M., Malik, M., Dobkin, C., Brown, W.T., & Li, X. (2011) IL-6 is increased in the cerebellum of autistic brain and alters neural cell adhesion, migration and synaptic formation. *J. Neuroinflammation*, **8**, 52.

Weintraub, K. (2011) The prevalence puzzle: Autism counts. *Nature*, **479**, 22–24.

Weir, R., Jacobs, B., Schumann, C., Weir, R., & Schumann, C. (2018) Protracted dendritic growth in the typically developing human amygdala and increased spine density in young ASD brains HHS Public Access. *J Comp Neurol*, **526**, 262–274.

Wen, Q. & Chklovskii, D.B. (2008) A cost-benefit analysis of neuronal morphology. *J. Neurophysiol.*, **99**, 2320–2328.

Williams, D.L., Goldstein, G., & Minshew, N.J. (2005) Impaired memory for faces and social scenes in autism: clinical implications of memory dysfunction. *Arch. Clin. Neuropsychol.*, **20**, 1–15.

Williams, D.L., Goldstein, G., & Minshew, N.J. (2006) The profile of memory function in children with autism. *Neuropsychology*, **20**, 21–29.

Williams, S.R. & Stuart, G.J. (2003) Role of dendritic synapse location in the control of action potential output. *Trends Neurosci.*, **26**, 147–154.

Won, H., Lee, H.R., Gee, H.Y., Mah, W., Kim, J.I., Lee, J., Ha, S., Chung, C., Jung, E.S., Cho, Y.S., Park, S.G., Lee, J.S., Lee, K., Kim, D., Bae, Y.C., Kaang, B.K., Lee, M.G., & Kim, E. (2012) Autistic-like social behaviour in Shank2-mutant mice improved by restoring NMDA receptor function. *Nat. 2012 4867402*, **486**, 261–265.

Wong, C. & Crawford, D.A. (2014) Lipid Signalling in the Pathology of Autism Spectrum Disorders. In *Comprehensive Guide to Autism*. Springer New York, 1259–1283.

Wong, C.T., Bestard-Lorigados, I., & Crawford, D.A. (2019) Autism-related behaviors in the cyclooxygenase-2-deficient mouse model. *Genes, Brain Behav.*, **18**.

Wong, C.T., Ussyshkin, N., Ahmad, E., Rai-Bhogal, R., Li, H., & Crawford, D.A. (2016) Prostaglandin E2 promotes neural proliferation and differentiation and regulates Wnt target gene expression. *J. Neurosci. Res.*, **94**, 759–775.

Wong, C.T., Wais, J., & Crawford, D.A. (2015) Prenatal exposure to common environmental factors affects brain lipids and increases risk of developing autism spectrum disorders. *Eur. J. Neurosci.*,.

Wright, C.L., Hoffman, J.H., & McCarthy, M.M. (2019) Evidence that inflammation promotes estradiol synthesis in human cerebellum during early childhood. *Transl. Psychiatry 2019 91*, **9**, 1–10.

Wright, C.L. & McCarthy, M.M. (2009) Prostaglandin E2-Induced Masculinization of Brain and Behavior Requires Protein Kinase A, AMPA/Kainate, and Metabotropic Glutamate Receptor Signaling. *J. Neurosci.*, **29**, 13274–13282.

Wu, A., Ying, Z., & Gomez-Pinilla, F. (2008) Docosahexaenoic acid dietary supplementation enhances the effects of exercise on synaptic plasticity and cognition. *Neuroscience*, **155**, 751–759.

Yamagata, K., Andreasson, K.I., Kaufmann, W.E., Barnes, C.A., & Worley, P.F. (1993) Expression of a Mitogen-Inducible Cyclooxygenase in Brain Neurons: Regulation by Synaptic Activity and Glucocorticoids, Neuron.

Yau, S.Y., Bettio, L., Chiu, J., Chiu, C., & Christie, B.R. (2019) Fragile-X syndrome is associated with NMDA receptor hypofunction and reduced dendritic complexity in mature dentate granule cells. *Front. Mol. Neurosci.*, **11**, 495.

Yau, S.Y., Bostrom, C.A., Chiu, J., Fontaine, C.J., Sawchuk, S., Meconi, A., Wortman, R.C., Truesdell, E., Truesdell, A., Chiu, C., Hryciw, B.N., Eadie, B.D., Ghilan, M., & Christie, B.R. (2016) Impaired bidirectional NMDA receptor dependent synaptic plasticity in the dentate gyrus of adult female Fmr1 heterozygous knockout mice. *Neurobiol. Dis.*, **96**, 261–270.

Yehuda, S. & Rabinovitz, S. (2016) The Role of Essential Fatty Acids in Anorexia Nervosa and Obesity. *Crit. Rev. Food Sci. Nutr.*, **56**, 2021–2035.

Yui, K., Imataka, G., Kawasaki, Y., & Yamada, H. (2016) Down-regulation of a signaling mediator in association with lowered plasma arachidonic acid levels in individuals with autism spectrum disorders. *Neurosci. Lett.*, **610**, 223–228.

Zablotsky, B., Black, L.I., & Blumberg, S.J. (2014) Estimated Prevalence of Children With Diagnosed Developmental Disabilities in the United States, 2014-2016 Key findings Data from the National Health Interview Survey.

Zaboski, B.A. & Storch, E.A. (2018) Comorbid autism spectrum disorder and anxiety disorders: A brief review. *Future Neurol.*,.

Zaqout, S. & Kaindl, A. (2016) Golgi-Cox Staining Step by Step. *Front. Neuroanat.*, **10**.

Zerbo, O., Qian, Y., Yoshida, C., Grether, J.K., Van de Water, J., & Croen, L.A. (2015) Maternal Infection During Pregnancy and Autism Spectrum Disorders. *J. Autism Dev. Disord.*, **45**, 4015–4025.

Zuo, Y., Lin, A., Chang, P., & Gan, W.B. (2005) Development of Long-Term Dendritic Spine Stability in Diverse Regions of Cerebral Cortex. *Neuron*, **46**, 181–189.

Zuo, Y., Yang, G., Kwon, E., & Gan, W.B. (2005) Long-term sensory deprivation prevents dendritic spine loss in primary somatosensory cortex. *Nature*, **436**, 261–265.

APPENDIX A

Copyright Information for Published Work

Figure 1 citation:
Weintraub, K. (2011) The prevalence puzzle: Autism counts. *Nature*, **479**, 22–24.

SPRINGER NATURE LICENSE
TERMS AND CONDITIONS

May 01, 2022

This Agreement between York University -- Shalini Iyer ("You") and Springer Nature ("Springer Nature") consists of your license details and the terms and conditions provided by Springer Nature and Copyright Clearance Center.

License Number	5300350280266
License date	May 01, 2022
Licensed Content Publisher	Springer Nature
Licensed Content Publication	Nature
Licensed Content Title	The prevalence puzzle: Autism counts
Licensed Content Author	Karen Weintraub
Licensed Content Date	Nov 2, 2011
Type of Use	Thesis/Dissertation
Requestor type	academic/university or research institute
Format	print and electronic
Portion	figures/tables/illustrations
Number of figures/tables/illustrations	1

High-res required	no
Will you be translating?	no
Circulation/distribution	1 - 29
Author of this Springer Nature content	no
Title	MSc Student
Institution name	York University
Expected presentation date	Jun 2022
Portions	Pie chart of reasons contributing to ASD prevalence on the top right of the second page.
Requestor Location	York University 4700 Keele Street Lumbers Building, Room 222 Toronto, ON M3J1P3 Canada Attn: York University
Total	0.00 USD

Figure 4 citation:
Wong, C. & Crawford, D.A. (2014) Lipid Signalling in the Pathology of Autism Spectrum Disorders. In *Comprehensive Guide to Autism*. Springer New York, 1259–1283.

SPRINGER NATURE LICENSE
TERMS AND CONDITIONS

May 01, 2022

This Agreement between York University -- Shalini Iyer ("You") and Springer Nature ("Springer Nature") consists of your license details and the terms and conditions provided by Springer Nature and Copyright Clearance Center.

License Number	5300350739137
License date	May 01, 2022
Licensed Content Publisher	Springer Nature
Licensed Content Publication	Springer eBook
Licensed Content Title	Lipid Signalling in the Pathology of Autism Spectrum Disorders
Licensed Content Author	Christine Wong, Dorota Anna Crawford
Licensed Content Date	Jan 1, 2014
Type of Use	Thesis/Dissertation
Requestor type	academic/university or research institute
Format	print and electronic
Portion	figures/tables/illustrations
Number of figures/tables/illustrations	1

Will you be translating?	no
Circulation/distribution	1 - 29
Author of this Springer Nature content	no
Title	MSc Student
Institution name	York University
Expected presentation date	Jun 2022
Portions	Figure 4: PGE2 signalling pathway and interaction with misoprostol
Requestor Location	York University 4700 Keele Street Lumbers Building, Room 222 Toronto, ON M3J1P3 Canada Attn: York University
Total	0.00 USD

Figure 5 citation:
Banker, S.M., Gu, X., Schiller, D., & Foss-Feig, J.H. (2021) Hippocampal contributions to social and cognitive deficits in autism spectrum disorder. *Trends Neurosci.*, **44**, 793–807.

ELSEVIER LICENSE
TERMS AND CONDITIONS

May 01, 2022

This Agreement between York University -- Shalini Iyer ("You") and Elsevier ("Elsevier") consists of your license details and the terms and conditions provided by Elsevier and Copyright Clearance Center.

License Number	5300341027445
License date	May 01, 2022
Licensed Content Publisher	Elsevier
Licensed Content Publication	Trends in Neurosciences
Licensed Content Title	Hippocampal contributions to social and cognitive deficits in autism spectrum disorder
Licensed Content Author	Sarah M. Banker,Xiaosi Gu,Daniela Schiller,Jennifer H. Foss-Feig
Licensed Content Date	Oct 1, 2021
Licensed Content Volume	44
Licensed Content Issue	10
Licensed Content Pages	15
Start Page	793
End Page	807

Type of Use	reuse in a thesis/dissertation
Portion	figures/tables/illustrations
Number of figures/tables/illustrations	2
Format	both print and electronic
Are you the author of this Elsevier article?	No
Will you be translating?	No
Title	MSc Student
Institution name	York University
Expected presentation date	Jun 2022
Portions	Figure 2 only
Requestor Location	York University 4700 Keele Street Lumbers Building, Room 222 Toronto, ON M3J1P3 Canada Attn: York University
Publisher Tax ID	GB 494 6272 12
Total	0.00 CAD